Chair of Energy Network Technology

Master's Thesis

# Techno-Economic Assessment of H2-Supply for an Industrial Site

Lukas Maximilian Wechner, BSc

May 2024

**MONTANUNIVERSITÄT LEOBEN**
www.unileoben.ac.at

## EIDESSTATTLICHE ERKLÄRUNG

Ich erkläre an Eides statt, dass ich diese Arbeit selbstständig verfasst, andere als die angegebenen Quellen und Hilfsmittel nicht benutzt, den Einsatz von generativen Methoden und Modellen der künstlichen Intelligenz vollständig und wahrheitsgetreu ausgewiesen habe, und mich auch sonst keiner unerlaubten Hilfsmittel bedient habe.

Ich erkläre, dass ich den Satzungsteil „Gute wissenschaftliche Praxis" der Montanuniversität Leoben gelesen, verstanden und befolgt habe.

Weiters erkläre ich, dass die elektronische und gedruckte Version der eingereichten wissenschaftlichen Abschlussarbeit formal und inhaltlich identisch sind.

Datum 06.05.2024

Unterschrift Verfasser/in
Lukas Maximilian Wechner

# ABSTRACT

To advance the mitigation of global warming by decarbonization, the industrial sector has to transform towards low emission energy sources. Green hydrogen is seen as an important part of this transformation. However, the absence of a well-established hydrogen transport infrastructure slows the implementation of production capacities and industrial applications. Moreover, investments in hydrogen infrastructure align close to the production of hydrogen and the industrial demand. Therefore, companies willing to transform toward clean energy have to make a strategic decision, if the supply should rely on regional infrastructure or if an investment in on-site production facilities should be considered. To support this decision-making process a calculation model is developed to evaluate the techno-economic concept for hydrogen supply of an industrial site.

The model is created within the Python programming environment utilizing the Open Energy Modelling Framework “OEMOF”. It is further supported by Excel spreadsheets to ease user interaction, result processing and graphical representation. The model can be tailored to investigate different scenarios focusing on on-site hydrogen production strategies through water electrolysis. Furthermore, an aboveground hydrogen storage as a flexibility option is taken into account evaluating the economic influence. The model is cost optimized by a mixed linear integer solver in regard of fluctuating electricity prices. Moreover, the flows, the capacities of the components component and their corresponding costs are determined to enable a detailed analysis.

Additionally, an exemplary calculation is carried out by providing technical and economic parameters for hydrogen production in near future. Together with an electricity price profile and a load profile the influences on costs and on the operational strategy are determined.

It turns out that the utilization of a hydrogen storage can reduce the hydrogen supply costs up to a certain point depending on the storage capacity. However, the implementation of larger hydrogen storage leads to a rise in hydrogen supply costs. Increasing the storage capacity by compressing or liquifying the hydrogen turned out to be not favourable under these assumptions.

The electricity price was identified as the main cost driver necessitating a further expansion of renewable energy sources to reduce electricity prices and utilize fluctuations.

For an industrial site with an annual hydrogen demand of 72 GWh the hydrogen supply costs for merchant hydrogen delivered by different transport routes and the on-site production lie within the same range. Depending on the underlying assumptions on-site production can be a competitive alternative for merchant hydrogen.

# KURZFASSUNG

Um die Auswirkungen der globalen Erwärmung abzumildern, muss die Industrie durch den Einsatz von emissionsarmen Energieträgern transformiert werden. Ein wichtiger Bestandteil dieser Transformation ist grüner Wasserstoff. Durch das Fehlen einer gut ausgebauten Wasserstofftransportinfrastruktur verlangsamt sich gleichermaßen der Ausbau von Produktionskapazitäten und die Umstellung der Industrieprozesse. Darüber hinaus sind Investitionen in die Wasserstofftransportinfrastruktur eng mit der Produktion und der industriellen Nachfrage verknüpft. Daher stehen Unternehmen, die eine Umstellung auf Wasserstoff anstreben, vor der strategischen Entscheidung, ob sie sich bei der Versorgung auf die regionalen Infrastrukturen und den Import von Wasserstoff stützen oder in Produktionsanlagen vor Ort investieren. Zur Unterstützung dieses Entscheidungsprozesses wird ein Berechnungsmodell entwickelt, um das technisch-wirtschaftliche Konzept für die Wasserstoffversorgung eines Industriestandortes zu bewerten.

Das Modell wird in der Programmierumgebung Python unter Verwendung des Open Energy Modelling Framework "OEMOF" erstellt. Es wird außerdem durch die Verwendung von Excel unterstützt, um die Benutzerinteraktion, die Ergebnisverarbeitung und die grafische Darstellung zu erleichtern. Das Modell kann so angepasst werden, dass verschiedene Szenarien untersucht werden können, die sich vor allem auf Strategien zur Wasserstofferzeugung vor Ort durch Wasserelektrolyse konzentrieren. Darüber hinaus wird eine oberirdische Wasserstoffspeicherung als Flexibilitätsoption berücksichtigt, und der wirtschaftliche Einfluss bewertet. Durch Einsatz eines „mixed linear Integer“ Solver wird das Modell unter Berücksichtigung eines vordefinierten Strompreisprofils kostenoptimiert. Darüber hinaus werden die Komponentengrößen ermittelt und die Prozessströme sowie deren Kosten zeitaufgelöst berechnet, um eine detaillierte Analyse zu ermöglichen.

Auf Basis, der durch Literaturrecherche ermittelten, technischen und wirtschaftlichen Parameter wird die Berechnung für einen exemplarischen Industriestandort in naher Zukunft durchgeführt. Zusammen mit dem Strompreisprofil und einem vordefinierten Lastprofil werden die Betriebsstrategie und die zugehörigen Kosteneinflüsse ermittelt.

Es zeigt sich, dass der Einsatz eines Wasserstoffspeichers als Flexibilitätsoption die Wasserstoffversorgungskosten in Abhängigkeit von der Speicherkapazität bis zu einem gewissen Grad reduzieren kann, wobei der Einsatz von noch größeren Wasserstoffspeichern zu einem erneuten Anstieg der Wasserstoffversorgungskosten führt. Die Erhöhung der Speicherkapazität durch Komprimierung oder Verflüssigung des Wasserstoffs hat sich als nicht vorteilhaft herausgestellt und führt zu Kostensteigerungen.

Da der Strompreis der Hauptkostentreiber der Wasserstoffversorgungskosten ist kann die Konkurrenzfähigkeit und Kosteneffizienz der Produktion am Standort von sinkenden Strompreisen profitieren. Das zeigt, dass der Ausbau erneuerbarer Energie, die Nutzung von

erneuerbaren Überschüssen und die dadurch fluktuierenden Preise, einen großen Einfluss auf die Kosten der Wasserstoffproduktion hat.

Weiters hat sich herausgestellt, dass für einen Industriestandort mit einem jährlichen Wasserstoffbedarf von 72 GWh die Wasserstoffversorgungskosten für importierten Wasserstoff, der über verschiedene Transportwege angeliefert wird, und die Vor-Ort-Erzeugung in der gleichen Größenordnung liegen. Je nach den zugrundeliegenden Annahmen kann die Vor-Ort-Erzeugung daher eine wettbewerbsfähige Alternative zu importiertem Wasserstoff darstellen.

# ACKNOWLEDGEMENT

At first, I would like to thank Univ.-Prof. Dipl.-Ing. Dr.techn. Thomas Kienberger, head of the Chair of Energy Network Technology of Montanuniversität Leoben for providing the topic of this master's thesis, the discussions, as well as reviewing and correcting my work.

The greatest thank goes to my supervisor at the Chair of Energy Network Technology, Dipl.-Ing. Roberta Cvetkovska, for her excellent support, review and corrections, advice, and for giving me access to many sources of information. She was always there to help me with my questions and problems, no matter the time or situation.

Many thanks to my fiancé Nicole for her personal support throughout all life situations and her excellent expertise and support in material science and academic research topics. She has broadened and enriched my view of science and helped to improve the quality of my work during my studies significantly.

Finally, I would like to thank my family especially my mum and my grandparents for all their emotional and financial support before and during my studies and thanks to everyone who has contributed for making all this possible.

# CONTENT

# NOMENCLATURE

## Abbreviations

| | |
|---|---|
| AEL | Alkaline Electrolyzer |
| AEMEL | Anion Exchange Membrane Electrolyzer |
| AEM | Anion Exchange Membrane |
| CAPEX | Captial Expenditures |
| CBC | Coin-OR Branch and Cut Solver |
| CCU | Carbon Capture and Utilization |
| CGH2 | Compressed Gaseous Hydrogen |
| DRI | Direct Reduced Iron |
| EPC | Equivalent Periodic Cost |
| F1 | Delivery on a Weekly Basis |
| F2 | Delivery Every Two Weeks |
| F3 | Delivery Every Three Weeks |
| GH2 | Gaseous Hydrogen |
| GLPK | GNU Linear Programming Kit |
| KPI | Key Point Indicator |
| LCOC | Levelized Cost of Carbon Dioxide |
| LCOCOM | Levelized Cost of Compressor |
| LCOEL | Levelized Cost of Electrolyzer |
| LCOH_Pro | Levelized Cost of Hydrogen Production |
| LCOOXY | Levelized Cost of Oxygen |
| LCOS | Levelized Cost of Storage |
| LH2 | Liquid Hydrogen |
| LPG | Liquified Petroleum Gas |
| NOx | Nitrogen Oxide Emissions |

| | |
|---|---|
| OEMOF | Open Energy Modelling Framework |
| OPEX | Operational Expenditures |
| PEM | Polymer Electrolyte Membrane |
| PEMEL | Polymer Electrolyte Membrane Electrolyzer |
| PFSA | Perfluorosulfonic Acid |
| PSA | Pressure Swing Adsorption |
| SOEC | Solid Oxide Electrolysis Cell |
| WACC | Weighted Average Costs of Capital |

## Indices

| | |
|---|---|
| EPC | Equivalent Periodic Cost [€/$kg_{H2}$] in case of hydrogen storage and compressor, [€/kWh] in case of electrolyzer |
| $C_{H2,Scenario}$ | Specific hydrogen supply costs for a scenario [€/$kg_{H2}$] |
| $C_{H2}$ | Specific hydrogen production cost [€/$kg_{H2}$] |
| $C_{CAPEX}$(EL,ST,COM) | Specific capital expenditures for electrolyzer, storage or compressor [€/$kg_{H2}$] |
| $C_{OPEX}$(EL,ST,COM) | Specific operational expenditures for electrolyzer, storage or compressor [€/$kg_{H2}$] |
| $i_d$ | Interest rate in a range of 10 years [%] |
| i | Interest rate for a single year [%] |
| n | Number of years |
| $M_{H2}$ | Total annual hydrogen amount [$kg_{H2}$] |
| Ca | Storage cost for reference implementation [€] |
| $S_{limit}$ | Storage capacity limit [GWh] |
| Sa | Storage capacity from reference implementation [$kg_{H2}$] |
| Cb | Storage cost for required storage [€] |
| Sb | Storage capacity for required storage [$kg_{H2}$] |

| | |
|---|---|
| f | Scale factor for hydrogen storage |
| $C_{OPEX,O\&M}$(EL,ST,COM) | Specific operation and maintenance expenditures for electrolyzer, storage or compressor [€/$kg_{H2}$] |
| $C_{electricity,limit}$ | Electricity price limit [€/MWh] |
| $C_{electricity}$ | Specific variable costs for electricity [€/kWh] |
| $C_{water}$ | Specific variable costs for water [€/$kg_{H2O}$] |
| $C_{CO2}$ | Carbon dioxide certificate costs [€/$kg_{CO2}$] |
| $W_{isothermal}$ | Compression work for isothermal hydrogen compression [J] |
| $W_{isen12}$ | Compression work for isentropic hydrogen compression [J] |
| κ | Isentropic exponent |
| $p_1$ | Pressure at the begin of the compression [Pa] |
| $p_2$ | Pressure at the end of the compression [Pa] |
| $V_1$ | Volume at the begin of the compression [$m^3$] |
| $n_{O2}$ | Amount of oxygen [mol] |
| $n_{H2}$ | Amount of hydrogen [mol] |
| $m_{O2}$ | Molar mass of oxygen [g/mol] |
| $m_{H2}$ | Molar mass of hydrogen [g/mol] |
| $m_{H2O}$ | Molar mass of hydrogen [g/mol] |
| CAPEX $H_2$ F1 | Specific capital expenditures for a gaseous hydrogen storage with a delivery frequency on a weekly basis [€/$kg_{H2}$] |
| $CAPEX_{Compressor}$ | Specific capital expenditures for the compressor [€/$kg_{H2}$] |
| $P_{com}$ | Specific compressor power [kW/$kg_{H2}$] |
| $W_{isen5.3}$ | Compression work for isentropic hydrogen compression regarding scenario 5.3 [J] |
| $P_{30}$ | Specific compressor power needed for hydrogen compression to 30 bar [kW/$kg_{H2}$] |
| $P_{200}$ | Specific compressor power needed for hydrogen compression to 200 bar [kW/$kg_{H2}$] |

| | |
|---|---|
| $EPC_{Compressor,5.3}$ | Equivalent periodic cost for compressor in scenario 5.3 [€/$kg_{H2}$] |
| $f_{material}$ | Scale factor to consider cost influence of storage material |
| y | Interpolation variable representing capital expenditures for hydrogen storage [€/$kg_{H2}$] |
| x | Interpolation variable representing hydrogen storage pressure [bar] |
| $CAPEX_{Storage,200}$ | Specific capital expenditures for hydrogen storage at 200 bar [€/$kg_{H2}$] |
| $CAPEX_{Storage,30}$ | Specific capital expenditures for hydrogen storage at 30 bar [€/$kg_{H2}$] |
| $CAPEX_{Storage}$ | Specific scaled capital expenditures for hydrogen storage [€/$kg_{H2}$] |
| $EPC_{Storage}$ | Equivalent periodic cost for hydrogen storage [€/$kg_{H2}$] |
| $EPC_{Storage,5.3}$ | Equivalent periodic cost for hydrogen storage in scenario 5.3 [€/$kg_{H2}$] |

# LIST OF FIGURES

# LIST OF TABLES

# 1 INTRODUCTION

The Austrian government has set an ambitious goal of decarbonizing the entire energy system of the country by 2040 to limit global warming below 2°C. To achieve this, the industrial sector, particularly the energy-intensive industry, must be transformed by finding sustainable and innovative solutions. Green hydrogen is seen as a major component in this transformation, as it can be used as feedstock for refineries and chemical plants, as reduction agent, and energy carrier for decarbonizing high-temperature applications [1].

Austria recently announced a hydrogen strategy that prioritizes key sectors for the use of hydrogen. Many companies are developing extensive strategies for their future hydrogen utilization and demand. While numerous planned electrolysis projects are progressing well on the production side, the limited capacity of renewable electricity production and transmission in Austria will not be enough for large-scale production of hydrogen produced by electrolysis. Therefore, hydrogen imports from other countries are necessary to ensure supply security in these industry sectors. The transportation of liquid hydrogen or its derivates can be facilitated through maritime, rail or truck transport, whereas pipeline networks are suitable for transporting gaseous hydrogen. Until 2030, the development of green hydrogen production facilities is expected to closely align with demand, primarily due to the absence of an existing hydrogen infrastructure. Companies with substantial hydrogen requirements have to make a strategic decision between importing the hydrogen or establish an on-site production facility to fulfill their requirements [1].

This thesis is focusing on an energy model to evaluate the techno-economic concept for the hydrogen supply of an industrial site. The model is tailored to consider on-site hydrogen production through low temperature electrolysis. It incorporates demand-driven production dynamics and considers flexibility options to optimize the costs. Following this, an exemplary calculation is carried out and the findings are compared with the hydrogen prices of various transportation options to discuss possible solutions for an exemplary industry site.

# 2 TASK ASSIGNMENT

The objective of this thesis is to evaluate the techno-economic concept for the hydrogen supply of an industrial site utilizing the computational framework "oemof" within the Python programming environment. The model is used to consider on-site hydrogen production through alkaline or polymer electrolyte membrane electrolysis. It considers demand-driven production dynamics and on-site hydrogen storage to optimize cost with respect to fluctuating electricity prices. Moreover, an exemplary calculation, including a sensitivity analysis, is carried out and the results are compared with the hydrogen prices of various transportation options.

## 2.1 Research Need

To achieve our goal of decarbonizing our energy system to limit climate change, hydrogen has an important role in transforming the energy intensive industry. In the absence of an established hydrogen infrastructure, placing hydrogen production and its utilization in industrial applications on site is demanding. It requires detailed research to outline the advantages and challenges associated with various hydrogen supply options.

Wang et al. [2] analysed the demand and the needed hydrogen infrastructure for supply and transport at a European level focusing on pipeline and ship transport. Ganter et al. [3] investigate low-carbon hydrogen supply chains for the chemical industry and refineries in the near term (2035) at a European level. They consider mature infrastructure technologies and focus on transport by truck. However, this large scale is not suitable for evaluating an average industrial consumer in Austria.

Focusing on Austria, the Austrian hydrogen strategy identifies the main sectors where hydrogen should be used to reach climate neutrality in 2040 [1]. Furthermore, hydrogen import routes are evaluated and the costs for green hydrogen are assessed by Kathan et al. [4]. It is indicated that hydrogen transport by pipeline is the most cost-effective solution. When using derivates like ammonia as feedstock other transport routes could be favorable as well. However, the production and distribution by various means of transportation in Austria and the corresponding costs for this hydrogen supply are not addressed. Additionally Carels et al.[5] recently analyzed hydrogen import routes for Germany. The situation in Germany is similar to Austria and pipeline transport seems to be favorable in terms of cost, however regional distribution and the corresponding hydrogen costs for individual industrial customers are not taken into account.

To address this gap and to facilitate strategic decision making in industrial context this study focuses on a representative industrial site to discuss possible solutions for hydrogen supply in Austria.

## 2.2 Research Objectives

The main objective of this thesis is to provide answers to the questions below:

- Can on-site hydrogen production through water electrolysis be a feasible and cost-effective alternative to other hydrogen supply routes?
- What economic influence has the implementation of an on-site hydrogen storage tank as a flexibility option?
- How is the operating strategy influenced when optimizing hydrogen supply costs considering storage capacity limits, electricity price limits and pressure limits?

## 2.3 Methodology Overview

The calculation model is developed through Python and Excel, and divided into an energy and an economic model as can be seen in Figure 1. The Energy Model contains the energy system for utilizing hydrogen gas in an industrial process. The input parameters are provided in an Excel sheet and extracted by the Python model. Major input parameters are the load profile and the electricity price profile to determine the component sizes and optimal operational strategies for cost efficiency. The results of the optimized Energy Model are forwarded to the Economic Model through a Python interface. The Economic Model computes the specific hydrogen supply costs for meeting the demand and writes the results to an Excel sheet for further analysis. Depending on the configuration different scenarios can be computed and compared. In conclusion, a sensitivity analysis is conducted to examine the cost influences.

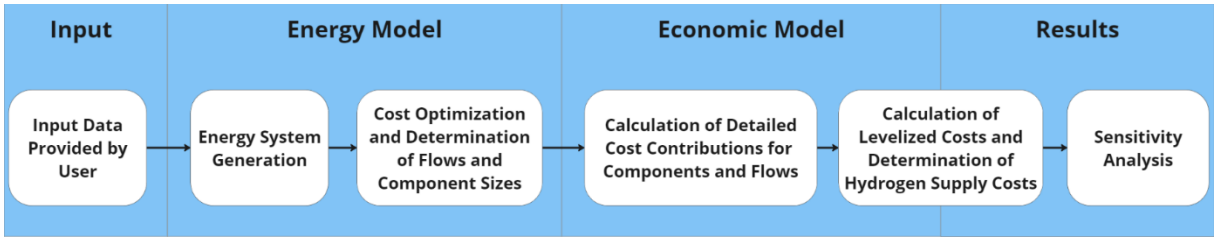


***Figure 1: Overview of the model sections and the calculation process.***

# 3 THEORETICAL BACKGROUND

This chapter provides an overview of the theoretical aspects regarding the industrial utilization of hydrogen. It will begin by examining the fundamental properties of hydrogen, followed by its current and potential future applications in various industries. Additionally, it will cover traditional methods of hydrogen production, as well as low emission techniques such as water electrolysis. Finally, the storage of hydrogen in different states is outlined.

## 3.1 Hydrogen Properties

Hydrogen consists of non-polar $H_2$ molecules with very weak intermolecular forces of attraction. This is reflected in its low boiling point, melting point and critical temperature. Hydrogen is a colorless, odorless and tasteless gas that is hardly soluble in water and the density is very low. Due to its low mass, the $H_2$ molecules in the gas move very fast, which results in a high diffusion capacity and a relatively high thermal conductivity [6]. The main properties of hydrogen are shown in Table 1 [6–8].

***Table 1: Properties of hydrogen [6–8].***

| Property | Unit | Value |
|---|---|---|
| Molecular weight | | 2.01594 |
| Density of gas at 0°C and 1,01325 bar | $kg/m^3$ | 0.08987 |
| Density of liquid at -253°C | $kg/m^3$ | 70.8 |
| Melting temperature | °C | -259 |
| Boiling temperature at 1,01325 bar | °C | -253 |
| Critical temperature | °C | -240 |
| Critical pressure | bar | 12.97 |
| Critical density | $kg/m^3$ | 31.2 |
| Heat of vaporization at -253°C | kJ/kg | 447 |
| Thermal conductivity at 25°C | kJ/kg | 0.019 |
| Heat capacity of gas at 25°C | kJ/kg K | 14.3 |
| Heat capacity of liquid at -256°C | kJ/kg K | 8.1 |
| Lower heating value | kWh/kg | 33.305 |

The presence of hydrogen can degrade the mechanical properties of various materials, particularly affecting their plasticity, a phenomenon referred to as hydrogen embrittlement. This phenomenon is significant for a wide range of metallic materials, including low-alloy steels, precipitation-hardening steels, superalloys, and aluminum alloys. Hydrogen embrittlement typically leads to failure at low stress levels, characterized by brittle fracture, often resulting in substantial economic losses or in severe cases, catastrophic consequences [9]. It has been widely concluded that hydrogen tends to reduce both macroscopic and microscopic tensile strength [10–15], as well as fatigue strength [16–18], and fracture toughness [19–23]. However, its impact on the rate of fatigue crack propagation in steels remains a topic of debate, often contingent upon factors such as frequency or stress ratio level [9, 24]. This has to be considered when developing or repurposing infrastructure for hydrogen use especially for hydrogen pipelines [9, 16, 17, 19, 20].

## 3.2 Hydrogen Industrial Applications

Today, industrial utilization of hydrogen is characterized by conventional applications like feedstock for refining, as a raw material in the chemical industry and for steel making. Hydrogen is crucial in the production of various chemicals such as ammonia and methanol, as well as in the steel industry where it acts as a reducing agent for the creation of direct reduced iron (DRI). Additionally, hydrogen finds application in smaller quantities in sectors like electronics, glassmaking, and metal processing, which will not be displayed here in detail [25].

In 2022, global hydrogen consumption reached 95 million metric tons, marking nearly 3% increase compared to 2021. Despite a rising global demand, these applications offer limited advantages for climate change mitigation, due to the reliance on fossil sources such as methane or coal for hydrogen production. In 2022, the production of low-emission hydrogen, sourced either from electrolysis or through fossil fuel and carbon capture and utilization (CCU), accounted for less than 0.7% of the total global production. Emerging applications in heavy industry, transportation, the synthesis of hydrogen-based fuels, as well as electricity generation and storage, currently represent a marginal fraction, constituting less than 0.1% of the overall global demand. This chapter aims to provide an overview of both common and new applications of hydrogen within the industrial sector [25].

### 3.2.1 Refining

Hydrogenation technology is the primary method used in producing oil products and is the core of refining chemical integration. The petrochemical industry employs several hydrogenation processes, which include hydrocracking, hydrodesulfurization, hydroconversion, C3 fraction hydrogenation and benzene hydrogenation. Despite its benefits, hydrogenation has some drawbacks, such as high investment and operational costs, and high

energy consumption. Therefore, researchers in the petrochemical field have focused on improving the activity and selectivity of hydrogenation catalysts while simultaneously reducing the amount of hydrogen consumed and overall process costs [26].

Hydrogen consumption in the refining industry has exceeded 41 million metric tons in 2022. Around 80% of this hydrogen was produced on-site by the refineries themselves. Out of this, about 55% was generated through dedicated hydrogen production, while the rest was produced as a by-product from various operations such as naphtha crackers. Less than 1% of the hydrogen used in refining in 2022 was produced using low-emission technologies. The remaining 20% of hydrogen used in refining was produced externally and mostly from fossil fuels. This hydrogen was sourced as merchant hydrogen. The production of hydrogen for use in refining resulted in 240-380 million tons of $CO_2$ being emitted into the atmosphere in 2022. Using low-emission hydrogen in refining can provide an accessible route to create a large demand for low-emission hydrogen and facilitate the scale-up of production. This is because it involves a like-for-like substitution rather than a fuel switch. However, the use of low-emission hydrogen in refineries has been limited so far and is progressing slowly. This is due to its higher production costs compared to hydrogen produced from fossil fuels. The use of merchant hydrogen in refineries is a common practice today and it could provide an alternative route to increase the supply of low-emission hydrogen in refineries [25].

### 3.2.2 Chemical Industry

Hydrogen is further used as a raw material to synthesize many chemical products, such as ammonia and urea. The production of ammonia, primarily achieved through the Haber Bosch process, offers a higher energy density compared to hydrogen. Ammonia possesses the advantage of being used to store energy and generate power without emitting carbon dioxide [27]. It is a promising fuel for maritime shipping by using it in a fuel cell or internal combustion engine [25]. Furthermore, its ability to remain stable as a liquid at room temperature and at around 10 bar pressure makes it suitable for transportation. The existing infrastructure for transporting and handling liquid ammonia facilitates its widespread utilization. Moreover, ammonia can react with $CO_2$ to form urea which is a vital nitrogen fertilizer. It is stable, nontoxic, and easier to store than hydrogen. Enterprises within the ammonia industry are actively exploring new ammonia synthesis processes like nitrogenase, photocatalytic synthesis, electrocatalytic synthesis, synthesis via cyclic processes, and supercritical synthesis. However, these novel methods are still immature and face challenges such as low efficiency, unstable reactions, and limited cost-effectiveness, necessitating further improvement. The future development focuses to use hydrogen produced from renewable resources, which could significantly improve existing processes and reduce greenhouse gas emissions [26].

Apart from urea, hydrogen can react with carbon dioxide to produce fundamental carbon-containing compounds such as methanol, methane, formic acid, and formaldehyde. These compounds can be used as liquid fuels with zero carbon emissions, which makes them ideal for renewable energy storage and transportation. Methanol, in particular, is important as a chemical raw material, being utilized in the synthesis of various compounds including formaldehyde, dimethyl ether, propylene, ethylene, and gasoline. With a high hydrogen content of 12.6% by mass and a notable energy density, methanol emerges as a liquid fuel. It can be transformed into hydrogen and carbon monoxide for use in polymer electrolyte membrane (PEM) fuel cells, or employed directly in methanol fuel cells, internal combustion engines, and turbines. The industrial hydrogenation of $CO_2$ to methanol is transitioning from the phase of industrial demonstration to large-scale commercial implementation [26].

Out of the 53 million metric tons of hydrogen consumed by industry in 2022, approximately 60% was used for ammonia production, 30% for methanol, and 10% for direct reduced iron (DRI) in the iron and steel subsector. Notably, nearly all are derived from fossil fuels within the same facilities where it is utilized. While carbon capture is a common practice in certain industry subsectors, the majority of the captured $CO_2$ finds alternative applications, such as in urea production and ends up being released into the atmosphere. Only a small fraction of projects involve underground storage of $CO_2$ [25].

### 3.2.3 Carbon Capture and Utilization

CCU presents an opportunity for the application of renewable hydrogen. This involves capturing $CO_2$ from industrial processes using various capture technologies and then combining it with hydrogen to produce synthetic methane which could be further processed into intermediate products like methanol, ethanol or ethylene [1, 28, 29]. These methods, called power to gas or power to liquid, were originally intended as an energy storage option for fluctuating renewable electric energy but are effective in reducing what are known as "hard to abate" $CO_2$ emissions [1, 28, 29]. These emissions occur in sectors like steel, cement or petrochemical industry and are difficult or impossible to avoid. However, the captured $CO_2$ can be used with hydrogen generated on-site from water electrolysis. This process provides an opportunity to use the oxygen, generated by the electrolysis, in place of air for combustion processes. This technology often referred to as oxyfuel increases the $CO_2$ concentration in the flue gas by avoiding dilution with nitrogen from the air, which in turn improves the separation by the CCU [30, 31].

### 3.2.4 Steel Industry

During the process of steel smelting, coke is used as a reduction agent for iron ore. This process generates a significant amount of carbon emissions, making ferrous metallurgy one

of the largest sources of carbon emissions. To address this issue, hydrogen can be used instead of coke as a reduction agent and energy carrier. This process produces only water as a by-product promoting the transformation to clean metallurgy. However, demonstration projects are still at the industrial test stage, and several problems need to be addressed. These include incomplete infrastructure facilities, lack of relevant standards, high costs, and safety concerns related to hydrogen. Currently, the main challenge in implementing hydrogen ferrous metallurgy technology is the cost of hydrogen production [26].

Beyond traditional applications in the chemical and steel sectors, hydrogen use also increases in new industrial applications, particularly 100%-hydrogen DRI steelmaking and high-temperature heating. Their share is marginal today but is expected to be 16% of the global hydrogen demand in 2030 according to the International Energy Agency [25].

### 3.2.5 Power Generation

Hydrogen is not commonly used as fuel in the power sector, accounting for less than 0.2% of the global electricity generation mix. In most cases, hydrogen is combined with other gases from steel production, refineries, or petrochemical plants rather than being used in its pure form. However, there are technologies available today that can use pure hydrogen for electricity generation. Fuel cells, internal combustion engines, and gas turbines can all run on hydrogen-rich gases or even pure hydrogen. Another option for electricity generation is using hydrogen in the form of ammonia by co-firing it or using it as a fuel for gas turbines. While using hydrogen and ammonia can reduce $CO_2$ emissions, nitrogen oxide emissions (NOx) need to be considered. Low NOx technologies are used in modern gas turbines to manage those emissions, allowing hydrogen co-firing shares of 30-60% depending on the burner design and combustion strategies implemented and research is carried out to establish low NOx gas turbines that can handle pure hydrogen. For NOx emissions from ammonia, flue gas treatment technologies such as selective catalytic reduction are available and already established for coal power plants. Ammonia combustion can also lead to nitrous oxide ($N_2O$) emissions, a strong greenhouse gas that has to be considered and treated [25].

### 3.2.6 Current and Future Hydrogen Applications

Even though the current hydrogen utilization focuses on industrial applications and refining, the Net Zero Emissions by 2050 Scenario of the International Energy Agency estimates a significant increase of hydrogen use in new applications in 2030. Beside the mentioned industrial sectors above, the transport sector and the generation of synthetic fuels are estimated to increase their demand significantly. Figure 2 shows the share of the hydrogen use according to the International Energy Agency scenario [25].

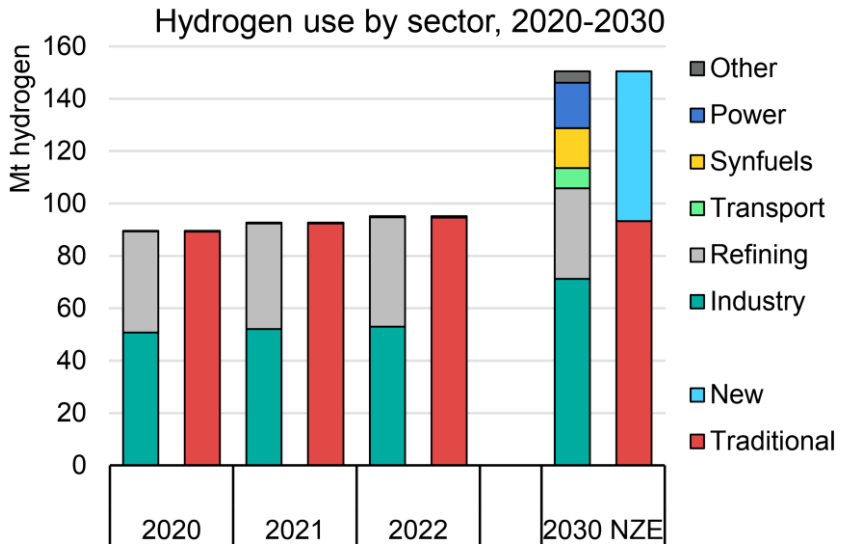


***Figure 2: Hydrogen use by sector in the IEA Net Zero Emissions by 2050 Scenario [25].***

## 3.3 Hydrogen Production

To meet the hydrogen demand for the applications mentioned above, multiple production pathways are available. This section will provide an overview of both conventional methods and electrolysis technologies aimed at producing low-emission hydrogen.

### 3.3.1 Steam Reforming

Steam reforming is the most commonly used method for hydrogen production. The best feedstocks for steam reforming are natural gas (the most common), refinery gas, liquified petroleum gas (LPG), and light naphtha. In its simplest form the reforming process for pure hydrogen production consists of four stages: a desulphurization unit, a steam methane reformer, a shift reactor, and finally pressure swing adsorption (PSA). These four main steps can be seen in Figure 3 [32].

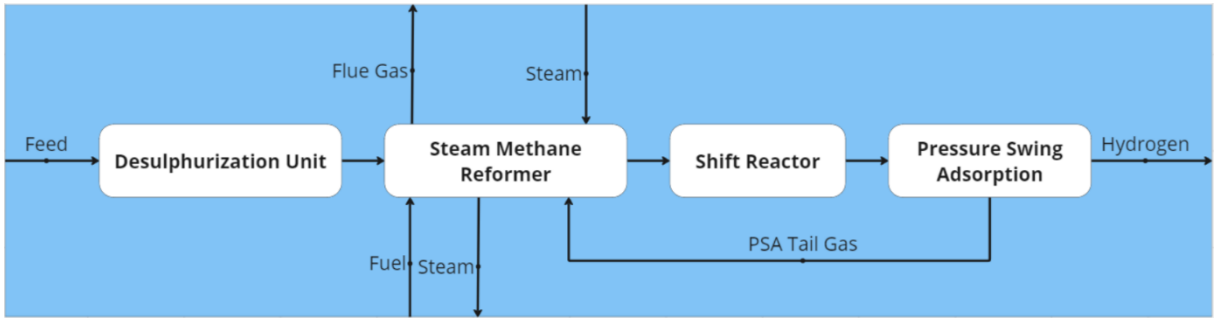


***Figure 3:The main steps of hydrogen production by steam methane reforming, based on [32].***

The reaction is typically carried out at 750 – 1000°C and a pressure of 20 – 40 bar over a fixed catalyst bed and can be seen in equation (1) [32].

$$CH_4 + H_2O \rightleftharpoons CO + 3\,H_2 \quad \left(\Delta H = -206\frac{kJ}{mol}at\ 15°C\right) \tag{1}$$

Desulphurization of the feedstock is required in order to protect the catalyst in the reformer furnace against deactivation. It is common practice to operate at excess steam/hydrocarbon ratios to prevent carbon formation. Heat for the endothermic reforming reaction is provided by the furnace burners. The reformed gas, a mixture of hydrogen, carbon dioxide, carbon monoxide, methane and steam, is cooled down to about 350°C by rising steam. After reforming, the CO in the gas reacts with steam to form additional hydrogen according to the shift reaction (equation (2)) [32].

$$CO + H_2O \rightarrow CO_2 + H_2 \quad \left(\Delta H = +41.2\frac{kJ}{mol}at\ 15°C\right) \tag{2}$$

The oxidation of the CO to $CO_2$ can be done in a converter reducing the CO content to less than 0.4 %. The product gas passes to a PSA which delivers ultra-pure hydrogen [32].

### 3.3.2 Gasification of Coke and Hydrocarbons

Coke gasification occurs within a gasifier using an oxygen-blown mode, yielding a gas that can be processed to extract hydrogen or synthesis gas, or utilized as a medium-calorific value fuel. The gasification reaction can be seen in equation (3) [32].

$$C + H_2O \rightarrow CO + H_2 \quad \left(\Delta H = -132\frac{kJ}{mol}at\ 15°C\right) \tag{3}$$

The resulting gas (syngas) comprises CO, $H_2$, $CO_2$, $CH_4$, and $H_2O$, along with sulfides that necessitate removal using an adsorbent. Particulates present in the gas are eliminated through a barrier filter, which typically contains a substantial carbon percentage. These particulates, often combined with ash, are directed to a combustor where any remaining carbon is incinerated [32].

Hydrocarbons are partially oxidized at elevated temperatures to yield a mixture of hydrogen and carbon monoxide. Unlike steam reforming, which relies on catalysts, partial oxidation can handle less pure feedstocks. Hydrogen processing in this system depends on how much of the gas is recovered as hydrogen, and how much is used as fuel. In cases where hydrogen production constitutes a minor fraction of the overall gas stream, a membrane is typically employed to extract a hydrogen-rich stream. This stream is subsequently refined in a purification unit [32].

Since the streams are available at a wide variety of compositions, flows, and pressures, the method of purification will vary. They include wet scrubbing, membrane systems, cryogenic

separation and PSA. This last technique is the most commonly used. In a PSA plant, the majority of impurities can be effectively removed to the desired extent. Multiple layers of absorbents, typically molecular sieves, are utilized to eliminate carbon dioxide, water, carbon monoxide, methane, and nitrogen from the outlet stream. Nitrogen, being the most challenging impurity to eliminate, often necessitates additional adsorbent for complete removal. However, as nitrogen primarily acts as a diluent, it is commonly left in the product. Following the PSA unit, hydrogen purity typically reaches around 99.9% with residual components such as CO typically below 10 ppm. Several adsorber beds are employed, with the gas flow periodically switched between vessels to facilitate the regeneration of the adsorbent through pressure reduction and purging, thereby releasing the adsorbed components [32].

### 3.3.3 Methane Pyrolysis

The thermal decomposition of methane, also known as methane pyrolysis, involves the endothermic breakdown of $CH_4$ into gaseous hydrogen and solid carbon. Unlike steam reforming, this process does not emit greenhouse gases. Typically, the reaction takes place within a temperature range of 800-1200 °C. Reaction temperature, decomposition rate, and the morphology of the solid carbon are controlled by catalysts. In contrast to water electrolysis (equation(8)), hydrogen produced through pyrolysis (equation (5)) demands a significantly lower specific energy requirement, of approximately 13 kWh/kg$H_2$ [33].

$$H_2O \rightarrow H_2 + \frac{1}{2}O \quad \left(\Delta H_R^\circ = 285{,}8\frac{kJ}{mol}\right) \tag{4}$$

$$CH_4 \rightarrow 2H_2 + C \quad \left(\Delta H_R^\circ = 74{,}8\frac{kJ}{mol}\right) \tag{5}$$

Various processes exist for methane pyrolysis, broadly categorized as catalytic and non-catalytic, further subdivided into molten, solid, and plasma pyrolysis. Catalysts include solid metals and oxides, graphite, or molten metals, each influencing reaction dynamics differently. While solid catalysts may degrade over time due to product absorption, this is not the case with molten metals and alloys, as long as no reaction products with carbon are formed. Alongside gaseous hydrogen, solid carbon is also generated, which, depending on its modification and purity, finds diverse applications. It can be utilized as a byproduct, applicable as a raw material in asphalt and refractory industries, in rubber and activated carbon products, as an additive in lubricants, casting powders, or anode material in metallurgical sectors like steel and aluminum production, and as a soil enhancer in agriculture, to make methane-pyrolysis economically interesting. High-purity pyrolysis carbons can also be used for

qualitatively more demanding applications such as electrode materials in batteries or electronics [33].

### 3.3.4 Electrolysis

The water electrolysis can be realized by technological variations based on diverse physical, chemical, and electrochemical aspects. Electrolyzers typically divide into four main technologies, distinguished by the electrolyte and operating temperature. Each technology consists of numerous variations, with significant differences in cell design, component variations, and technology maturity levels. Figure 4 shows the four different types of commercially available elecrtolyzers together with their functional principles which are discussed in detail in the sections below [34].

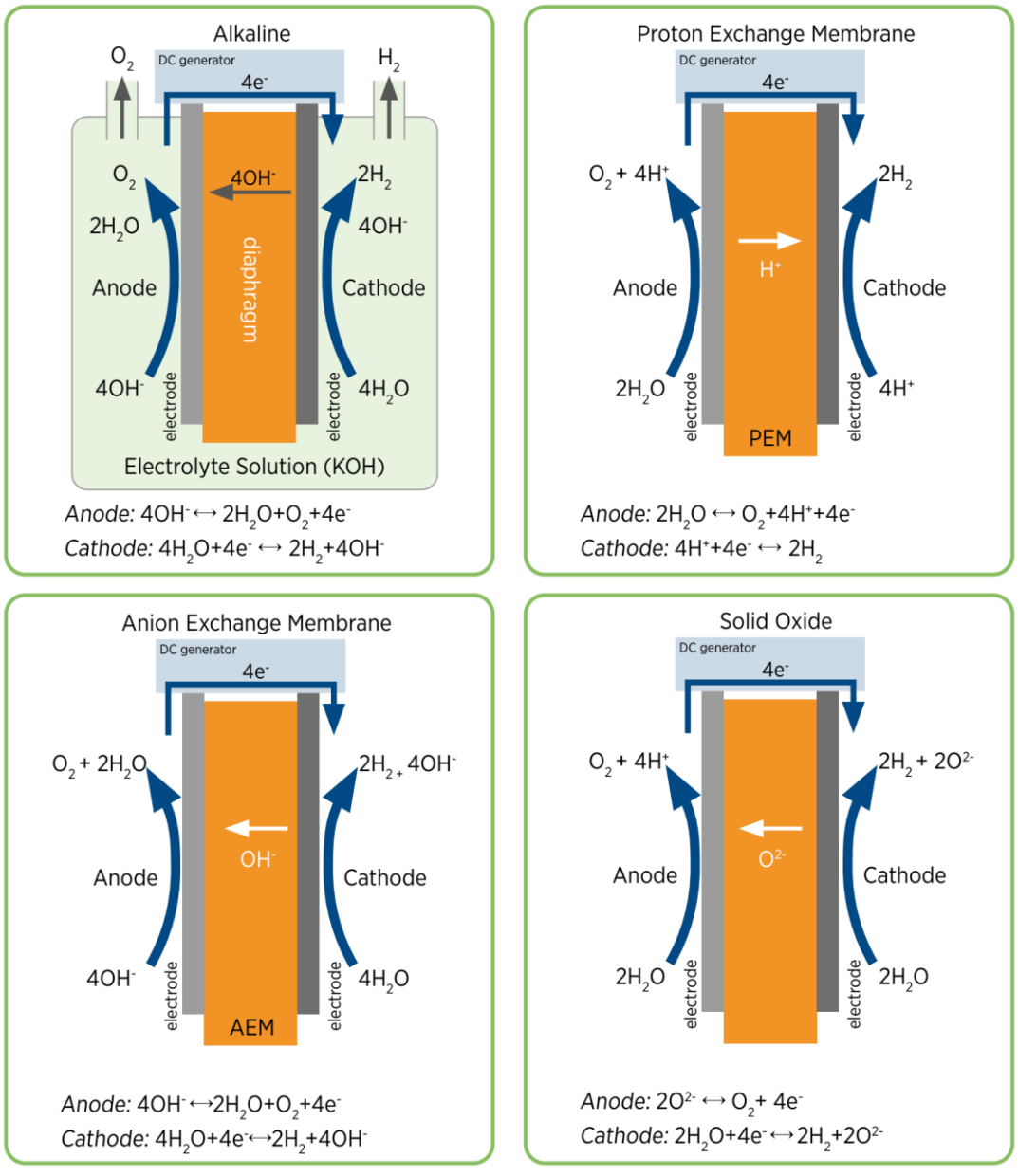


***Figure 4: Different types of commercially available electrolysis technologies [34].***

Alkaline (AEL) and polymer electrolyte membrane (PEMEL) technologies are already commercialized, while anion exchange membrane (AEMEL) and solid oxide (SOEC) technologies hold considerable potential but are less mature, with only a few companies engaged in their manufacturing and commercialization. This chapter will give an overview with a focus on alkaline and polymer electrolyte membrane technologies [34].

**Solid Oxide Electrolyzers**

The SOEC is operating at high temperatures (700-850 °C) and uses a solid electrolyte like yttria-stabilized zirconia. These systems benefit from favorable kinetics, allowing the use of relatively inexpensive nickel electrodes. This results in reduced electricity demand, and part of the energy for separation can be provided through heat. Additionally, there is the potential for reversibility by functioning as both a fuel cell and an electrolyzer or enabling co-electrolysis processes to combine $CO_2$ and water to produce syngas. However, thermo-chemical cycling, particularly during shutdown or ramping periods, accelerates degradation, leading to shorter lifetimes. Other challenges include stack degradation issues such as sealing difficulties under higher differential pressure, electrode contamination from silica sealants, and additional contaminants from piping, interconnects, and sealing materials. Presently, SOEC are mainly deployed at the kW-scale, although some ongoing demonstration projects have already reached 1 MW. The typical system design of a SOEC plant is shown in Figure 5 [34].

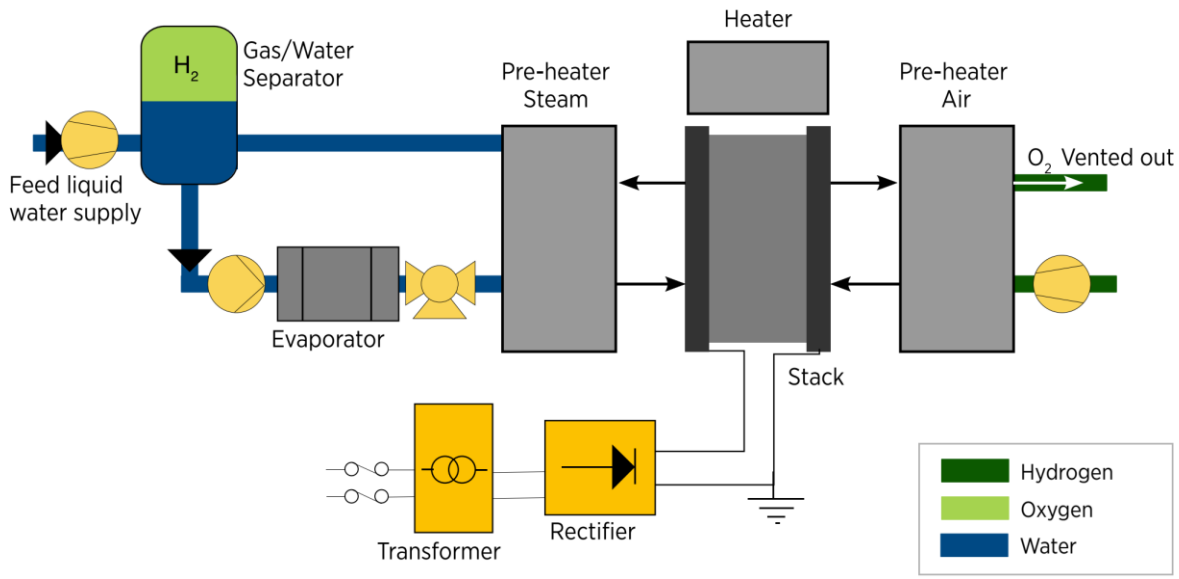


***Figure 5:Typical system design of a plant for a solid oxide electrolyzer [34].***

By coupling with heat-producing technologies like waste heat from industrial processes or concentrated solar power plants, these systems achieve higher overall efficiency. The water electrolysis becomes increasingly endothermic with rising temperatures and therefore the energy demand decreases rapidly due to the Joule heating of the cell [34].

**Alkaline Electrolyzers**

AEL electrolyzers have a simple stack and system design, making them relatively easy to manufacture. They utilize a high concentration of KOH as the electrolyte, along with robust $ZrO_2$-based diaphragms and nickel-coated stainless-steel electrodes with an area up to 3 square meters. The hydroxyl ion $OH^-$ serves as the ionic charge carrier, with KOH and water permeating through the porous structure of the diaphragm to facilitate the electrochemical reaction. However, this setup allows the hydrogen and oxygen gases ($H_2$ and $O_2$) produced to dissolve into the electrolyte, limiting their operational range and ability to function effectively at higher pressures. To mitigate gas intermixing, thicker diaphragms and spacers between electrodes and diaphragms are used. Nevertheless, these thicker diaphragms and added spacers result in higher ohmic resistances across the electrodes, significantly reducing efficiency and current density at a given voltage. Modern designs have addressed this performance gap by implementing zero-gap electrodes, thinner diaphragms, and novel electrocatalyst concepts to enhance current density, thus approaching the efficiency levels of PEM technology. Nonetheless, traditional alkaline designs are robust and reliable with lifetimes exceeding 30 years [34].

In operation, AEL electrolyzers necessitate recirculating the electrolyte (KOH) within the stack components, which creates a pressure drop requiring specific pumping characteristics and leads to efficiency losses. Alternatively, some alkaline systems operate without external pumping peripherals. The extracted alkaline solution must be separated from the produced gases. Gas-water separators, positioned above the stack at a specified height, facilitate this process. The KOH/water mixture flows back into the stack, with the water phase removed at the bottom and the gas phase at the top, as can be seen in Figure 6 . This separator also serves as a buffer storage for fluctuating load specifications. Effective water management is crucial, regulating the filling level of each gas separator while accounting for water permeation via the diaphragm [34].

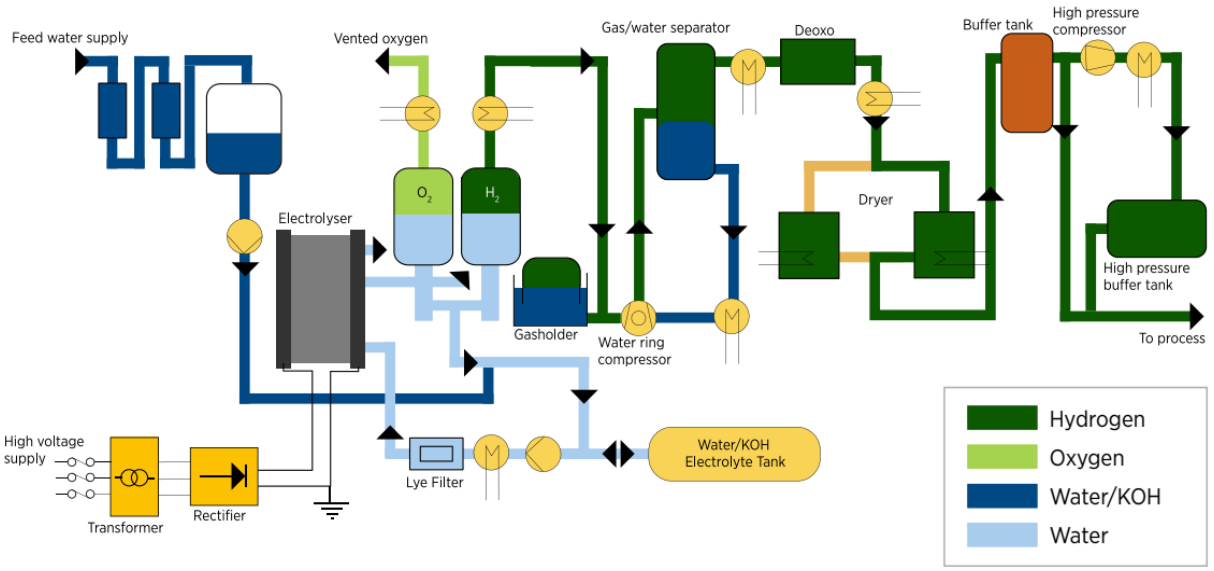


***Figure 6: System design of an alkaline electrolyzer plant [34].***

### Polymer Electrolyte Membrane Electrolysers

The PEM electrolyzers utilize a thin perfluorosulfonic acid (PFSA) membrane and an advanced electrode architecture. They achieve higher efficiencies due to reduced resistance. The PFSA membrane, known for its chemical and mechanical resilience, enables operation under high pressure differentials, reaching up to 70 bar while maintaining atmospheric pressure on the oxygen side. However, the harsh oxidative environment generated by the membrane, coupled with high voltages and oxygen evolution at the anode, necessitates materials capable of withstanding such conditions. Titanium-based materials, noble metal catalysts, and protective coatings are needed to ensure long-term stability, optimal electron conductivity, and overall cell efficiency. These requirements contribute to the higher costs associated with PEM stacks compared to alkaline electrolyzers. PEM systems are susceptible to water impurities such as iron, copper, chromium, and sodium, which can lead to calcination. While electrode areas are approaching 0.2 square meters today, future concepts focus on larger stacks with outputs of up to multiple megawatts, although their reliability and lifetime characteristics on such scales require validation [34].

In contrast to alkaline systems, PEM electrolyzers are simpler and typically require circulation pumps, heat exchangers, and pressure control and monitoring primarily at the anode (oxygen) side. At the cathode side, additional components like a gas separator, a de-oxygenation unit to eliminate residual oxygen (often unnecessary for differential pressure), a gas dryer, and a final compressor are necessary. The system design of a PEM electrolyzer plant can be seen in Figure 7 [34].

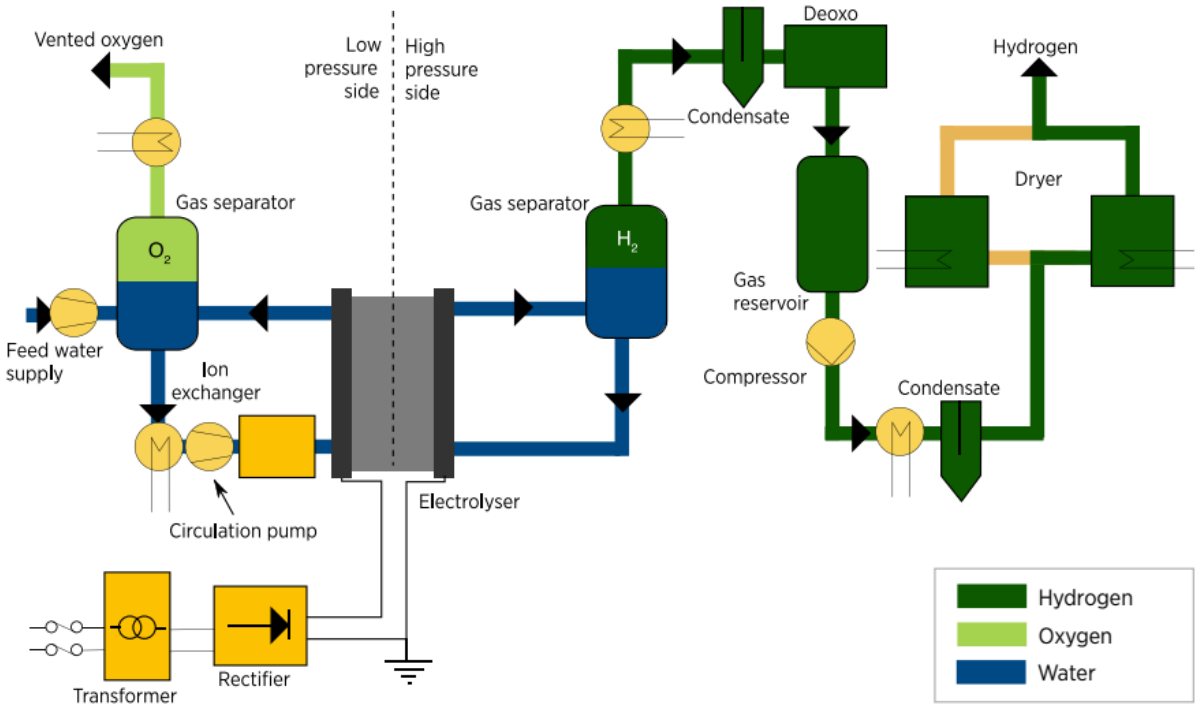


***Figure 7: System design of an polymer electrolyte membrane electrolyzer [34].***

PEM systems offer more design flexibility, including atmospheric, differential, or balanced pressure operation modes, thereby reducing costs, system complexity, and maintenance. With balanced pressure operation, the anode and cathode are operated under the same pressure level, while atmospheric pressure operation maintains a constant pressure mode. Operating under differential pressure (typically 30 bar to 70 bar) necessitates a thicker membrane for improved mechanical stability and reduced gas permeation, potentially requiring an additional catalyst to reconvert any permeated hydrogen back to water [34].

**Anion Exchange Membrane Electrolyzers**

AEM electrolyzers are the latest development in technology, and it is currently being commercialized by only a handful of companies, with deployment still limited. The potential of AEM lies in combining the less demanding environment of AEL electrolyzers with the simplicity and efficiency of PEM electrolyzers. This technology enables the use of non-noble catalysts, titanium-free components, and, like PEM, operation under differential pressure. However, AEM membranes face challenges in chemical and mechanical stability, leading to inconsistent lifetime profiles. Additionally, performance has not met expectations due to low conductivity, suboptimal electrode architectures, and slow catalyst kinetics. Efforts to enhance performance often involve adjusting membrane conductivity properties or introducing supporting electrolytes like KOH or sodium bicarbonate ($NaHCO_3$), which could compromise durability. The OH- ion conductivity is three times slower than with $H^+$ ion conductivity in PEM. This forces developers to consider thinner membranes or those with higher charge density. While AEM electrolyzers share similar system design concepts with

PEM electrolyzers, the technology's low maturity limits information related to high differential pressure operation. The typical system design is depicted in Figure 8 [34].

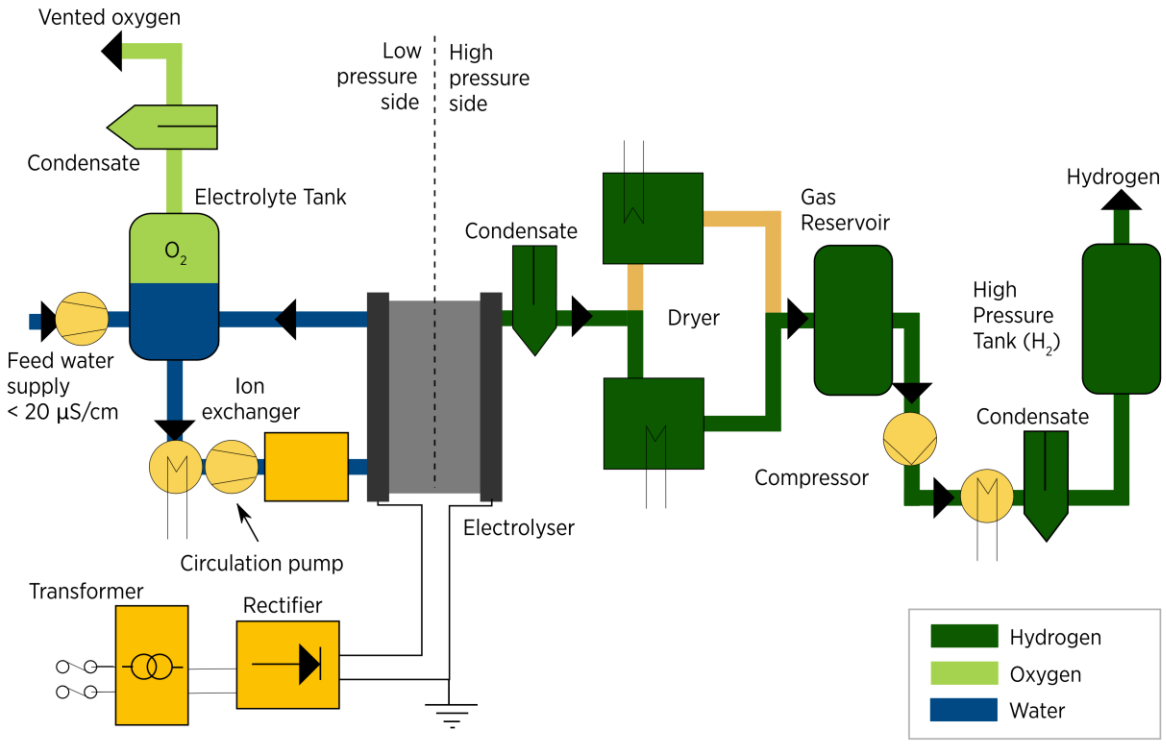


***Figure 8: Typical system design of a plant for an anion exchange membrane electrolyzer [34].***

Early-stage improvements are anticipated in mechanical membrane stability, gas purity, ability to withstand high pressure differentials, and wider power range compared to alkaline systems. However, they are still limited to a narrower power input range compared to PEM mainly attributed to the plant sizing rather than the stack itself [34].

## 3.4 Hydrogen Storage Technologies

To buffer the production and to utilize renewable energy surplus numerous storage technologies have been developed to address the challenges posed by hydrogen. In particular its low volumetric energy density under atmospheric conditions and its small molecular size. Below, an overview of hydrogen storage options is presented. Figure 9 shows volumetric and gravimetric energy densities for different hydrogen storage options [35–37]. A crucial technical differentiation lies in whether hydrogen is stored in its pure form or bound in a material [38]. In addition, with the current infrastructure, it is possible to add hydrogen in proportions of up to 20% to the natural gas grid [39], store it together and then use it to generate energy [38].

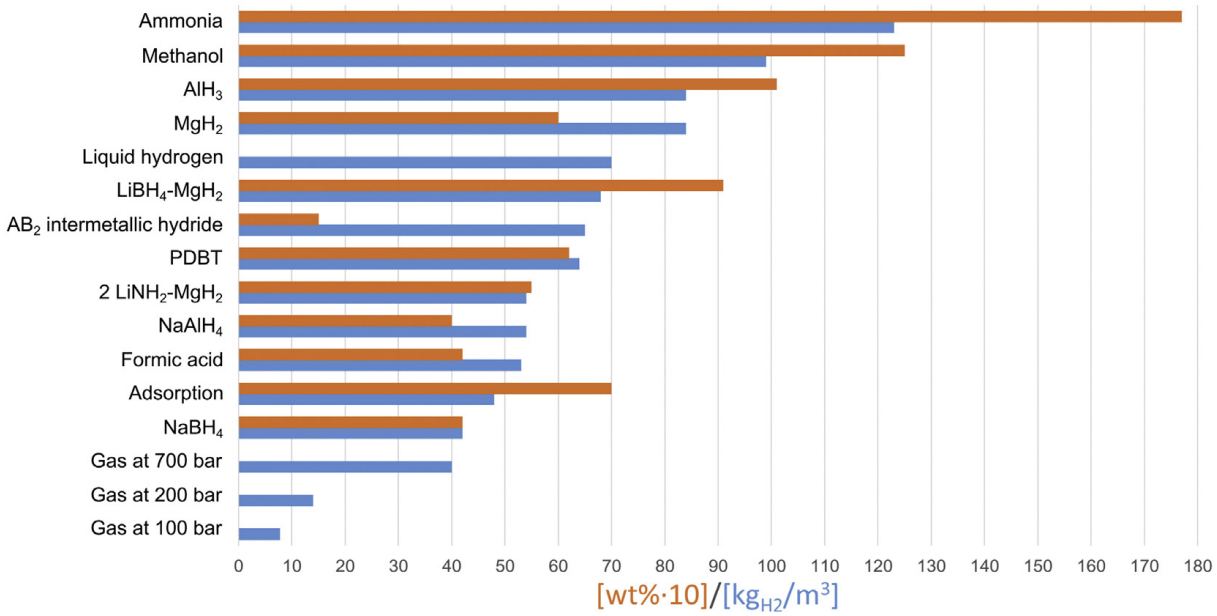


***Figure 9: Volumetric (kg/m3, in blue) and gravimetric (wt% multiplied by ten, in orange) hydrogen storage densities of considered technologies [35–37].***

### 3.4.1 Compressed hydrogen storage

Currently, pressure storage tanks are the dominant method for storing hydrogen, with pressures exceeding 700 bar achieved in certain applications, like in vehicles. Historically, a challenge in high-pressure hydrogen storage was the diffusion loss due to its small molecule size. However, advancements in materials have largely mitigated this issue. In applications such as vehicle storage, high-pressure tanks must be designed to be very pressure-stable to withstand the material stress [38].

The aboveground storage tanks are categorized into four types based on vessel design. Type I vessels are the heaviest as they are entirely made from metal, while Type II vessels feature a metal liner wrapped in composite material. Type I operates at 175–200 bar pressure, whereas Type II operates at 263–300 bar. While suitable for industrial use, both types are unsuitable for vehicles due to their weight and susceptibility to hydrogen-induced cracking [40, 41].

Type III vessels utilize a composite cylinder with a metal liner, typically aluminum, which prevents hydrogen-induced cracking. These vessels are 25%–75% lighter than Types I and II and can withstand pressures up to 450 bar, making them ideal for vehicles. However, they are costly and cannot withstand pressure cycling at 700 bar [40, 41].

Type IV vessels are the lightest, featuring a composite cylinder with a plastic liner as a hydrogen barrier. They offer durability, easy manufacturing, and a long lifetime, suitable for vehicle applications, withstanding pressures up to 1000 bar. However, the high cost, primarily attributed to carbon fiber which accounts for 75% of the vessel cost, is a drawback. Storing

hydrogen under high pressure is associated with safety concerns if it escapes from a damaged vessel [40, 41].

To achieve these pressures a significant amount of energy is needed. This energy consumption depends on the underlying thermodynamic process. The ideal process is the isothermal compression as depicted in equation (6), with $V_1$ the volume at the beginning, $p_1$ the pressure at the beginning and $p_2$ the pressure at the end of the compression. However, it cannot be realized in practice [42].

$$W_{isothermal} = p_1 \cdot V_1 \cdot \ln\left(\frac{p_2}{p_1}\right) \tag{6}$$

The adiabatic or isentropic compression is more closely describing the thermodynamic process for ideal gases. Equation (7) shows the calculation of the isentropic compression work ($W_{isen12}$), with κ representing the isentropic exponent, $V_1$ the volume at the beginning, $p_1$ the pressure at the beginning and $p_2$ the pressure at the end of the compression [42, 43].

$$W_{isen12} = \frac{\kappa}{\kappa - 1} \cdot p_1 \cdot V_1 \left[\left(\frac{p_2}{p_1}\right)^{\frac{\kappa-1}{\kappa}} - 1\right] \tag{7}$$

Furthermore, the compression work depends on the nature of the gas descried by the isentropic exponent and the specific volume at the beginning. Comparing hydrogen and methane, the five-atomic methane has a lower specific volume (V1 = 1,39m³/kg) and isentropic exponent ($\kappa$ = 1.31) whereas the diatomic hydrogen has a specific volume of V1 = 11.11 m³/kg and an isentropic exponent of $\kappa$ = 1.41, resulting in a higher compression work. The development of the needed compression work as a function of pressure, for hydrogen, helium and methane can be seen in Figure 10 [42].

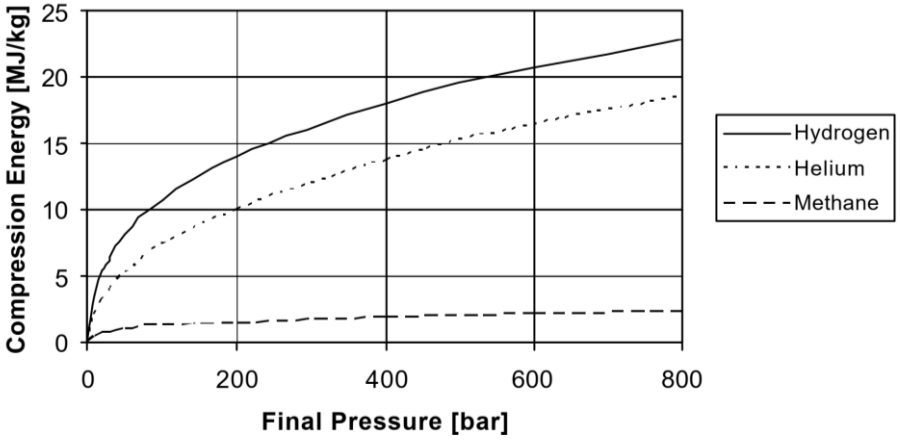


***Figure 10: Adiabatic compression work for hydrogen, helium and methane [42].***

In industrial applications multistage compressors with intercoolers are used to compress the hydrogen gas. They operate between the adiabatic and the isothermal process as can be seen

in Figure 11. A typical 5 stage compressor with a hydrogen mass flow of 1000 kg/h consumes about 7.2% of the hydrogen higher heating value when compressing it from 1 to 200 bar. For a compression to 800 bar the energy consumption rises to about 13% of the higher heating value [42].

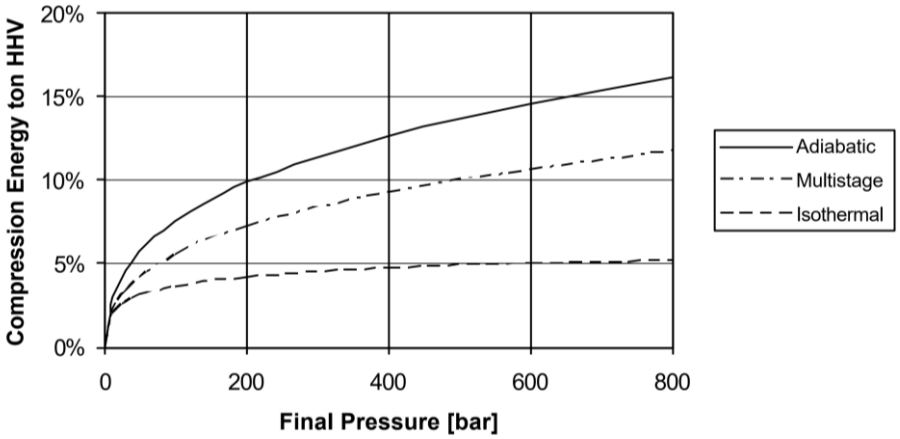


***Figure 11: Energy demand for hydrogen compression compared to its higher heating value (HHV) [42].***

Even if the generation of high pressures necessitates energy input, compressed gas storage tanks remain relatively efficient. Another viable option for storing large quantities of energy involves pressure storage in underground caverns, such as salt caverns [38]. Figure 12 shows an artificial underground storage in a salt cavern [44].

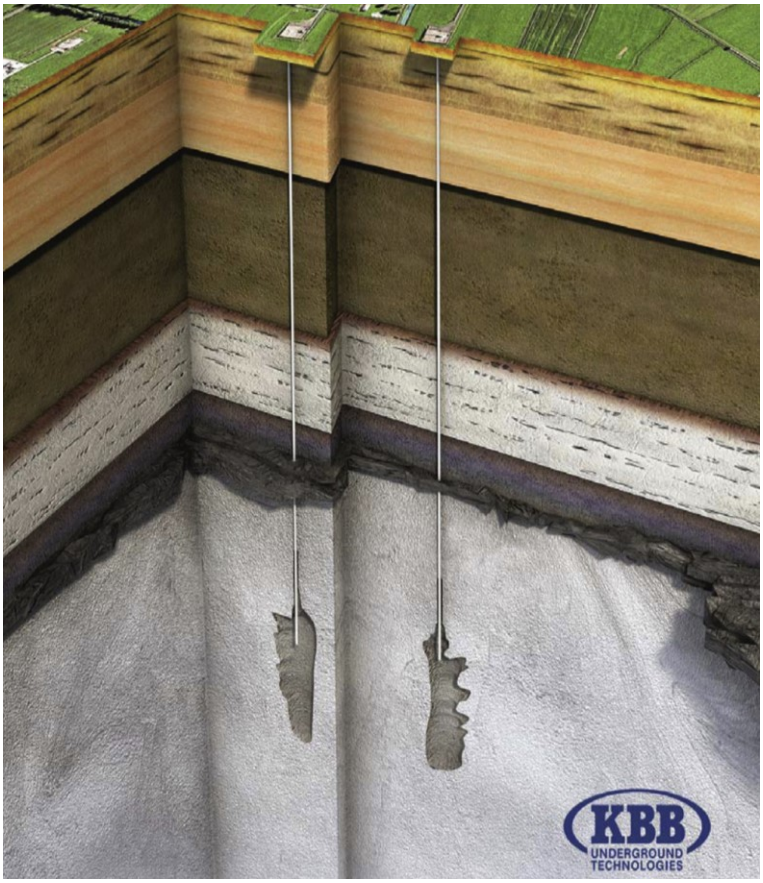


***Figure 12: Artificial underground salt cavern [44].***

Those formations, found at considerable depths offer ideal conditions for establishing high-pressure gas storage facilities. They show very high gas tightness even at elevated pressures, ensuring secure containment. With operational depths reaching nearly 2000 meters, they enable higher energy densities due to increased operational pressures within caverns. Their volumes can exceed 500000 $m^3$, allowing storage capacities of several thousand tons of hydrogen. Moreover, they occupy minimal surface land at low specific investment costs per MWh of storage. Additionally, they provide high security against manipulation and obstruction [44].

While depleted oil and gas fields, as well as aquifer formations, represent potential hydrogen storages, they pose challenges. Figure 13 shows a gas storage in a depleted oil or gas field [44].

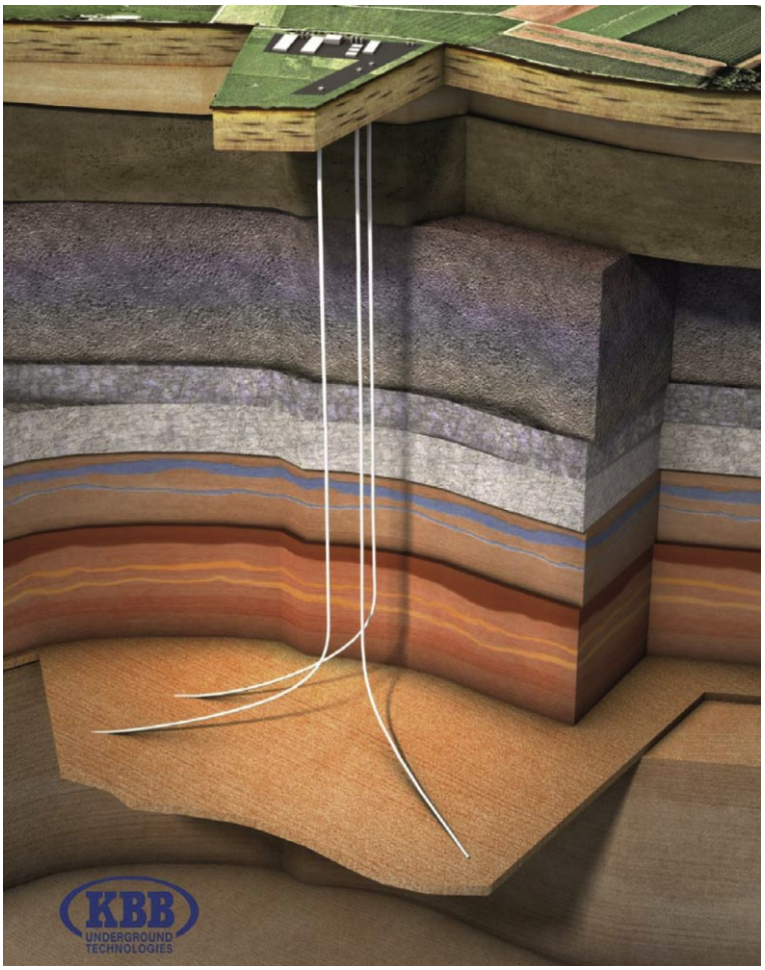


***Figure 13: Gas storage in depleted oil and gas fields [44].***

Depleted oil and gas fields may retain residual hydrocarbons, resulting in unpredictable gas compositions upon hydrogen release. This unpredictability hinders various applications. Furthermore, the reactivity of hydrogen may lead to the formation of biological or chemical byproducts, potentially clogging reservoir pores and limiting hydrogen flow during discharge. Additionally, depleted gas fields charged with hydrogen may exhibit variations in fuel quality,

presenting challenges for grid operators and consumers. Both formations also face limitations in dynamic operation due to the high-pressure drops required for gas penetration through numerous pores. Consequently, artificial salt caverns emerge as the most promising option for underground hydrogen storage due to their favorable characteristics and greater operational flexibility [44].

### 3.4.2 Liquified Hydrogen Storage

Liquefaction offers an alternative method to increase the density of pure hydrogen besides compression. This process condenses hydrogen into a liquid state, allowing for high storage densities of 70 kg/m$^3$ [8] at atmospheric pressure [35]. It is therefore primarily considered for hydrogen distribution [45].

The energy demand for hydrogen liquefaction is substantial due to two primary reasons: the extremely low boiling point of hydrogen (-253 °C) and the lack of cooling during adiabatic, isenthalpic expansion processes for temperatures above approximately -73 °C. To address this issue, precooling is required, often achieved through the evaporation of liquid nitrogen [46]. Modern hydrogen liquefaction plants require around 10 kWh$_{el}$/kg, but advancements suggest that values closer to 6 kWh$_{el}$/kg may be achievable with larger plants and process improvements [45, 47, 48] .

Despite potential reductions in energy demand, the capital costs of liquefaction plants remain a significant part (40-50%) of overall liquefaction costs, especially for new plants with an exemplary capacity of 100 tons per day [49].

Once liquefied, it is crucial to minimize evaporation to prevent ventilation losses over time. To mitigate this evaporation known as boil-off, storage vessels are designed with minimized surface-to-volume ratios, often adopting spherical shapes, and incorporate advanced insulation techniques. Commonly, liquid hydrogen storage vessels feature double walls with a high vacuum between them, effectively reducing heat transfer through conduction and convection [50].

### 3.4.3 Cryo-Compressed Hydrogen Storage

Another method of storing hydrogen in its pure form involves cryogenic storage at elevated pressures. This approach allows for relatively high energy densities without necessitating a phase change of hydrogen. Typically, storage occurs at temperatures around -223 °C and pressures equivalent to those used in pressurized gas storage. Storing cryo-compressed hydrogen is technically complex and demands significant amounts of energy for cooling and storage. Nevertheless, it offers the potential to further increase the volumetric energy content compared to other storage methods for pure hydrogen [38].

### 3.4.4 Metal Hydride Storage

Storing hydrogen in a metal hydride involves chemisorption. In this process, hydrogen diffuses into the lattice of a metal, forming a metal hydride. Since the reaction is exothermic, supplying heat to the system is necessary to release hydrogen from the metal hydride [38].

Effective thermal management is crucial for optimizing the efficiency of metal hydride storage. While these systems have the potential to achieve high volumetric storage densities for hydrogen, several technical challenges, such as cycle stability, must be addressed to realize their full potential [38].

### 3.4.5 Chemical Hydrides

Chemical hydrides similar to metal hydrides are chemically bond hydrogen. However, due to their composition of lighter elements, they exhibit fundamentally different properties. They are typically liquid at standard conditions, simplifying their transport, storage, and facilitating heat and mass transfer during hydrogenation and dehydrogenation processes. Some suggested chemical hydrides for hydrogen storage, such as methanol, ammonia, and formic acid, are already commonly synthesized bulk chemicals and the existing infrastructure for their production, handling, and transport is already in place [35].

The use of low-emission hydrogen derived from water electrolysis for the production of these bulk chemicals can be used to store hydrogen and directly reduce emissions by replacing fossil sources [35].

Methanol ($CH_3OH$) is the simplest alcohol, with gravimetric and volumetric hydrogen storage capacities of 12.5 wt. % and 99 kg/m$^3$, respectively [51].

Ammonia ($NH_3$) emerges as a promising hydrogen storage medium due to its high hydrogen storage density, 17.7 wt. % gravimetrically, and 123 kg/m$^3$ volumetrically for liquid ammonia at 10 bar. Moreover, its synthesis, handling, and transportation are well-established [52].

Formic acid ($HCO_2H$) exhibits the lowest hydrogen storage capacity, at 4.4 wt. gravimetrically and 53 kg/m$^3$ volumetrically. However, its advantage lies in the ability to undergo dehydrogenation under very mild conditions, sometimes even at room temperature [53].

### 3.4.6 Liquid Organic Hydrogen Storage

Liquid organic hydrogen storages (LOHC) are liquid compounds capable of being charged and discharged with hydrogen. Examples include N-ethylcarbazole, benzyltoluene, or dibenzyltoluene. LOHCs undergo chemical hydrogenation for charging at elevated pressures (20 to 50 bar) and temperatures (150 to 200 °C) in a hydration reactor. For discharge, they are catalytically dehydrogenated in a reactor at low pressures and high temperatures (270 to 310 °C). LOHCs offer significant advantages, especially in terms of hydrogen transport, as they are much easier to handle technically than pure hydrogen. However, energy is still required for charging and discharging, which reduces the efficiency of storage [38].

### 3.4.7 Activated Carbon

Activated carbon possesses a highly porous structure. The resulting large surface area enables the adsorptive binding of hydrogen to the carbon. This binding is primarily based on van der Waals forces, which only allows a stable hydrogen storage at low temperatures of approximately -203 °C. Therefore, appropriate cooling is necessary for hydrogen storage in activated carbon [38].

### 3.4.8 Metal Organic Framework

Metal-organic frameworks (MOF), similar to activated carbon, are highly porous materials with a large surface area (approximately 1 000 $m^2/g$), allowing for hydrogen storage through adsorption. Compared to activated carbon, the structure of MOF enables chemical optimization of the adsorption behavior. However, this form of storage also requires temperatures below -173 °C and thus appropriate cooling for stable hydrogen storage [38].

# 4 METHODOLOGY

Within this chapter a detailed description of the investigated scenarios is outlined, followed by the description of the modeling environment utilizing OEMOF and “oemof.solph”. Furthermore, an overview of the entire model including Excel files is provided, outlining the major sections and the calculation in detail. Finally, the parameters employed in the analysis are presented, along with a discussion concerning the assumptions and limitations.

## 4.1 Investigated Scenarios

Depending on the user configuration, different scenarios can be defined and investigated. This chapter displays the used scenarios and their sub scenarios within this thesis. Scenarios 1-3 investigate the supply of hydrogen via different transportation and storage options. They are calculated from literature data provided in chapter 4.5, to generate comparable values for the

discussion of the on-site production results. The sub-scenarios differentiate depending on the type of stored hydrogen and the frequency of delivery as shown in Figure 14. Scenario 1 represents liquid hydrogen transport by truck. It is divided into a sub scenario using a liquid hydrogen storage tank on-site (scenario 1 LH2) and a second sub scenario where the hydrogen is stored gaseous necessitating a reconversion before storing it (scenario 1 GH2).

Scenario 2 represents the transport by railway and is divided into six sub scenarios. The first three of these sub scenarios store the hydrogen in liquid state and are distinguished by the delivery frequency indicated by the letter F and a number (scenario 2 LH2 F1 to F3; e.g. F1 – delivery once per week). The delivery frequencies are presented together with the other parameters in chapter 4.5. The other three use the same delivery frequency but utilize a gaseous hydrogen storage on site (scenario 2 GH2 F1 to F3).

Scenario 3 represents the transport of gaseous hydrogen by pipeline without the necessity of a hydrogen storage or reconversion on site.

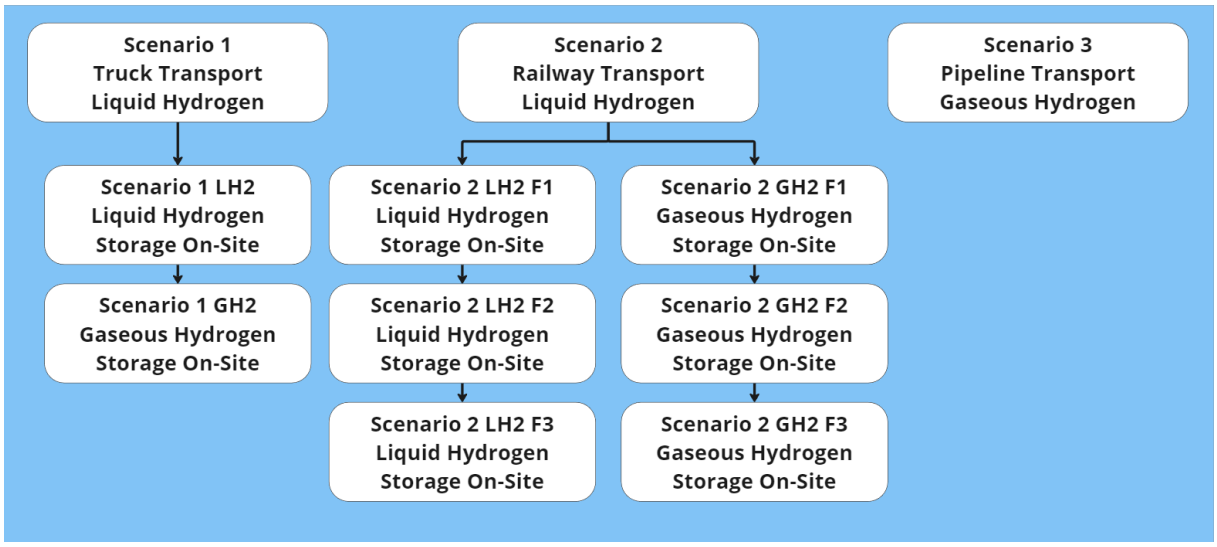


***Figure 14: Subdivision of scenarios 1-3 regarding their hydrogen state and delivery frequency.***

To carry out the calculation, parameters such as annual hydrogen demand, transport capacity, delivery distance, and frequency are assumed to calculate the specific hydrogen supply costs. These costs include the production cost of the imported hydrogen, the distribution expenses, the reconversion costs and the levelized costs of storage (LCOS). Distribution and reconversion costs are determined through extensive literature review [2, 54–56] and consultation with industrial and logistic experts. LCOS is computed for each storage option as described in chapters 4.2 and 4.3 based on the required capacity.

Scenarios 4 and 5 involve the utilization of either an AEL or PEM electrolyzer for hydrogen production. This offers decentralized production, minimizing the necessity for transportation infrastructure. Scenario 4 aims to fulfill demand without using a storage, whereas scenario 5 involves a hydrogen storage to optimize costs with respect to fluctuating electricity prices. By

configuring parameters such as pressure, storage capacity limits, production limits, and electricity price limits, the model can be tailored accordingly.

Scenario 5 is segmented into the three sub-scenarios 5.1, 5.2, and 5.3. Scenario 5.1 uses different storage capacity limits and is therefore additionally divided into three parts denoted as 5.1a, 5.1b, and 5.1c. Figure 15 shows scenario 4 and the subdivision of scenario 5.

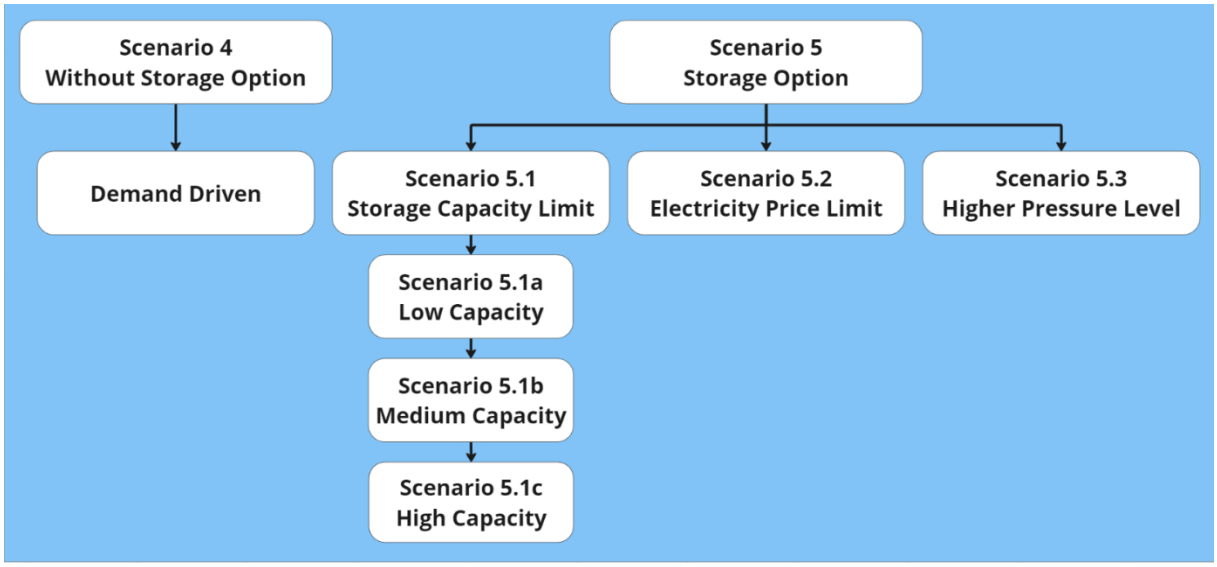


***Figure 15: Scenario 4 and the Subdivision of scenario 5 to investigate different limits and pressure levels.***

Scenario 5.1a features a storage tank with a low-capacity limit, while 5.1c uses the largest among these three. Most of the other parameters remain constant across these sub-scenarios and can be seen in chapter 4.5. Scenario 5.2 operates using an electricity price limit indicating hydrogen production only when the electricity price is under the assumed limit value. Scenario 5.3 investigates a higher pressure level while using the same storage capacity limit as 5.1c. The specific values for these parameters are also provided in chapter 4.5.

## 4.2 Modelling Environment

The model is developed using Python programming language and the Open Energy Modelling Framework (OEMOF), which is a Python toolbox designed for energy system modeling and optimization [57]. The optimization process is conducted with the package oemof.solph which is the corresponding model generator for energy system modelling and optimization [58]. Its basis is a graph structure consisting of buses and components connected by directed edges representing the flow of energy carriers and resources, their conversion and consumption. The graph holds information on the topology and relationships between the nodes, whereas solph converts this graph into an optimisation model [59]. It is implemented in Python based on the optimisation package pyomo [60]. In addition, the code is supported by several Excel spreadsheets regarding the data input, storing of data and results as well as their processing and graphical representation.

The Energy Model is generated with oemof.solph by defining an energy system object with a time range and time resolution. The energy system layout is then assembled with the mentioned nodes and edges. Nodes are the main building blocks and are divided into two types, components and buses. Buses represent a balanced grid or network without losses therefore the overall sum of inflows and outflows is zero. Edges connect these nodes and represent flows, like mass or energy flows. Figure 16 shows an example energy system with buses and the components sink, source, converter, and generic storage. The edges are indicated by the lines connecting these blocks [61].

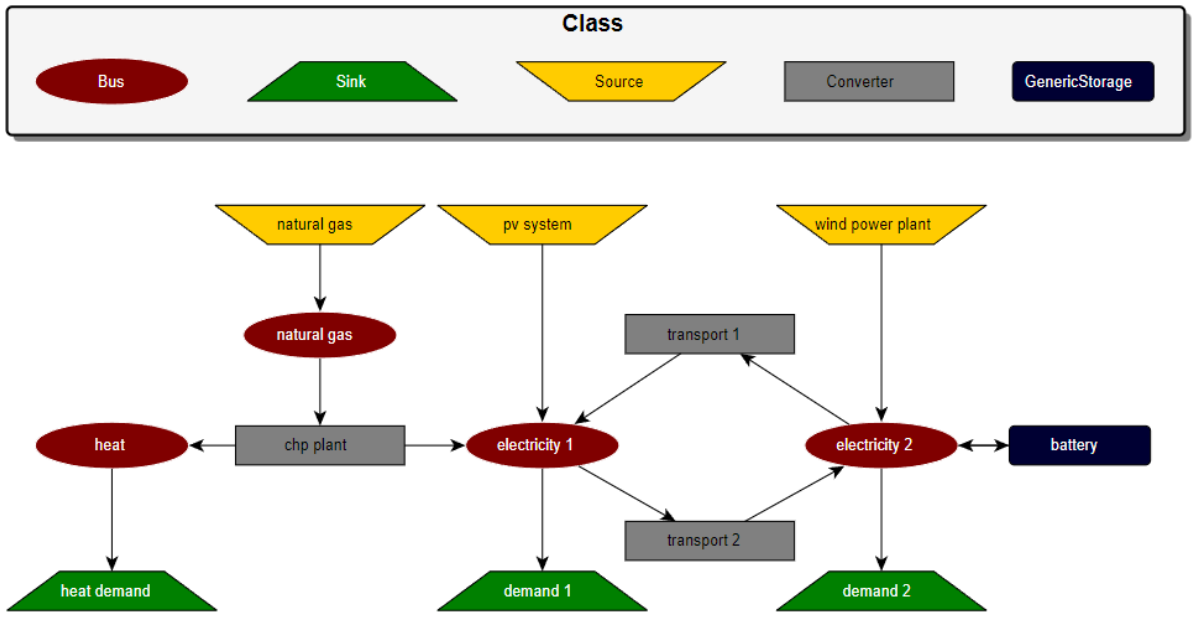


***Figure 16: Example energy system showing the nodes (blocks) and edges (lines) used in oemof.solph [61].***

Sinks are used to define the demand or can be used to detect excesses and are specified by a single nominal value or a demand series [61].

Source represents the input to the energy system like a pv-system, a wind power plant, or an import of natural gas. They can be specified by a single nominal value or a series and the corresponding variable costs. The source can be restricted by a maximum value or an annual limit like for example the total amount of full load hours [61].

Converters are nodes with multiple inputs and outputs such as a power plant, a heat pump or an electrolyzer. It is specified by an efficiency value for the transformation process which can be provided as a predefined series as well. When implementing a series the efficiency has to be constant within a timestep to get a linear transformation [61].

The generic storage is designed to take a single inflow and a single outflow and can be specified by the nominal storage capacity, the initial storage level, efficiency factors for in and outflow and a loss rate. In addition an investment object can be added and the inflows and outflows can be coupled or decoupled with the storage capacity [61]. The investment object

takes equivalent periodical costs (EPC) to find the optimal capacity of the component and to decrease cost. The EPC are typically calculated as annuities consisting of the capital expenditures (CAPEX), the lifetime and the weighted average cost of capital (WACC) according to equation (8) [61].

$$EPC = \frac{CAPEX \cdot (WACC \cdot (1 + WACC)^{lifetime})}{((1 + WACC)^{lifetime} - 1)} \tag{8}$$

The assembled model is optimized by an external mixed linear integer solver [59]. For the model developed within this thesis two solvers can be used, the COIN-OR Branch and Cut solver (CBC) [62] or the GNU Linear Programming Kit (GLPK) [63]. They can optimize for economic, environmental, technical or any other type of cost [59]. The optimization variable of the model in this thesis is minimizing of the total costs of hydrogen production according to equation (9) with $C_{H2,Scenario}$ representing the specific hydrogen supply costs for the corresponding scenario, $C_{H2}$ the specific hydrogen production costs according to equation (10), LCOS the specific storage costs according to equation (11) and LCOC the specific carbon dioxide costs according to equation (17). The auxiliary conditions are defined depending on the scenario using the the total annual amount of hydrogen ($M_{H2}$), the storage capacity limit ($S_{limit}$) and the electricity price limit ($C_{electricity,limit}$) as can be seen in equation (9).

$$Minimize: C_{H2,Scenario} = C_{H2} + LCOS + LCOC$$

$$with\ auxiliary\ conditions:$$

$$0 \leq M_{H2} \leq 73\ GWh \quad \text{(all scenarios)} \tag{9}$$

$$0.38\ GWh \leq S_{limit} \leq 3.37\ GWh \quad \text{(scenarios utilizing storage capacity limit)}$$

$$C_{electricity,limit} \leq 149\ €/MWh \quad \text{(scenarios utilizing electricity price limit)}$$

$$C_{H_2} = \frac{\sum_n C_{CAPEX}(EL,\ COM) + \sum_n i_d \cdot C_{OPEX}(EL,\ COM)}{i_d \cdot M_{H_2}} \tag{10}$$

$$LCOS = \frac{\sum_n C_{CAPEX}(ST) + \sum_n i_d \cdot C_{OPEX}(ST)}{i_d \cdot M_{H_2}} \tag{11}$$

$$i_d = \frac{1}{(1 + i)^n} \tag{12}$$

$C_{CAPEX}$(EL,ST,COM) represent the specific capital expenditures and $C_{OPEX}$(EL,ST,COM) represents the specific variable costs for electrolyzer, storage or compressor. Further, $i_d$ is the interest rate in a range of 10 years calculated according to equation (12).

## 4.3 Model Description

The model is divided into the following sections: Input parameters, optimization Energy Model, Economic Model and Results processing. Figure 17 shows an overview of the whole model including the main aspects of the calculation. The purple fields at the bottom indicate parts of the model that are realized in python code whereas the green parts represent Excel spreadsheets.

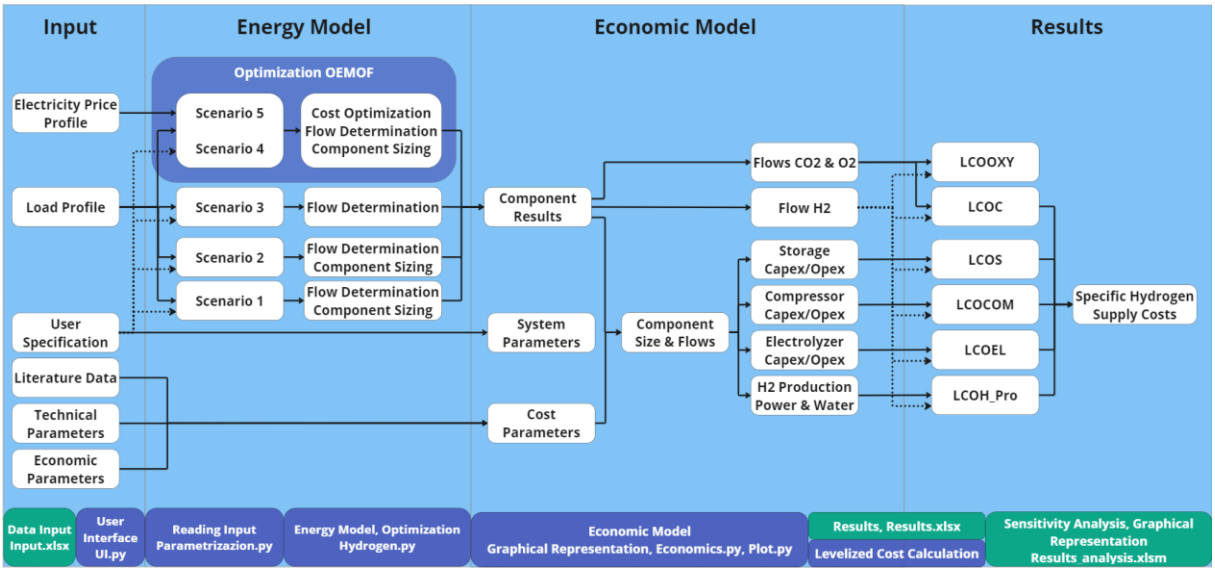


***Figure 17: Overview of the used model to calculate the specific hydrogen supply costs, consisting of the input section, the Energy Model, the Economic Model and the results section. The purple parts are realized in python code and the green represent Excel spreadsheets.***

The following chapters will provide a detailed introduction to each of this sections, starting from the input on the left towards the results on the right.

### 4.3.1 Input Section

In the input section, the user can set the electricity price profile and the load profile for the investigated year with a time resolution of one hour. The file contains the mentioned information needed to calculate the hydrogen transport costs, including hydrogen production costs, transport costs, delivery frequency, scaled storage costs, and reconversion costs, such as those for liquid hydrogen. Furthermore the economic parameters like WACC and discount rate as well as the technical parameters like lifetimes, efficiencies, pressure and substance data can be provided there. These inputs are structured within the Excel spreadsheet „Input.xlsx“ for user convenience.

When initiating the calculation process, a user interface within the Python terminal prompts the user to select a scenario and to configure the setup. Aditionally an optional help section is provided to guide the user through this process. After completing the setup the user input can

be stored in a distinct Excel file. This file can be used to restart the calculation with the same configuration or optionally a predefined default setting can be used instead.

The data from the Input section is then processed in the Energy Model in regard to the user input to determine the flows and component sizes. The Economic Model uses this information to calculate levelized costs which are further processed to the specific hydrogen supply costs.

### 4.3.2 Energy Model

The provided information from the input section is read from the Excel file “Input.xlsx” by the parameterization code and checked by an automated verfication. The user input is passed on from the user interface code to the respective sections. Following that in the precalculation phase of the “Hydrogen.py” code the EPC for the investment optimization are calculated. For scenarios 1 and 2 no Energy Model is needed and the input data is handed over to the Economic Model.

For sceanrio 3 a simple energy model is set up, as can be seen in Figure 18. The source represents the gaseous hydrogen from the pipeline which is transformed into thermal energy by the burner.

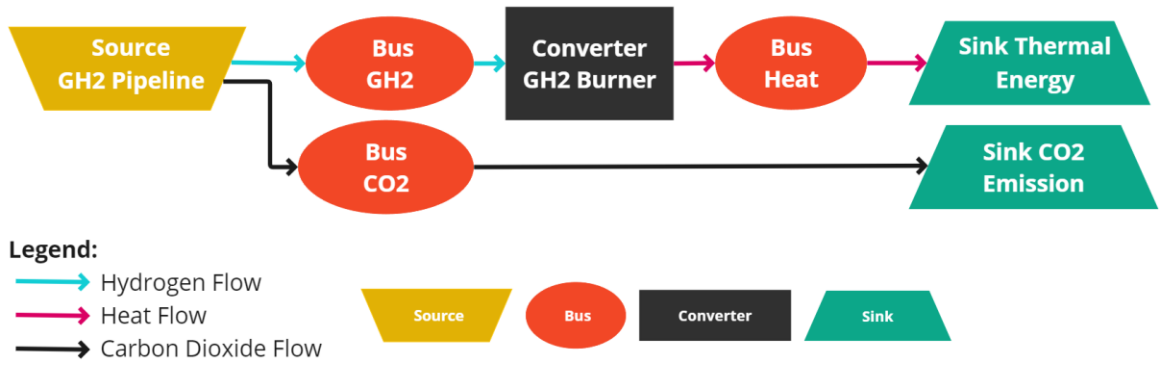


***Figure 18: Energy Model for scenario3 (Pipeline).***

The $CO_2$ emissions originate from upstream emissions related to hydrogen production and transportation. The process itself does not directly generate $CO_2$ emissions. In the context of pipeline supply, optimization is unnecessary, and the energy model is utilized to determine the flow sizes concerning the load profile. The resulting data is then forwarded to the Economic Model.

The Energy Model for scenario 4 is set up as can be seen in Figure 19 whereby the dotted line area is not included. The two source blocks represent the electrical distribution network and the public water supply. They are transformed in the electrolyzer to gaseous hydrogen and oxygen, both at 30 bar. The compressor is optional, depending on the user input. If the output pressure of the electrolyzer is sufficient for the industrial application it will not be considered

in the calculation. Otherwise the hydrogen gas is compressed using electrical energy and is further labeled as compressed hydrogen gas (CGH2). Finally it is transformed into heat at the burner. The $CO_2$ emissions originate from upstream emissions related to the electrical energy production and water production. The energy model is then forwarded to the solver and is cost optimized in regard to the EPC from the precalculation. The resulting flows and component sizes are then passed on to the Economic Model.

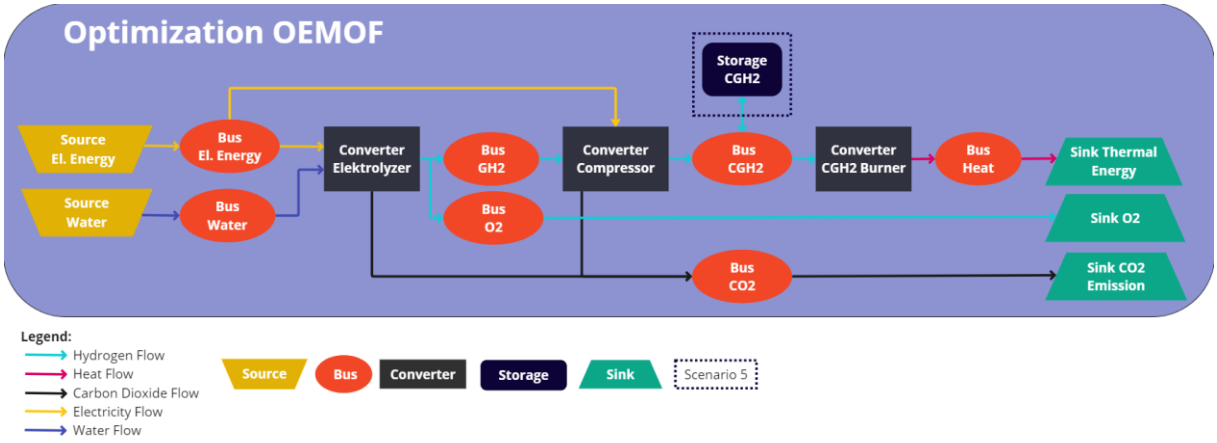


***Figure 19: Energy Model for scenario 4 and 5, the dotted line indicates the additional storage for scenario 5.***

Scenario 5 uses the same layout as scenario 4 but in addition a storage tank is added. Depending on user input, the tank can be filled with hydrogen at elevated pressures. Due to the significant energy consumption associated with liquefaction, only gaseous storage is taken into account. The storage tank is positioned on the industrial site, and while higher energy densities achieved through compression or cooling may reduce the volume of the storage tank, they will cause additional costs.

Scenario 5 is the most demanding situation for the solver, as it strongly depends on the input data and user-defined setup to converge. The behavior of the storage tank can be altered by a maximum storage capacity, the inflow and outflow conversion factors and the loss rate. The electrolyzer size or power can be adjusted by restricting the inflow into the storage tank. Additionally, an electricity price limit can be set to stop hydrogen production when exceeding it. These configurations define the boundaries within the solver computes a cost-optimal operational strategy to meet the demand. The component sizes and flows for the Economic Model are determined by optimizing costs using the electricity price profile, the variable costs and the EPC.

### 4.3.3 Economic Model

The Economic Model receives three sets of information as input, as illustrated in Figure 20. Firstly, the cost parameters provided by the input section of the program. Secondly, the

system parameters defined by the user through the user interface. Thirdly, the results of the Energy Model, like mass flows and component sizes.

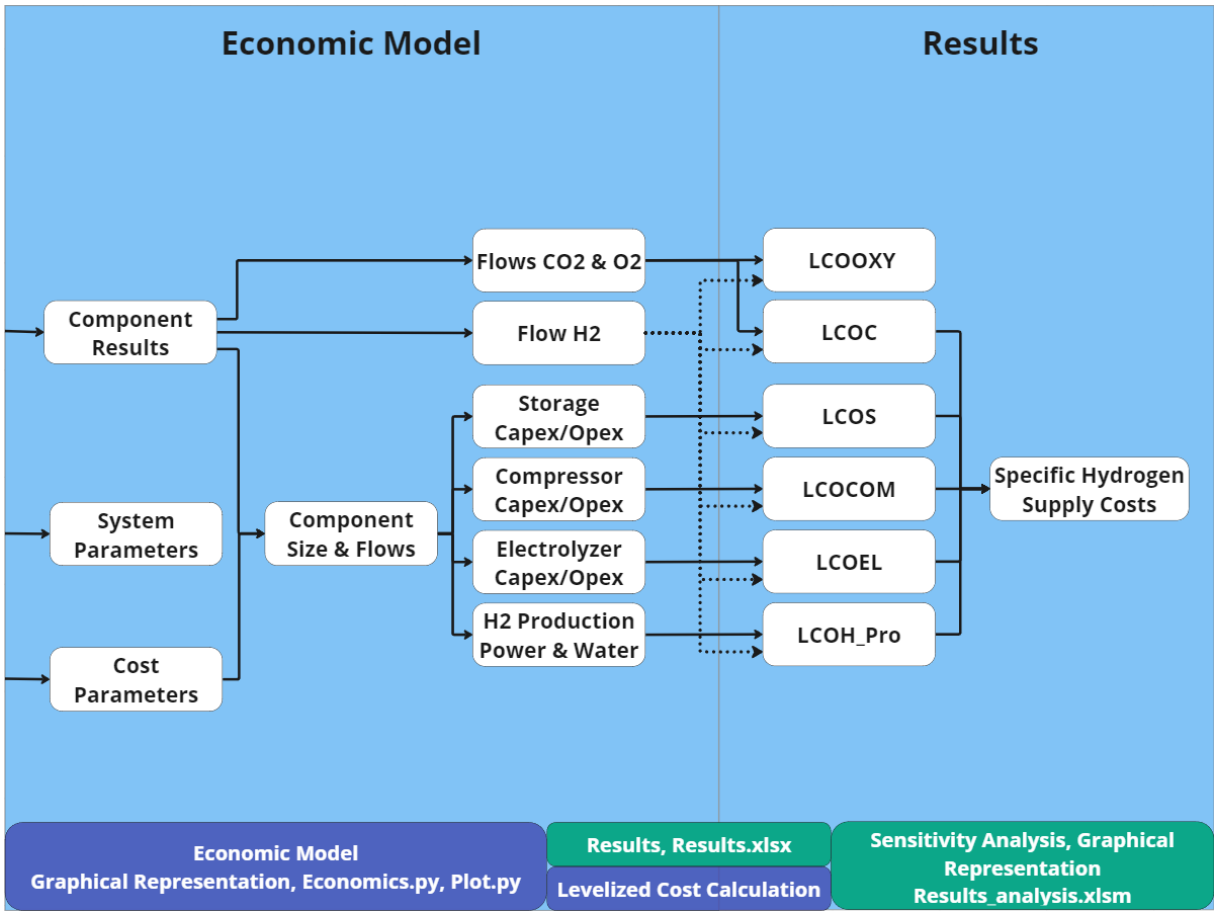


***Figure 20: Detail view of Figure 17 Economic Model and its linking points to the other program sections.***

From this data, the CAPEX and operation and maintenance expenditures (OPEX) for each component are computed based on their size and operation. The storage costs are scaled from literature data according to equation (13) [64, 65].

$$C_b = C_a \left(\frac{S_b}{S_a}\right)^f \tag{13}$$

$C_a$ represents the reference implementation from literature [64] with the corresponding storage capacity $S_a$. $C_b$ are the costs for the required storage with the corresponding capacity $S_b$. The scale factor f amounts to f = 0,6 for chemical applications or in this case liquid hydrogen storage and f = 0,3 for pressurized tanks or in this case gaseous hydrogen storage [65].

The variable costs for water and electricity are calculated separately to determine the costs of the produced hydrogen. Additionally, the carbon dioxide flow is evaluated and priced according to the $CO_2$ certificate costs [66], while the oxygen flow is priced based on its value as a technical gas for applications like oxyfuel combustion [67]. These costs are levelized to a reference value, which in this case is the total hydrogen demand. The concrete values can be

seen in section 4.5. The resulting levelized costs reflect the cost contributions for each component and for the energy and water input. They can be utilized to identify the primary cost driver behind the selected supply route. They are labeled as levelized costs of storage (LCOS), levelized costs of the electrolyzer (LCOEL), levelized costs of the compressor (LCOCOM), levelized cost of hydrogen production (LCOH_Pro) and levelized costs of carbon dioxide (LCOC). They are calculated according to equation (11) and (14) to (17). Finally, based on user input, the specific hydrogen supply costs are computed as the sum of the levelized costs. This value is used as a benchmark for comparing with other supply options for the industrial site.

$$LCEl = \frac{\sum_n C_{CAPEX}(EL) + \sum_n i_d \cdot C_{OPEX,O\&M}(EL)}{i_d \cdot M_{H_2}} \tag{14}$$

$$LCCOM = \frac{\sum_n C_{CAPEX}(COM) + \sum_n i_d \cdot C_{OPEX,O\&M}(COM)}{i_d \cdot M_{H_2}} \tag{15}$$

$$LCOH\_Pro = \frac{\sum_n C_{electricity}(EL, COM) + C_{water}(EL)}{M_{H_2}} \tag{16}$$

$$LCOC = \frac{\sum_n C_{CO2}(EL, COM)}{M_{H_2}} \tag{17}$$

$C_{CAPEX}$(EL,ST,COM) represents the specific capital expenditures and $C_{OPEX,O\&M}$(EL,ST,COM) represents the specific operation and maintenance costs for electrolyzer, storage or compressor. $C_{electricity}$ and $C_{water}$ represent the specific variable costs for electricity and water. $C_{CO2}$ represents the $CO_2$ certificate costs caused by electricity production based on the European energy mix [66, 68]. Further, $i_d$ is the interest rate in a range of 10 years and $M_{H2}$ is the total annual amount of hydrogen.

## 4.4 Result Processing

The Energy Model and Economic Model results, along with their corresponding data, are stored in an Excel spreadsheet called "Results.xlsx" as can be seen in Figure 20. This documentation includes the entire process, not just the final results, providing a detailed database for the sensitivity analysis. To improve calculation time and prevent data loss, the sensitivity analysis is decoupled from both the calculation process in Python and the “Results.xlsx” Excel spreadsheet. This is implemented by using an Excel Macro which extracts the stored results, transferring them to the sensitivity analysis file “Results_analysis.xlsm”. Moreover, an automated verification procedure checks the result plausibility, detecting potential calculation errors or configuration issues. The analysis spreadsheet can contain multiple scenario calculations for comparative purposes.

The graphical representations of the operational strategies for all components are displayed within the Excel analysis spreadsheet, allowing hourly resolution analysis. Additionally, key performance indicators (KPI) for the electrolyzer are computed. Those factors are operating hours, full load hours, part load hours and load shifts. Full load hours and load shifts are tracked due to their supposed influence on the lifespan of the electrolyzer [34]. The operating hours, part load hours, and full load hours are determined by analyzing the inflows and outflows of the electrolyzer as provided by the Energy Model. Load shifts from 0 to at least 90% load are calculated by examining the gradient in electrical energy inflow between two consecutive time steps.

To assess the operational strategy, the operation of the electrolyzer and storage are investigated, taking into account the electricity price limit. When the electricity price exceeds this limit, but hydrogen production is still necessary to meet demand or charge the storage tank the process is not cost-optimal. A KPI tracks the hours of production at high prices throughout the year to compare different settings and scenarios. This is implemented by an automated analysis examining electrical inflows alongside the electricity price profile. In Figure 21 an example is shown. The red box highlights instances where the electrolyzer operates at prices exceeding the limit.

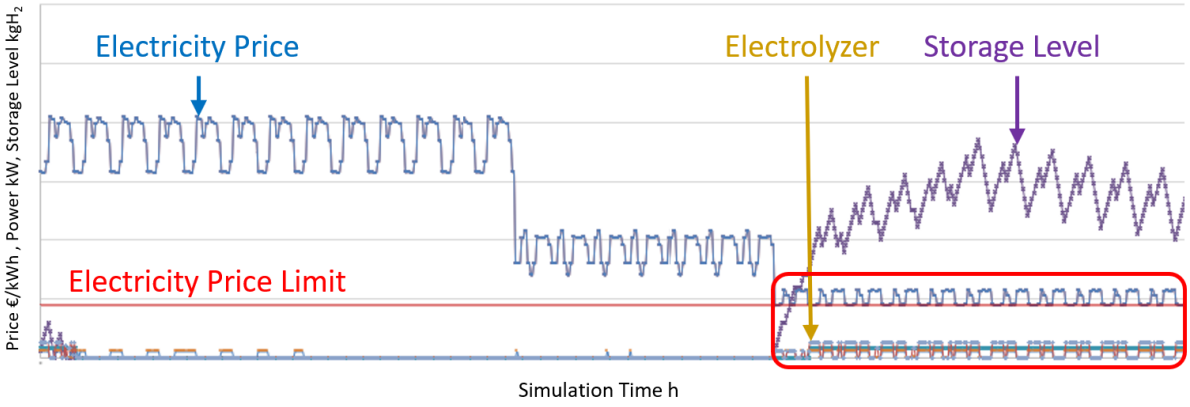


***Figure 21: Exemplary evaluation of the electrolyzer KPI, red box indicates production hours at electricity prices exceeding the electricity price limit.***

If the capacity limit of the storage tank is reached, the electrolyzer may need to reduce production during periods of low electricity prices which is not cost optimal. This situation is analyzed by another KPI that tracks the hours of low electricity prices with a full storage tank. The automated calculation involves analyzing the storage level provided by the Energy Model in conjunction with the electricity price profile and is implemented in the Excel analysis spreadsheet. In Figure 22 an example is shown. The KPI counts the hours when the storage level represented by the jagged purple line hits the storage level limit represented by the solid purple line.

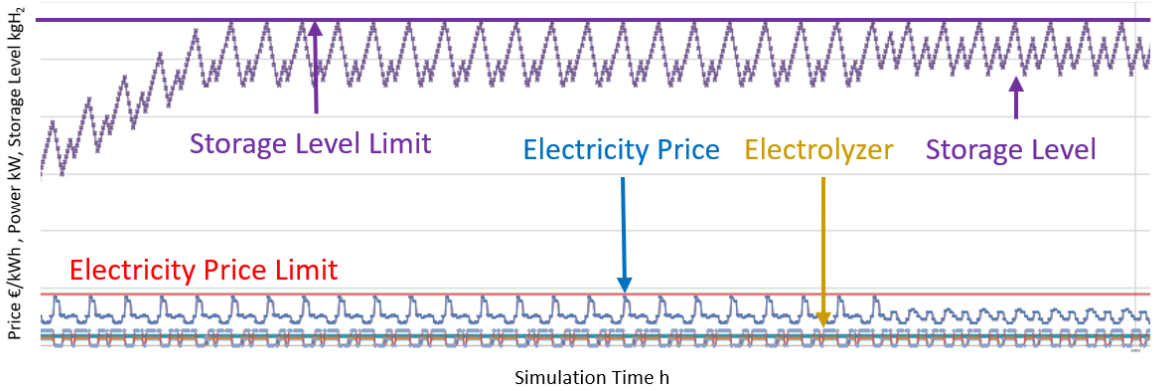


***Figure 22: Exemplary evaluation of the hydrogen storage KPI, the electricity prices are below the electricity price limit, but the storage capacity limit is reached at several points.***

Parallel to the analysis in the Excel spreadsheet a new scenario calculation can be carried out through the Python model without interfering with the current sensitivity analysis. If a new set of results is available, the user can save the current analysis and refresh the data by starting the import Macro again. When working within the "Results.xlsx" instead of the "Results_analysis.xlsm", the calculation carried out in the python code tries to write data into the "Results .xlsx" file while it is opened. This will lead to a writing permission error and full data loss.

## 4.5 Model Parameters

This chapter presents the used technical and economic parameters and discusses the underlying assumptions and limitations of the model.

### 4.5.1 Technical Parameters

The used load profile is one of the main technical parameters and is characterised within this thesis by a constant load of a continuous industrial process with a downtime in the first quarter of the year due to a maintenance period. It is representing a burner with 10 000 kW power as depicted in Figure 23. The burner is inactive during a period of approximately 1400 h. There is only one burner taken into account therefore the total hydrogen demand falls to zero during the maintenance period. The first 24 h of the calculation start with an active burner to initialize the calculation with positive values and due to further numerical reasons.

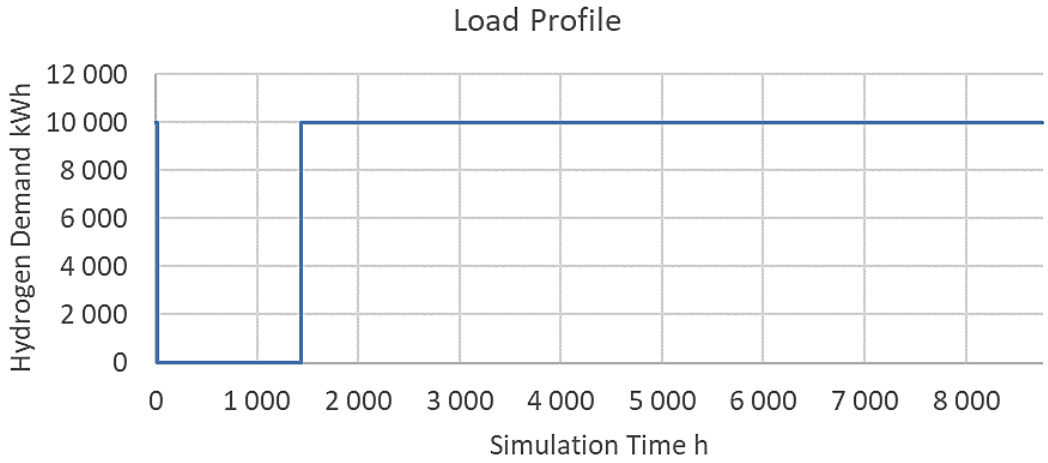


***Figure 23: Load profile for the representative industrial site.***

Table 2 displays the technical parameters utilized in the computation of the previously discussed calculations.

The electrolyzer lifetimes are approximated as a compromise between AEL systems, which lasts up to 30 years, and PEMEL systems, with lifetimes exceeding 10 years [34]. Their operation is estimated with 5000h per year. The efficiency of the electrolyzer systems is derived from a mean value of literature data, resulting in 62% for both technologies [55, 65]. Not mentioned efficiencies are calculated ideal.

The lower limit of the storage pressure is set to the typical output pressure of a PEMEL [34]. While the upper pressure limit is technically feasible at approximately 1000bar, although for industrial application, pressures around 300 bar are recommended [40, 41].

***Table 2: Technical parameters used in the calculation.***

| Parameter | Unit | Value | Reference |
|---|---|---|---|
| Heat Demand | kW | 10000 | |
| $CO_2$ Emission Intensity | $kg_{CO2}/kWh_{H2}$ | 0.188 | [68] |
| Lifetime Storage | Years | 10 | |
| Lifetime Electrolyzer | Years | 10 | |
| Lifetime Compressor | Years | 10 | |
| Efficiency Burner | % | 100 | |
| Efficiency Storage | % | 100 | |
| Efficiency Electrolyzer | % | 62 | [55, 65] |
| Efficiency Compressor | % | 100 | |

| | | | |
|---|---|---|---|
| Storage Pressure | bar | 30-1 000 | [34] |
| Water Consumption | $kg_{H2O}/kg_{H2}$ | 8.9360 | [69] |

The compression work ($W_{isen12}$) for compressing the gaseous hydrogen is calculated as an isentropic compression at constant efficiency according to equation (10).

The water consumption $m_{H2O}$ is calculated according to equation (18) to (21) with a hydrogen molar mass of 2.016 g/mol ($m_{H2}$), an oxygen molar mass of 31.998 g/mol ($m_{O2}$) [69].

$$H_2O_{(l)} \rightarrow H_{2\,(g)} + \frac{1}{2}\,O_{2\,(g)} \tag{18}$$

$$\frac{m_{O2}}{m_{H2}} = \frac{n_{O2} \cdot M_{O2}}{n_{H2} \cdot M_{H2}} = \frac{1\,mol \cdot 31.998\,\frac{g}{mol}}{2\,mol \cdot 2.016\frac{g}{mol}} = 7.936 \tag{19}$$

$$m_{H2O} = m_{H2} + m_O = m_{H2} \cdot (1 + 7.936) \tag{20}$$

$$\frac{m_{H2O}}{m_{H2}} = 8.936\,\frac{kg_{H2O}}{kg_{H2}} \tag{21}$$

### 4.5.2 Economic Parameters

The used electricity price profile is depicted in Figure 24. It represents fluctuating electricity prices on an hourly resolution and was created with the "Low-carbon Expansion Generation Optimization model" [70, 71]. The electricity price limit is set by defining 5000 cost-effective operating hours of the electrolyser. It was determined by sorting the electricity prices in ascending order and using the 5 001$^{st}$ value of this profile. The horizontal black line in Figure 24 indicates this limit.


***Figure 24: Used electricity price profile [70, 71], the black line indicates the electricity price limit of 0,149 €/kWh.***

Table 3 shows the utilized economic parameters to calculate the levelized costs for each scenario. A description of the parameters is provided below.

The water costs are estimated based on current Austrian tap water prices in Upper Austria and Tyrol [72, 73]. It is used to calculate the variable costs caused by water in scenarios 4 and 5.

The hydrogen production costs for truck, railway and pipeline transport represent the mean value of the mentioned extensive literature review representing import from different production countries. The hydrogen is transported either with maritime vessels, in liquid state, as ammonia or within LOHC, or gaseous via pipeline to the distribution hub in Austria [4, 74].

Transportation costs for transporting hydrogen from the distribution hub to the industrial site, depend on the delivery frequency which correlates with the number of vessels and their respective capacities. In case of truck transport the costs are provided for a single truck with a capacity of 124 MWh of liquid hydrogen [55, 75]. The delivery frequency is Monday to Friday including the amount needed for the weekend.

For transport by railway a tank waggon with a capacity of 257 MWh of liquid hydrogen is considered [55]. The delivery can occur on a weekly basis (F1), every two weeks (F2) or every three weeks (F3) which affects the number of waggons per train. The costs contain the rental costs for the waggons and the hauling engine and for the transport of the liquid hydrogen [76].

The pipeline costs represent a repurposed natural gas pipeline with a capacity of 3020 MWh per day and a transport distance of 100 km to the supply point [55, 75]. The costs are estimated by a mean value from literature data [54–56]. The uncertainty is high due to the influence of transport distance and amount of transported hydrogen. They lie within a range of 0.0002 to 0.0049 €/kg/km [54–56]. The conversion was carried out with an average exchange rate of 0.893 €/USD [77]. Figure 25 shows this influence on distribution costs for pipelines with two different transport capacities compared to the truck transport [55].

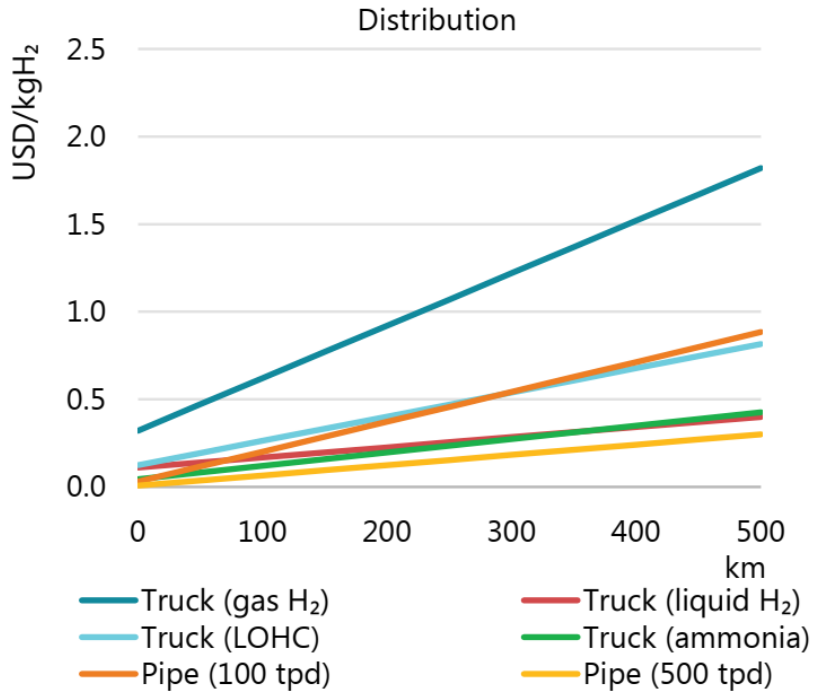


***Figure 25: Cost of hydrogen distribution to a large centralized facility [55].***

The size of the hydrogen storage depends on the delivery frequency and the state of the hydrogen. It is scaled based on a hydrogen storage tank with 5 000 000 $kg_{H2}$ capacity and capital expenditures of 325.09 €/$kg_{GH2}$ or 811.83 €/$kg_{LH2}$ [64]. Equation (22) demonstrates the scaling using the example of the value "Capital Expenditures Storage Gaseous $H_2$ F1" denoted as CAPEX $H_2$ F1. The delivery occurs every week, with a needed storage capacity of 1.8 GWh or respectively 54 508 $kg_{GH2}$ and a scaling factor of 0.3 for gaseous hydrogen.

$$\text{CAPEX } H_2 \text{ F1} = 325.09 \frac{€}{kg_{GH2}} \left( \frac{54\,508\ kg_{GH2}}{5\,000\,000\ kg_{GH2}} \right)^{0.3} = 83.8 \frac{€}{kg_{GH2}} \tag{22}$$

To carry out the calculation for the exemplary industrial site the storage capacities are set to 54 508,3 $kg_{H2}$ for F1, 101 229,7 $kg_{H2}$ for F2 and 155 738 $kg_{H2}$ for F3, in accordance with the delivery frequencies and vessel capacities. The capacity for truck delivery amounts to 11 301 $kg_{H2}$ and is needed to buffer the hydrogen throughout the week. Optionally, the model can scale the cost parameters automatically when a different storage capacity is considered.

The storage capacities for the scenarios 4 and 5 are set equal to the scenarios 1 and 2 to enable a direct comparison as can be seen in Table 5.

The operational expenditures for operation and maintenance amount to 2% of the scaled capital expenditures [64, 78].

***Table 3: Economical parameters used in the calculation.***

| Parameter | Unit | Value | Reference |
|---|---|---|---|
| Electricity Price Limit | €/$kWh_{el}$ | 0.149 | |
| Water Costs | €/$kg_{H2O}$ | 0.00185 | [72, 73] |
| Hydrogen Production Cost Truck | €/$kg_{H2}$ | 8.35 | [4, 74] |
| Hydrogen Production Cost Railway | €/$kg_{H2}$ | 8.35 | [4, 74] |
| Hydrogen Production Cost Pipeline | €/$kg_{H2}$ | 8.35 | [4, 74] |
| $CO_2$ Certificate Costs | €/$t_{CO2}$ | 55 | [66] |
| Oxygen Costs | €/$kg_{O2}$ | 0.08 | [67] |
| Hydrogen Transport Cost Truck | €/$kg_{H2}$ | 0.18 | [55] |
| Hydrogen Transport Cost Railway F1 | €/$kg_{H2}$ | 0.03 | [76] |
| Hydrogen Transport Cost Railway F2 | €/$kg_{H2}$ | 0.02 | [76] |
| Hydrogen Transport Cost Railway F3 | €/$kg_{H2}$ | 0.01 | [76] |
| Hydrogen Transport Cost Pipeline | €/$kg_{H2}$ | 0.16 | [55] |
| Capital Expenditures Storage Gaseous $H_2$ | €/$kg_{H2}$ | 325.09 | [64] |
| Capital Expenditures Storage Liquid $H_2$ | €/$kg_{H2}$ | 811.83 | [64] |
| Capital Expenditures Storage Gaseous $H_2$ F1 | €/$kg_{H2}$ | 83.8 | [64] |
| Capital Expenditures Storage Gaseous $H_2$ F2 | €/$kg_{H2}$ | 100.9 | [64] |
| Capital Expenditures Storage Gaseous $H_2$ F3 | €/$kg_{H2}$ | 114.82 | [64] |
| Capital Expenditures Storage Liquid $H_2$ F1 | €/$kg_{H2}$ | 53.95 | [64] |
| Capital Expenditures Storage Liquid $H_2$ F2 | €/$kg_{H2}$ | 78.21 | [64] |
| Capital Expenditures Storage Liquid $H_2$ F3 | €/$kg_{H2}$ | 101.28 | [64] |
| Capital Expenditures PEMEL | €/$kWh_{el}$ | 519.16 | [65] |
| Capital Expenditures AEL | €/$kWh_{el}$ | 718.88 | [65] |
| Operational Expenditures Storage Gaseous $H_2$ | €/$kg_{H2}$ | 6.5 | [64] |
| Operational Expenditures Storage Liquid $H_2$ | €/$kg_{H2}$ | 16.24 | [64] |

| | | | |
|---|---|---|---|
| Operational Expenditures Storage Gaseous $H_2$ F1 | €/$kg_{H2}$ | 1.68 | [64] |
| Operational Expenditures Storage Gaseous $H_2$ F2 | €/$kg_{H2}$ | 2.02 | [64] |
| Operational Expenditures Storage Gaseous $H_2$ F3 | €/$kg_{H2}$ | 2.3 | [64] |
| Operational Expenditures Storage Liquid $H_2$ F1 | €/$kg_{H2}$ | 1.08 | [64] |
| Operational Expenditures Storage Liquid $H_2$ F2 | €/$kg_{H2}$ | 1.56 | [64] |
| Operational Expenditures Storage Liquid $H_2$ F3 | €/$kg_{H2}$ | 2.03 | [64] |
| Operational Expenditures PEMEL | €/$kg_{H2}$ | 7.79 | [65] |
| Operational Expenditures AEL | €/$kg_{H2}$ | 10.78 | [65] |
| Liquefaction Costs | €/$kg_{H2}$ | 1.47 | [4] |
| Regasification Costs | €/$kg_{H2}$ | 0.33 | [4] |
| WACC | % | 5 | |

Depending on the state of the delivered hydrogen and the type of hydrogen storage on the industrial site costs for liquefaction or regasification have to be considered [4].

### 4.5.3 Scenario Parameters

This chapter presents scenario specific parameters that are used to calculate the results within this thesis. To facilitate the tracing of calculations especially when it comes to the sensitivity analysis, identifiers are established due to multiple parameter options within the same scenario. Table 4 shows the used storage capacity mentioned before and the corresponding identifiers for scenarios 1-3.

***Table 4: Specific parameters for scenarios 1-3 as mentioned in chapter 4.1.***

| Scenario | Storage Capacity | Identifier |
|---|---|---|
| | $kg_{H2}$ | |
| Scenario 1 LH2 | 11301.0 | ft |
| Scenario 1 GH2 | 11301.0 | fu |
| Scenario 2 LH2 F1 | 54508.0 | fv |
| Scenario 2 LH2 F2 | 101229.7 | fw |
| Scenario 2 LH2 F3 | 155738.0 | fx |
| Scenario 2 GH2 F1 | 54508.0 | fy |
| Scenario 2 GH2 F2 | 101229.7 | fz |
| Scenario 2 GH2 F3 | 155738.0 | faa |
| Scenario 3 | 0.0 | fab |

Table 5 presents the detailed parameters for the investigated sub-scenarios mentioned in chapter 4.1. In scenario 5.3 a compressor is considered to increase the storage pressure from

30 to 200 bar. The compressor EPC are calculated according to equation (8) presented in chapter 4.2.

***Table 5: Specific parameters for scenario 4 and 5 as mentioned in chapter 4.1.***

| Scenario | Storage Pressure | EPC Storage | EPC Electrolyzer | EPC Compressor | Electricity Price Profile | Inflow Storage | Full Load Hours Min | Full Load Hours Max | Electricity Price Limit | Storage Capacity Max | Identifier |
|---|---|---|---|---|---|---|---|---|---|---|---|
| | bar | €/$kg_{H2}$ | €/kWh | €/$kg_{H2}$ | | $kg_{H2}$/h | h | h | €/kWh | $kg_{H2}$ | |
| 5.1a | 30.00 | 0.41 | 67.23 | 0.00 | default | 200 | 0 | 8 760 | n.a. | 11301 | gk |
| 5.1b | 30.00 | 0.41 | 67.23 | 0.00 | default | 200 | 0 | 8 760 | n.a. | 54508 | gm |
| 5.1c | 30.00 | 0.41 | 67.23 | 0.00 | default | 200 | 0 | 8 760 | n.a. | 101230 | gn |
| 5.2 | 30.00 | 0.41 | 67.23 | 0.00 | default | 1 000 | 0 | 8 760 | 0.149 | inf+ | go |
| 5.3 | 200.00 | 0.49 | 67.23 | 1 045.77 | default | 200 | 0 | 8 760 | n.a. | 11301 | gs |
| 4 | 30.00 | 0.41 | 67.23 | 0.00 | default | 200 | 0 | 8 760 | n.a. | n.a. | gu |

The CAPEX related to the compressor are determined by equation (23) [78] and are used to compute the compressor EPC. The compression power to scale the CAPEX of the compressor is calculated according to equation (7).

$$\mathrm{CAPEX}_{\mathrm{Compressor}} = 4948 \cdot \mathrm{P}_{\mathrm{com}}^{0.66} \tag{23}$$

The example below (equation (24) to (28)) illustrates the calculation of the compressor EPC for scenario 5.3 using a specific hydrogen volume of 11.11 $m^3/kg_{H2}$ [42].

$$P_{200} = \frac{W_{isen,5.3}}{1\,h} = \frac{\frac{1.41}{1.41-1} \cdot 10^5 Pa \cdot 11.11 \frac{m^3}{kg_{H2}} \left[ \left( \frac{200\,bar}{1\,bar} \right)^{\frac{1.41-1}{1.41}} - 1 \right]}{3.6 \cdot 10^6 \frac{J}{kWh}} = 3.8925 \frac{kW}{kg_{H2}} \tag{24}$$

$$P_{30} = \frac{W_{isen,5.3}}{1\,h} = \frac{\frac{1.41}{1.41-1} \cdot 10^5 Pa \cdot 11.11 \frac{m^3}{kg_{H2}} \left[ \left( \frac{30\,bar}{1\,bar} \right)^{\frac{1.41-1}{1.41}} - 1 \right]}{3.6 \cdot 10^6 \frac{J}{kWh}} = 1.7921 \frac{kW}{kg_{H2}} \tag{25}$$

$$\mathrm{P}_{\mathrm{com}} = \mathrm{P}_{200} - P_{30} = 2.1004 \frac{kW}{kg_{H2}} \tag{26}$$

$$\mathrm{CAPEX}_{\mathrm{Compressor,5.3}} = 4948 \cdot (2.1004)^{0.66} = 8075.15 \frac{€}{kg_{H2}} \tag{27}$$

$$EPC_{\mathrm{Compressor,5.3}} = \frac{8075.15 \frac{€}{kg_{H2}} \cdot (0.05 \cdot (1+0.05)^{10})}{((1+0.05)^{10} - 1)} = 1045.77 \frac{€}{kg_{H2}} \tag{28}$$

The increased pressure in scenario 5.3 is causing higher storage costs. This is being addressed by adapting the storage EPC with a scale factor termed "$f_{material}$". This factor is determined through a linear interpolation using literature data [79] and the found linear equation is shown in equation (29) with y representing the CAPEX of the hydrogen storage and x representing the storage pressure in bar.

$$y = 0.03183 \cdot x + 262.94 \tag{29}$$

The example below (equations (30) to (34)) shows the calculation of the storage EPC for scenario 5.3. In the other scenarios the compressor is not needed which leads to a scale factor equal to 1.

$$\mathrm{CAPEX}_{Storage,200} = 0.3183 \frac{€}{\mathrm{kg_{H2}\ bar}} \cdot 200\ \mathrm{bar} + 262.94 \frac{€}{\mathrm{kg_{H2}}} = 326.6 \frac{€}{\mathrm{kg_{H2}}} \tag{30}$$

$$\mathrm{CAPEX}_{Storage,30} = 0.3183 \frac{€}{\mathrm{kg_{H2}\ bar}} \cdot 30\ \mathrm{bar} + 262.94 \frac{€}{\mathrm{kg_{H2}}} = 272.489 \frac{€}{\mathrm{kg_{H2}}} \tag{31}$$

$$\mathrm{f_{material}} = \frac{326.6\ \frac{€}{\mathrm{kg_{H2}}}}{272.489\ \frac{€}{\mathrm{kg_{H2}}}} = 1.1985 \tag{32}$$

$$\mathrm{CAPEX}_{Storage} = 325.09\ \frac{€}{\mathrm{kg_{H2}}} \cdot \left(\frac{1\ kg_{H2}}{5\ 000\ 000\ kg_{H2}}\right)^{0,3} = 3.18 \frac{€}{\mathrm{kg_{H2}}} \tag{33}$$

$$EPC_{\mathrm{Storage}} = \frac{3.18 \frac{€}{\mathrm{kg_{H2}}} \cdot (0.05 \cdot (1 + 0.05)^{10})}{((1 + 0.05)^{10} - 1)} = 0.41 \frac{€}{kg_{H2}} \tag{34}$$

$$EPC_{\mathrm{Storage,5.3}} = EPC_{\mathrm{Storage}} \cdot \mathrm{f_{material}} = 0.41 \frac{€}{kg_{H2}} \cdot 1.1985 = 0.49 \frac{€}{kg_{H2}}$$

### 4.5.4 Assumptions and Limitations

This chapter outlines the assumptions and limitations for facilitating the techno-economic analysis. It is important to consider these factors when using the software and interpreting the results. In general, the reference point for the calculation is 2030 and the annual depreciation was assumed with 5%.

**Hydrogen Delivery**

For various hydrogen delivery strategies, the industrial site relies on regional infrastructure. In this context, the industrial site is assumed to meet all necessary infrastructural requirements to receive hydrogen via truck, railway, or pipeline. The site is presumed to be interconnected with the regional railway grid, with an existing railway terminal onsite. Additionally, an established connection to a natural gas pipeline allowing the reception of hydrogen through a repurposed segment of the pipeline is available. A blending of natural gas with hydrogen is not considered. The distance between the distribution hub and the industrial consumer is assumed with 100 km.

The site utilizes hydrogen for continuous heat generation through a dedicated hydrogen burner under ideal conditions. The annual hydrogen demand amounts to 72 GWh.

**Electrolysis**

For scenarios 4 and 5, it is assumed that a constant and sufficient water supply is accessible from the public grid. The installation of a water purification plant is not considered, and the effects of water impurities on degradation are not addressed in detail. Additionally, it is presumed that there is sufficient access to electrical energy from the public power grid, particularly for operating electrolyzers with an output of several MW.

The presented calculation was carried out with an PEM electrolyzer. As mentioned before the efficiency is assumed as a mean value therefore depending on the used electrolyzer other efficiencies can be achieved. It is assumed that the industrial site is using technical oxygen for their processes. This oxygen is assumed to be delivered in liquid state by truck. The resulting levelized costs for the produced oxygen by the electrolysis represent the value of the substituted purchased oxygen. The costs for the delivery and the according carbon dioxide emissions are not considered.

**Compression and Hydrogen Storage**

The compression process is assumed to operate isentropic, although actual compressor efficiencies may vary depending on the thermodynamic process employed. Further it is assumed that the compression process uses only electrical energy. Alternative options such as direct operation with hydrogen through a hydrogen gas turbine are not considered. Furthermore, liquefaction and regasification processes are also assumed to utilize electrical energy.

Regarding hydrogen storage options, this thesis refers to an industrial consumer with a substantial energy demand necessitating a large storage volume. The possible storage pressure was limited to a few hundred bar. This is because weight and space requirement on the industrial site are assumed to be less important than costs and necessary safety measures. However, the site has no access to an underground storage like a salt cavern or a depleted gas field and there is no company near to offer this service. The considered storage technologies include only liquid and compressed gaseous storage. Moreover, compliance with regulations and safety restrictions concerning the storage of such volumes of hydrogen is presumed, and the costs for safety measures are not accounted within this thesis. There is no storage option available in in scenario 3 and 4.

**Data and Uncertainties**

Depending on the used data significant uncertainties have to be considered. The costs for the components like electrolyzers, storage tanks or compressors are estimated and scaled based

on literature review. Ongoing research and the evaluation of current and further demonstration projects adds a high uncertainty. Furthermore, the projections to the year 2030 and the assumed cost reduction caused by learning and scale effects has to be considered with a high uncertainty too.

The electricity price profile is a main aspect of this calculation and due to recent changes in electricity price levels and the increasing fluctuations caused by renewable energy sources a high uncertainty has to be considered.

The hydrogen production costs for the transport scenarios are estimated as a mean value based on literature review and lie within a range of 3.175 €/$kg_{H2}$ to 12.2 €/$kg_{H2}$ [4, 74]. The costs depend on the hydrogen import routes to the supply point therefore high uncertainty needs to be considered.

The used load profile cannot represent all industrial companies. Depending on their load profiles different operation strategies, component sizes and costs may occur.

To address these issues the model was designed to be easily adjusted according to new input data, electricity price and load profiles. Further the scenarios can be tailored individually for specific industrial consumers to evaluate hydrogen supply costs considering their limitations and assumptions.

**Software**

The entire model is designed to be easily adaptable with respect to new data inputs, and interfaces for extension are incorporated, such as the implementation of time-resolved hydrogen delivery prices or $CO_2$ prices. However, when modifying input data beyond numerical values, it is essential to also update the verification code found in “parametrization.py” accordingly.

The calculation time varies depending on the scenario and settings, typically ranging from a few minutes to approximately 30 min. Employing a finer resolution for example a 15 min resolution would significantly increase the calculation time. Furthermore, the model is not tested with a finer resolution.

The software includes a support class “Plot.py” for generating plots directly from the Python environment using matplotlib. However, it is not advisable to use it with a high resolution in simulation time. For in-depth examination of component operations, the Excel analysis tool is recommended. Additionally, when utilizing the analysis tool, enabling the use of Excel Macros is necessary for a proper function.

The model is programmed in Python 3.11 and utilizes the pandas library version 2.0.3 along with numpy version 1.25.1. The energy model is constructed using oemof version 0.5.0

together with oemof.tools version 0.4.2. The optimization tasks are performed using either the GLPK solver version 5.0 or alternatively the CBC solver version 2.10.5. The Excel spreadsheets are created with Microsoft Excel version 2402 Build 16.0.17328.20124.

# 5 RESULTS

The following section outlines the outcomes of the techno-economic analysis based on the presented methodology and performed using the presented parameters. Firstly, the outcomes of the scenarios 1-3 are presented, followed by scenario 4 and 5. A detailed investigation of the results is provided in the discussion in chapter 5.4.

All scenarios use the same load profile therefore the total annual hydrogen demand is equal. In regard of scenario 4 and 5 this corresponds to the hydrogen production amounting to 2203720.37 $kg_{H2}$ and water costs of 36431.07 €. Furthermore, this is also the case for oxygen production and the resulting LCOOXY used in the sensitivity analysis in chapter 5.4.

## 5.1 Transport Scenarios

In this section, the results for scenarios 1-3 are presented. The resulting specific hydrogen supply costs are depicted in Figure 26. The indicators represent the uncertainty of the hydrogen production prices, as discussed above. It shows that transport by pipeline is the most cost-effective option due to its simplicity and the absence of a hydrogen storage. When deliveries occur on a weekly basis, the costs for transport trough truck or railway are similar. With increasing delivery frequency, the costs rise mostly due to the needed hydrogen storage capacities. Regarding the state of the stored hydrogen, the costs for liquid storage compared to gaseous storage are nearly equal, as the influence of the hydrogen state is low at small storage capacities.

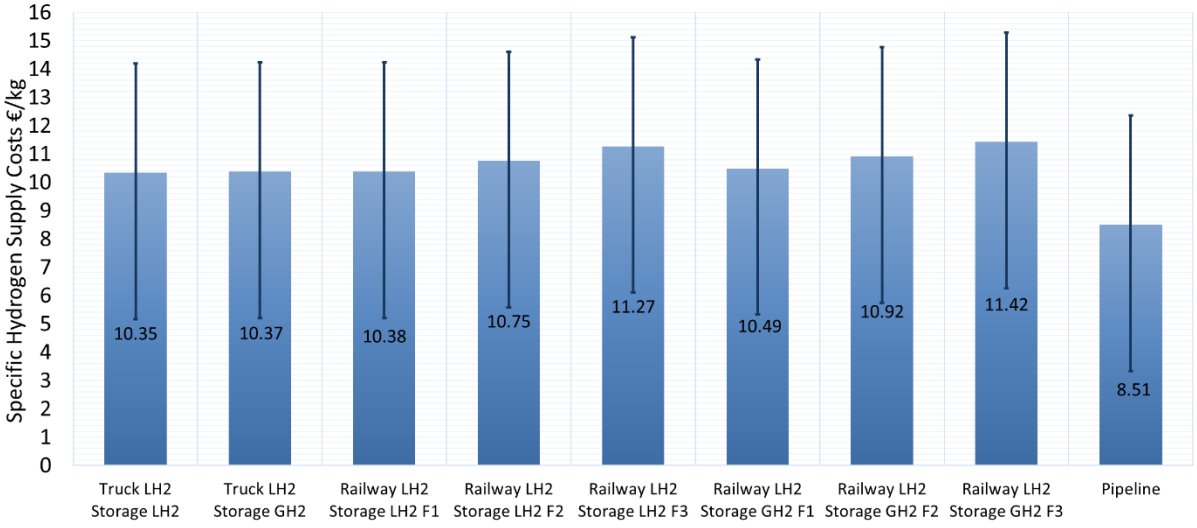


***Figure 26: Specific hydrogen supply costs for scenarios 1-3.***

## 5.2 On-Site Production Without Storage

This chapter represents the results for scenario 4. The resulting specific hydrogen supply costs and the corresponding levelized costs for the components can be seen in Figure 27. The influence of the costs for $CO_2$ emissions (red) are low due to the certificate costs. The hydrogen production is spread over the whole year necessitating a low production capacity of the electrolyzer resulting in low the costs. Therefore, the dominant cost influence are the production costs for the hydrogen mostly caused by the electricity costs. The demand driven operation strategy leads to high operating hours and low load shifts. However, the production at elevated electricity prices amounts to nearly a third of the operation time leading to a cost inefficient hydrogen production.

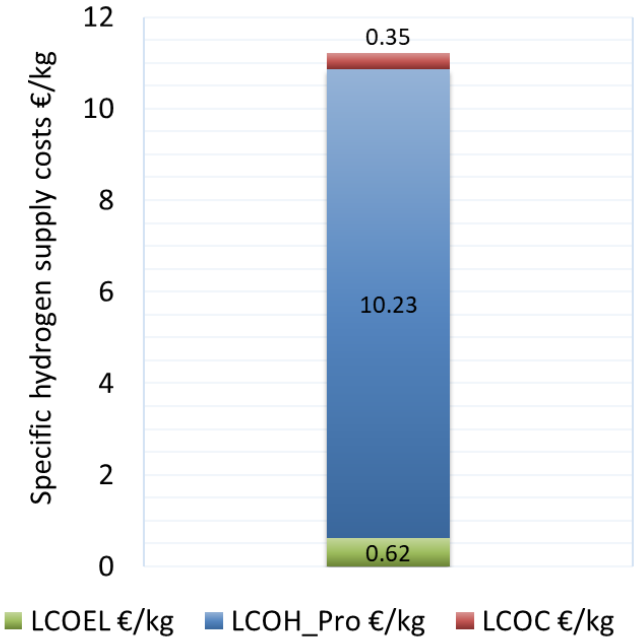


***Figure 27: Resulting specific hydrogen supply costs for Scenario 4.***

The detailed flow and component results for scenario 4 are shown in Table 6.

***Table 6: Component results for scenario 4.***

| Parameter | Unit | Value |
|---|---|---|
| **Electrolyzer** | | |
| Power | kW | 16129.03 |
| Maximum Outflow | $kg_{H2}/h$ | 300.03 |
| CAPEX | € | 8373615.6 |
| OPEX | € | 125604.23 |

| | | |
|---|---|---|
| Operating Hours | h | 7345 |
| Full Load Hours | h | 7345 |
| Part Load Hours | h | 0 |
| Load Shifts | | 3 |
| Production at High Electricity Price | % | 31.9 |
| Storage Full at Low Electricity Price | h | 0 |
| Electricity Costs | € | 22515600.4 |
| **Carbon Dioxide** | | |
| Total Annual Electricity Demand | GWh | 118.47 |
| Total Annual Emissions | $kg_{CO2}$ | 13979193.55 |

## 5.3 On-Site Production Utilizing a Storage

This chapter represents the on-site hydrogen production utilizing a hydrogen storage option. The resulting specific hydrogen supply costs and the corresponding levelized costs for the components can be seen in Figure 28. The LCOCOM amount to zero except for scenario 5.3.

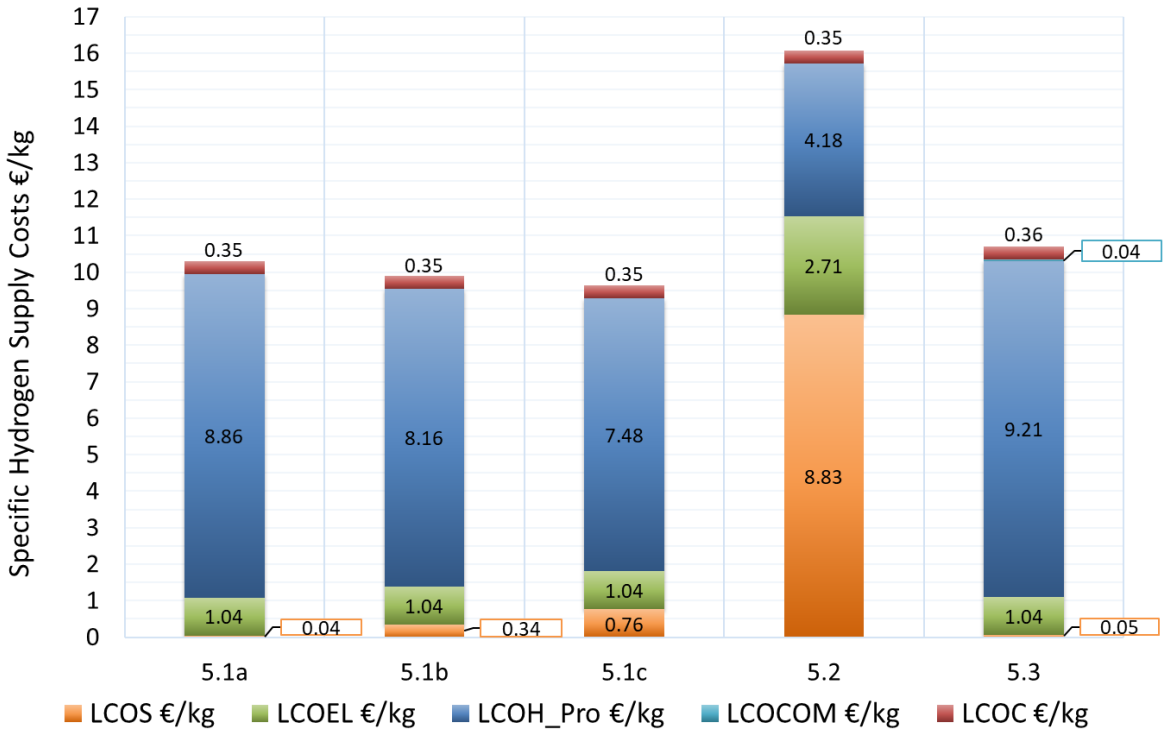


***Figure 28: Resulting specific hydrogen supply costs for scenario 5.1 to 5.3.***

The resulting operation strategies for electrolyzer and hydrogen storage are depicted in Figure 29. The purple line indicates the electricity price profile whereas the green, red and blue lines are representing the hydrogen storage level regarding the scenarios. The orange line represents the electrolyzer power according to the electricity price profile. The implemented storage capacity allows hydrogen production during more favorable periods of the year. Additionally, the stored hydrogen is used to avoid high electricity prices and meeting the demand. This influence is becoming more significant with increasing storage capacity (5.1a - 5.1c).

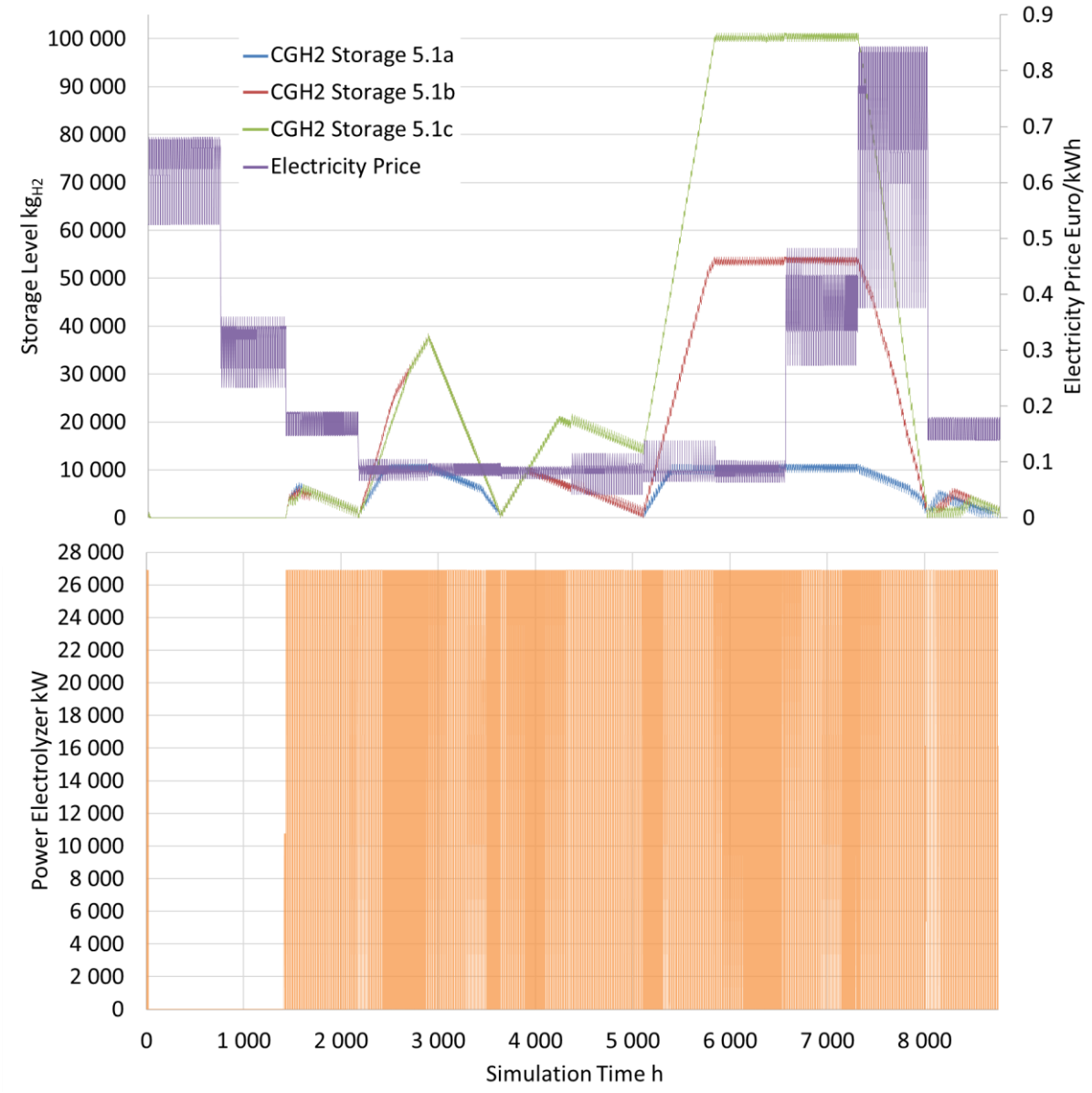


***Figure 29: Resulting operation strategies for hydrogen storage level and electrolyzer regarding scenarios 5.1a to 5.1c.***

The detailed scenario results are provided in the following chapters. Firstly, the results of scenario 5.1a, 5.1b and 5.1c are presented. Secondly scenario 5.2 and finally, scenario 5.3 are

outlined. The trends in comparison to each other and with scenario 4 are discussed in chapter 5.4.

### 5.3.1 On-Site Production with Low Storage Capacity Limit

The detailed flow and component results for scenario 5.1a utilizing a low storage capacity limit are shown in Table 7. This small hydrogen storage enables flexibility at low investment costs as well as low maintenance costs. However, it is necessary to use an electrolyzer with a higher production capacity compared to scenario 4 to take advantage of the fluctuating electricity prices. This is reflected in the investment and maintenance costs of the electrolyzer and the electrical power consumption. Furthermore, the storage option lowers the operating hours of the electrolyzer and significantly increases the number of load shifts. The high rate of production at elevated prices indicates that the small hydrogen storage cannot realize the full optimization potential. Furthermore, the storage tank is used to its full capacity and shows hardly any bottleneck for production at low electricity prices.

***Table 7: Component results of scenario 5.1a.***

| Parameter | Unit | Value |
|---|---|---|
| **Storage** | | |
| Capacity | $kg_{H2}$ | 11301 |
| Maximum Inflow | $kg_{H2}/h$ | 199.97 |
| Maximum Outflow | $kg_{H2}/h$ | 500 |
| CAPEX | € | 590693.8 |
| OPEX | € | 11813.88 |
| **Electrolyzer** | | |
| Power | kW | 26879.03 |
| Maximum Outflow | $kg_{H2}/h$ | 500 |
| CAPEX | € | 13954630.4 |
| OPEX | € | 209319.46 |
| Operating Hours | h | 4519 |
| Full Load Hours | h | 4334 |

| | | |
|---|---|---|
| Part Load Hours | h | 185 |
| Load Shifts | | 1127 |
| Production at High Electricity Price | % | 25,9 |
| Storage Full at Low Electricity Price | h | 71 |
| Electricity Costs | € | 19497104.84 |
| **Carbon Dioxide** | | |
| Total Annual Electricity Demand | GWh | 118.47 |
| Total Annual Emissions | $kg_{CO2}$ | 13979193.55 |

### 5.3.2 On-Site Production with Medium Storage Capacity Limit

The detailed flow and component results for scenario 5.1b utilizing a medium storage capacity limit are shown in Table 8. The medium storage tank improves flexibility but leads to significantly higher investment and maintenance costs. The KPI are in a similar range compared to the small hydrogen storage. However, the rate of production at elevated prices indicates that the medium hydrogen storage still cannot realize the full optimization potential.

***Table 8: Component results of scenario 5.1b.***

| Parameter | Unit | Value |
|---|---|---|
| **Storage** | | |
| Capacity | $kg_{H2}$ | 54508 |
| Maximum Inflow | $kg_{H2}/h$ | 199,97 |
| Maximum Outflow | $kg_{H2}/h$ | 500 |
| CAPEX | € | 4567818.02 |
| OPEX | € | 91356.36 |
| **Electrolyzer** | | |
| Power | kW | 26879,03 |
| Maximum Outflow | $kg_{H2}/h$ | 500 |
| CAPEX | € | 13954630,38 |

| | | |
|---|---|---|
| OPEX | € | 209319,45 |
| Operating Hours | h | 4494 |
| Full Load Hours | h | 4332 |
| Part Load Hours | h | 162 |
| Load Shifts | | 1068 |
| Production at High Electricity Price | % | 24,4 |
| Storage Full at Low Electricity Price | h | 34 |
| Electricity Costs | € | 17941488,53 |
| **Carbon Dioxide** | | |
| Total Annual Electricity Demand | GWh | 118,47 |
| Total Annual Emissions | $kg_{CO2}$ | 13979193,55 |

### 5.3.3 On-Site Production with High Storage Capacity Limit

The detailed flow and component results for scenario 5.1c utilizing a high storage capacity limit are shown in Table 9. The large hydrogen storage further improves flexibility showing approximately the same operating hours and load shifts compared to the other scenarios utilizing a capacity limit. The size causes high investment and maintenance costs at a similar level like the electrolyzer. Even though the rate of production at elevated prices has improved it is still above 20%.

***Table 9: Component results of scenario 5.1c.***

| Parameter | Unit | Value |
|---|---|---|
| **Storage** | | |
| Capacity | $kg_{H2}$ | 101230 |
| Maximum Inflow | $kg_{H2}/h$ | 199.97 |
| Maximum Outflow | $kg_{H2}/h$ | 500 |
| CAPEX | € | 10214391.03 |
| OPEX | € | 204287.82 |

| **Electrolyzer** | | |
|---|---|---|
| Power | kW | 26879.03 |
| Maximum Outflow | $kg_{H2}/h$ | 500 |
| CAPEX | € | 13954630.38 |
| OPEX | € | 209319.45 |
| Operating Hours | h | 4493 |
| Full Load Hours | h | 4333 |
| Part Load Hours | h | 160 |
| Load Shifts | | 999 |
| Production at High Electricity Price | % | 22.2 |
| Storage Full at Low Electricity Price | h | 33 |
| Electricity Costs | € | 16449958.91 |
| **Carbon Dioxide** | | |
| Total Annual Electricity Demand | GWh | 118.47 |
| Total Annual Emissions | $kg_{CO2}$ | 13979193.55 |

### 5.3.4 On-Site Production with Electricity Price Limit

The resulting operation strategies are depicted in Figure 30. The purple line indicates the electricity price profile whereas the red line is representing the hydrogen storage level. The black horizontal line shows the electricity price limit, and the orange line represents the electrolyzer power according to the electricity price profile. Due to the absence of a storage capacity limit the hydrogen production has significantly increased during the favorable periods of the year. This surplus hydrogen is stored to fully avoid high electricity prices. This is also reflected in the reduced operation time of the electrolyzer as can be seen in Figure 30.

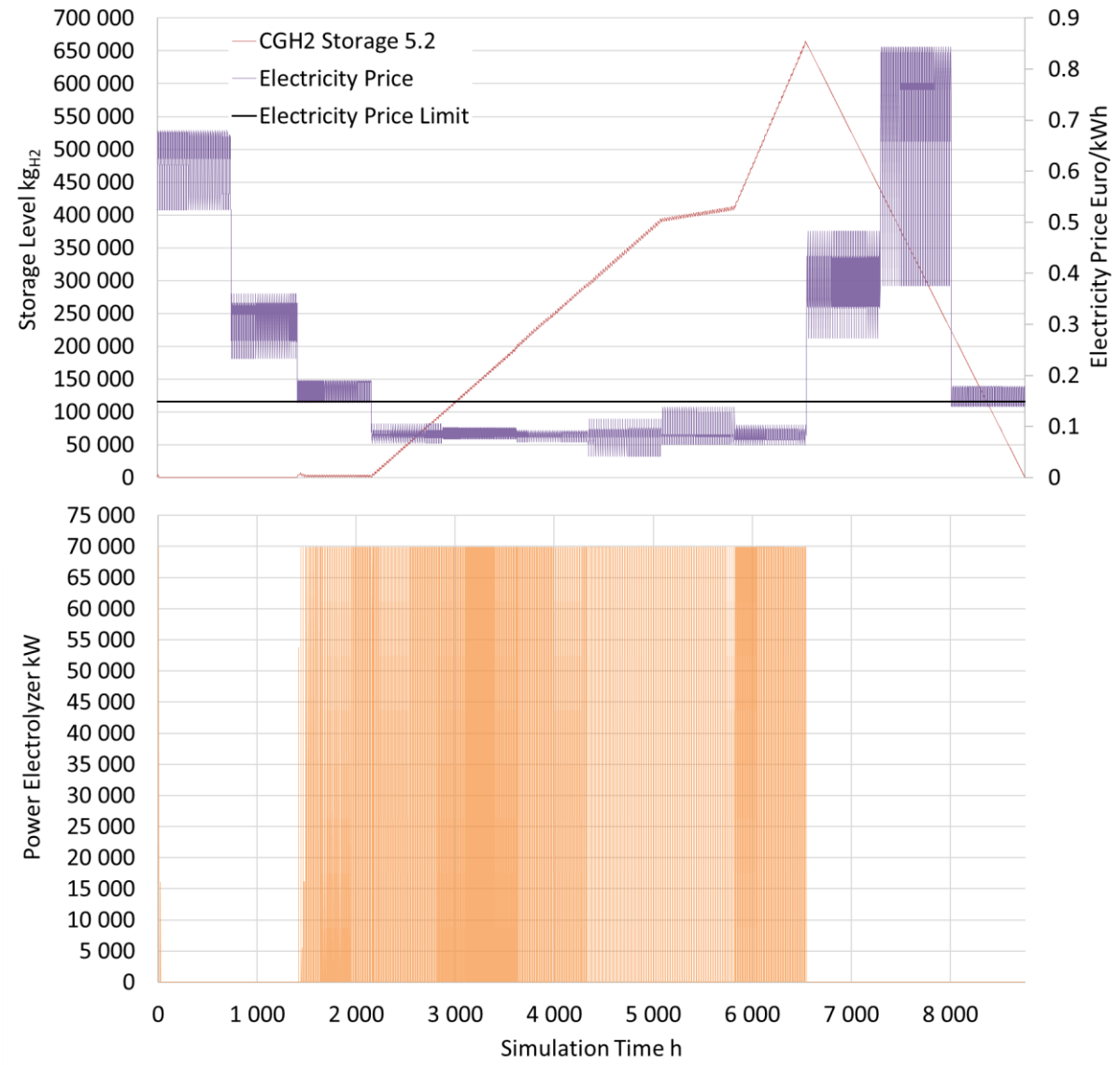


***Figure 30: Resulting operation strategy for hydrogen storage level and electrolyzer regarding scenario 5.2.***

The detailed flow and component results for scenario 5.2 are shown in Table 10. The resulting large hydrogen storage leads to very high investment and maintenance costs. To enable the charging and discharging in shorter periods the inflow and the outflow of the storage tank is increased significantly. Furthermore, the operation strategy necessitates an electrolyzer with a high production capacity resulting in a high electrical power consumption and very low full load hours. Even though the rate of production at elevated prices can be reduced close to zero, this operation strategy leads to a cost inefficient situation due to the high investment and maintenance costs. Additionally unpractical component sizes are assumed especially for the hydrogen storage tank.

*Table 10: Component results of scenario 5.2.*

| Parameter | Unit | Value |
|---|---|---|
| **Storage** | | |
| Capacity | $kg_{H2}$ | 664866.49 |
| Maximum Inflow | $kg_{H2}/h$ | 1000 |
| Maximum Outflow | $kg_{H2}/h$ | 1300.03 |
| CAPEX | € | 117995446.18 |
| OPEX | € | 2359908.92 |
| **Electrolyzer** | | |
| Power | kW | 69887.1 |
| Maximum Outflow | $kg_{H2}/h$ | 1300.03 |
| CAPEX | € | 36282876.36 |
| OPEX | € | 544243.15 |
| Operating Hours | h | 1710 |
| Full Load Hours | h | 1678 |
| Part Load Hours | h | 32 |
| Load Shifts | | 704 |
| Production at High Electricity Price | % | 0,5 |
| Storage Full at Low Electricity Price | h | 4 |
| Electricity Costs | € | 9182418.11 |
| **Carbon Dioxide** | | |
| Total Annual Electricity Demand | GWh | 118.47 |
| Total Annual Emissions | $kg_{CO2}$ | 13979193.55 |

### 5.3.5 On-Site Production with Elevated Pressure Level

The resulting operation strategies are depicted in Figure 31. The purple line indicates the electricity price profile whereas the red line is representing the hydrogen storage level. The increased storage capacity by compressing the hydrogen allows hydrogen production during more favorable periods of the year and using it to avoid high electricity prices. The implementation of a compressor and its operation causing additional investment, maintenance and electricity costs. However, the rate of production at elevated prices is high and shows no improvement caused by the hydrogen compression.

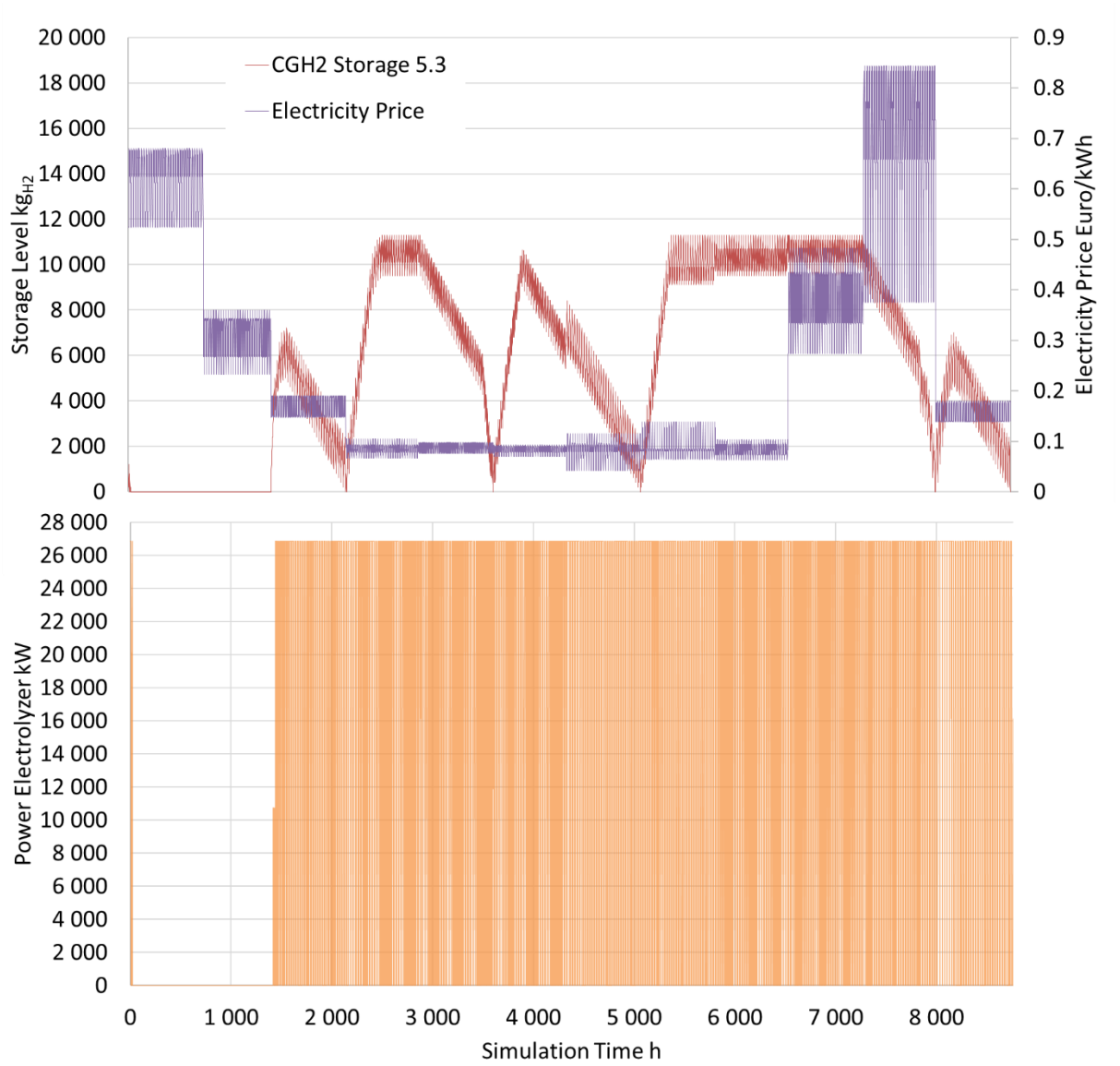


***Figure 31: Resulting operation strategy for hydrogen storage level and electrolyzer regarding scenario 5.3.***

The detailed flow and component results for scenario 5.3 with a hydrogen storage at a pressure level of 200 bar are shown in Table 11.

***Table 11: Component results of scenario 5.3.***

| Parameter | Unit | Value |
|---|---|---|
| **Storage** | | |
| Capacity | $kg_{H2}$ | 11301 |
| Maximum Inflow | $kg_{H2}/h$ | 199.97 |
| Maximum Outflow | $kg_{H2}/h$ | 399.94 |
| CAPEX | € | 707994.06 |
| OPEX | € | 14159.88 |
| **Electrolyzer** | | |
| Power | kW | 26879.03 |
| Maximum Outflow | $kg_{H2}/h$ | 500 |
| CAPEX | € | 13954630.38 |
| OPEX | € | 209319.46 |
| Operating Hours | h | 4553 |
| Full Load Hours | h | 4287 |
| Part Load Hours | h | 266 |
| Load Shifts | | 1078 |
| Production at High Electricity Price | % | 26.3 |
| Storage Full at Low Electricity Price | h | 56 |
| Electricity Costs | € | 19497104.84 |
| **Carbon Dioxide** | | |
| Total Annual Electricity Demand | GWh | 123.1 |
| Total Annual Emissions | $kg_{CO2}$ | 14525383.04 |
| **Compressor** | | |
| Power | kW | 1050.21 |
| CAPEX | € | 488057.61 |
| OPEX | € | 9761.15 |

## 5.4 Discussion

Within this section the research questions are answered by using the mentioned results and assumptions above. Moreover, findings and trends in connection with the sensitivity analysis are discussed.

### 5.4.1 Comparison of the Hydrogen Supply Routes

The investigated transport supply routes for this industrial site cause specific hydrogen supply costs in a range of 8,51 to 11,42 €/$kg_{H2}$ as can be seen in Figure 26. The supply through a repurposed hydrogen pipeline is the most cost effective under these assumptions due to the absence of a hydrogen storage infrastructure and the delivery of gaseous hydrogen.

The costs of the other transport options, except for railway transport with a F3 delivery frequency, lie close together. There is no significant difference between liquid hydrogen storage and gaseous hydrogen storage on site visible under these assumptions. With an increasing delivery frequency, the supply costs rise at an increasing rate leading to the highest costs stated by a railway delivery every three weeks. This is caused by the storage costs needed to buffer the delivery volume and the costs for regasification of the liquid hydrogen.

The resulting costs from scenario 4 lie at the upper end of the mentioned cost range at approximately the same level as the railway delivery every three weeks. Compared to the pipeline transport the supply costs are approximately 30% higher. The costs for the electrolyzer and the carbon dioxide emissions represent a minor role amounting to less than 10% of the supply costs. The cost driver behind the higher supply costs is the electricity price. This can be seen at the higher LCOH_Pro compared to the hydrogen production costs of the transport routes.

Scenario 5.1a shows a similar situation, although the LCOH_Pro are significantly reduced by using the small storage tank. It shows lower hydrogen supply costs than most of the transport scenarios but still with approximately 20% higher costs than pipeline transport. The LCOH_Pro of scenario 5.1a are slightly higher than the production costs of the transport scenarios.

Scenarios 5.1b and 5.1c continue this trend by utilizing higher storage volumes. The medium storage tank in scenario 5.1b leads to LCOH_Pro that fall below the production costs of the transport routes, whereas Scenario 5.1c shows even a reduction of 10%. Compared to the pipeline transport the costs are approximately 13% higher but are well within the range. Therefore scenario 5.1c seems to be a competitive alternative to the transport scenarios under these assumptions.

Scenario 5.2 causes high costs due to the used electricity price limit and can be regarded as an outlier. A more detailed analysis why this occurred is provided in the chapter below.

Scenario 5.3 has higher hydrogen supply costs similar to scenario 4. This is caused by the use of the compressor. The compressor itself described by the LCOCOM has neglectable influence, amounting to less than 1% of the hydrogen supply costs. However, the increased electricity consumption leads to significantly higher LCOH_Pro compared to scenarios 5.1a which utilizes the same storage capacity. If the pressure is further increased the CAPEX and OPEX for the compressor and for the storage will rise due to higher material requirements. Furthermore, the higher electricity consumption will lead to higher LCOC and higher LCOH_Pro. Therefore, a pressure increase for stationary storages should only be considered when the space at the installation site is limited. The advantage of gained storage capacity by compressing the hydrogen is nullified and the costs will rise with increasing pressure. This trend will be even more significant when the hydrogen is liquified before storing it.

### 5.4.2 Economic Influence of the Flexibility Option

This chapter addresses the second research question and analyses the influence of different operation strategies on the hydrogen supply costs.

The total annual hydrogen demand is equal for scenarios 4 and 5 but the specific hydrogen supply costs and the cost composition varies significantly depending on the limitations. The total annual electricity demand is also equal for most of the scenarios and therefore the total annual $CO_2$ emissions are equal too. The LCOC lie therefore within a range of 2 to 3.6% of the supply costs for scenarios 4 and 5 and represent a minor influence under these assumptions.

**Scenario 4**

The specific hydrogen supply costs of scenario 4 are the second highest behind scenario 5.2. This is because the operation of the electrolyzer is demand driven. When considering the electricity price profile in Figure 24 and the load profile in Figure 23, it can be seen that the electrolyzer has to operate regardless of the current electricity price. The advantage is that this constant operation leads to the lowest power requirement and therefore to the smallest electrolyzer. The LCOEL are approximately 41% lower than in scenarios 5.1a to 5.1c and 5.3 and approximately 77 % lower than in scenario 5.2. This would be even more significant when using an AEL due to the lower CAPEX and OPEX of PEMEL in 2030. This This influence is put into perspective because the LCOEL amount to only approximately 6% of the specific hydrogen supply costs. The disadvantage is that due to the missing flexibility option there is no possibility to avoid high electricity prices leading to high production costs. The LCOH_Pro are therefore the highest of all investigated scenarios and amount to 91% of the hydrogen supply costs. The elevated prices at the first quarter of the year have less effect on the costs because there is no hydrogen demand during the maintenance period as can be seen in Figure 23. With a different price distribution, a different maintenance period or a continuous production

throughout the whole year by using multiple burners, this effect will become even more significant.

**Scenario 5.1a**

Introducing a storage tank with a low capacity decreases the specific hydrogen supply costs by approximately 8% compared to scenario 4. As mentioned before this is influenced by avoiding high electricity prices as can be seen in Figure 29. Focusing on the last quarter of the year the storage level represented by the blue line is kept high to use the stored hydrogen in the eleventh month when electricity prices are at their highest. This optimization reduces costs in the longer term. Within a month the costs are optimized similarly by filling or emptying the storage tank depending on the fluctuation of the electricity prices. Figure 32 shows this in a detail of Figure 29. The red box further depicts the operation of the storage before a price leap. The storage is filled to its maximum capacity to soften the impact of increased prices as long as possible.

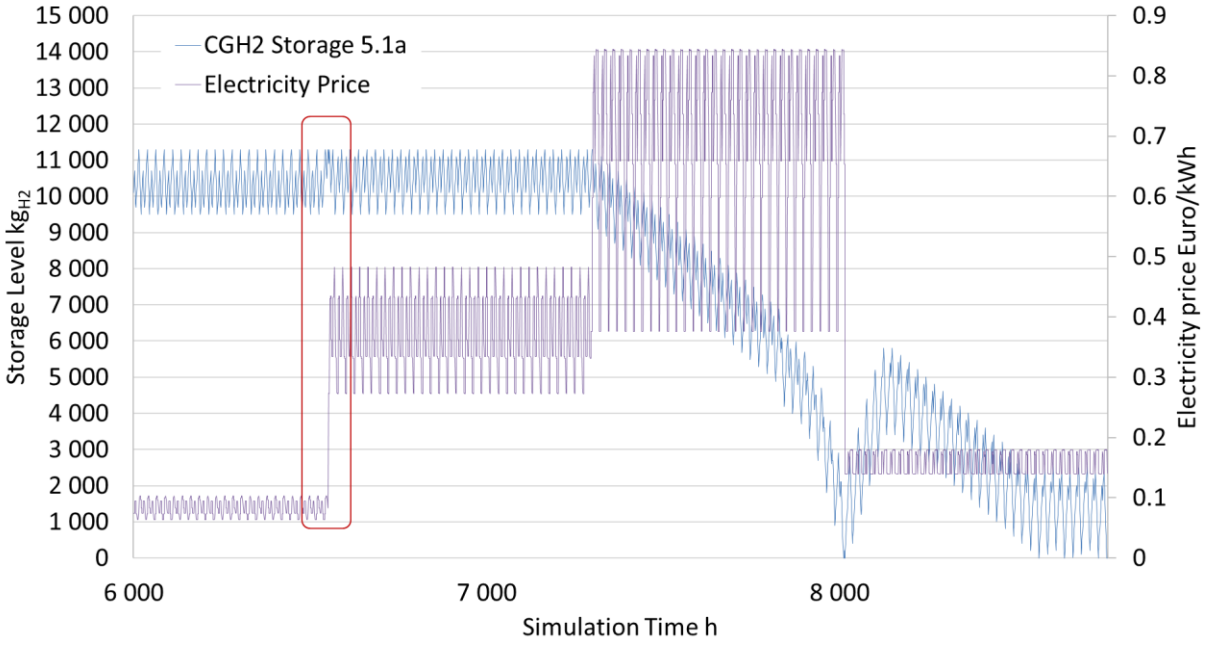


***Figure 32: Detail of Figure 29 showing the storage level of scenario 5.1a at the last quarter of the year according to the electricity price. The red box shows the operation of the storage to soften a leap in electricity costs.***

This optimization measures reduces the operation time by 2826 h compared to scenario 4 which leads to a lower capacity utilization with a downtime of approximately half the year. Furthermore, switching the electrolyzer leads to a sharp increase in load shifts compared to scenario 4 which could have negative effect on the lifetime.

The hours with favourable electricity prices and a full storage are low compared to the operation time amounting to approximately 1.5%. Despite of the reduction of 6% compared to scenario 4 the production at high electricity prices is still high.

Due to the small storage the LCOS amount to less than 1% of the hydrogen supply costs. However, they cannot be neglected as they are amounting still to nearly 600 000 € of CAPEX and operation and maintenance costs of approximately 12 000 €.

To enable the flexibility and charge the storage tank within short periods an electrolyzer with additional 10.8 MW of power is needed. This leads to a 4.5% rise in LCOEL compared to scenario 4 amounting to 10% of the hydrogen supply costs.

The LCOH_Pro are decreased as mentioned above due to the reduced electricity costs amounting to 86% of the hydrogen supply costs. The electricity price is still the main cost driver.

**Scenario 5.1b**

Utilizing a nearly five times larger storage tank than in scenario 5.1a, leads to a 11.7 % decrease of the hydrogen supply costs compared to scenario 4. This is due to the ability to store cheaper hydrogen for longer terms as in scenario 5.1a. This also reduces the number of load shifts and operation hours slightly. The hours with favourable electricity prices and a full storage are halved and the production at high electricity prices decreased by 7.5% compared to scenario 4.

The LCOS amount to approximately 3.5% of the hydrogen supply costs, caused by almost eight times higher CAPEX and corresponding operation and maintenance costs than in scenario 5.1a.

The size of the electrolyzer is sufficient and has not changed compared to scenario 5.1a leading to the same costs per $kgH_2$ with a LCOEL share of 10.5% regarding the hydrogen supply costs.

The LCOH_Pro are further decreased by the same reasons described in scenario 5.1a and are still the cost driver with an 82.5% share.

**Scenario 5.1c**

The used storage tank within this scenario is nine times larger than in scenario 5.1a leading to a 14% decrease of the hydrogen supply costs. As can be seen in Figure 29 the storage tank can be charged for longer periods reducing the number of load shifts slightly whereas the operating hours stay constant. The hours with favourable electricity prices and a full storage are constant too and the production at high electricity prices decreased by 9.7% compared to scenario 4. The LCOS amount to nearly 8% of the hydrogen supply costs caused by almost 17 times higher CAPEX and corresponding operation and maintenance costs.

The lower reduction rate in hydrogen supply costs indicates that the potential of larger storage tanks is increasingly exhausted. This trend of reducing hydrogen supply costs with increasing

storage was investigated using two further storage capacities (gray and light blue dot) to interpolate between the scenarios 5.1a (blue), 5.1b (red), 5.1c (green) and 5.2 (orange) as can be seen in Figure 33. It reaches its minimum between a storage capacity of approximately 100 000 $kgH_2$ and 150 000 $kgH_2$ and reverses with further storage capacity. Regarding security measures and the operation of such large storage tanks, smaller storage tanks should be preferred since the supply costs in scenario 5.1a and 5.1b show still a good cost reduction at lower capacities.

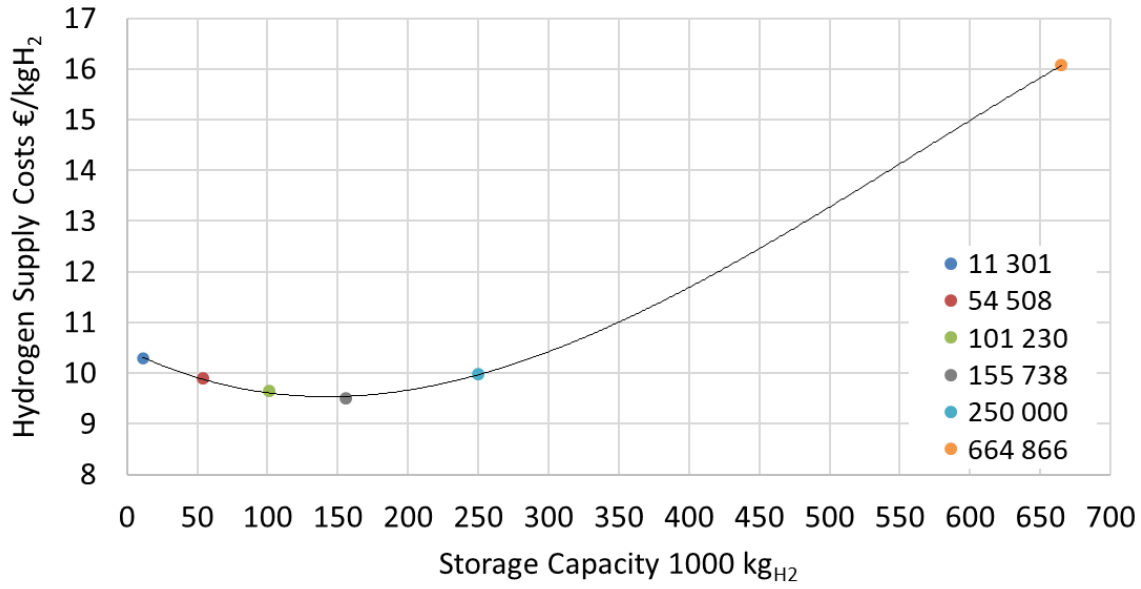


***Figure 33: Interpolation of the hydrogen storage capacity to estimate the minimum hydrogen supply costs.***

The size of the electrolyzer is sufficient and has not changed compared to scenario 5.1a leading to the same costs per $kgH_2$ and a share of 10.8% regarding the hydrogen supply costs.

The LCOH_Pro are further decreased and are still the cost driver with an 77.6% share.

**Scenario 5.2**

The used electricity price limit within this scenario leads to an extremum in operation strategy. Nearly the whole last quarter of the year exceeds the electricity price limit as can be seen in Figure 29. As described before to avoid high prices the solver tries to meet the demand during this phase of high prices by emptying the storage tank. To store this amount of hydrogen a storage tank with more than 650 000 $kgH_2$ is needed. Apart from the third month the storage tank is always charged until the electricity price limit is exceeded.

This also reduces the number of load shifts and operation hours significantly as can be seen in Figure 30. The hours with favourable electricity prices and a full storage and the production at high electricity prices amount to almost zero.

The hydrogen supply costs increased by 43% compared to scenario 4 due to the high LCOS. They amount to a share of 45% representing the cost driver of this scenario. As can be seen in Figure 33 the reduction of LCOS_Pro is nullified by the dominant storage costs. They are caused by almost 200 times higher CAPEX and corresponding operation and maintenance costs as in scenario 5.1a.

To charge this storage tank the size of the electrolyzer has increased by 54 MW compared to scenario 4 with approximately four times higher LCOEL amounting to a share of about 17% of the supply costs.

This scenario is not competitive and due to the high values of storage capacity and electrolyzer power assumed to be not suitable for an industrial site with this hydrogen demand.

**Scenario 5.3**

As mentioned in the section before the cost reducing influence of the storage capacity is partially counteracted by the compressor. The operation of the storage tank is done similarly to scenario 5.1 and is not affected significantly by the storage pressure.

The number of load shifts and operation hours are slightly lower compared to scenario 5.1a. The hours with favourable electricity prices are reduced slightly. The production at high electricity prices was reduced by 20%. These effects can be allocated to the improved storage capacity.

The LCOH_Pro are reduced by about 10% compared to scenario 4, amounting to a share of 86% of the hydrogen supply costs. The cost driver is the electricity price.

**Sensitivity Analysis**

Regarding the uncertainty of the input data a sensitivity analysis is carried out. It represents the influence of the $CO_2$ Certificate costs, the electricity price, the storage capacity, and the storage pressure when varying the data by 50% in both directions. The analysis of $CO_2$ Certificates and electricity price was based on the parameters of scenario 5.1a. The storage capacity analysis was based on parameters of scenario 5.1b and the storage pressure on scenario 5.1c. Figure 34 shows the influence on the hydrogen supply costs. The $CO_2$ certificate costs, the storage costs and the storage pressure show a minor influence on the hydrogen supply costs ranging from -2% to 3%. The electricity price shows a significant influence of -43% to 86% substantiating being the cost driver as discussed above.

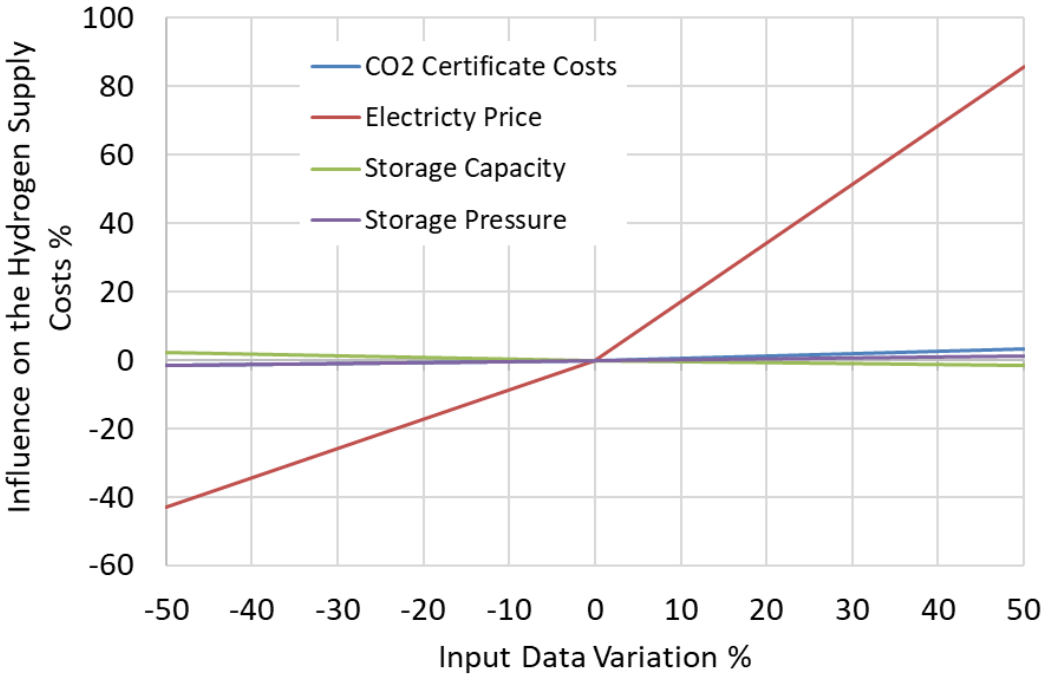


***Figure 34: Sensitivity analysis to investigate the influence of the input data on the hydrogen supply costs for the on-site scenarios.***

Within the sensitivity analysis the influence of utilizing the produced oxygen to substitute oxygen purchases is evaluated. The LCOOXY amount to -23.84 €/$kg_{H2}$ which indicates that there is a potential to reduce the hydrogen supply costs by using the produced oxygen. Due to the high uncertainty and the assumptions discussed in section 4.5.4 the LCOOXY are not included in the hydrogen supply costs. Under these assumptions, their influence would be very high putting the hydrogen supply costs into perspective. It is therefore suggested to investigate the cost reduction potential of oxygen on a case-by-case basis using more detailed information provided from a specific industrial consumer.

Regarding the uncertainty of scenarios 1-3, the influence on the hydrogen supply costs is analyzed by varying the hydrogen production costs by -62% and 46.1%. This represents the lower and upper boundary of hydrogen production costs found in the literature [4] and can be seen in Figure 35. The hydrogen supply costs for truck transport are the least affected showing a variation within a range of -50 to 37.2%. The difference caused by the different state of stored hydrogen is neglectable therefore the lines overlap. The railway transport shows a variation of hydrogen supply costs in a range of -49.8 to 37.1%, whereby the influence is decreasing with longer delivery intervals. The hydrogen supply costs for pipeline transport closely align with the hydrogen production price due to the low distribution costs showing a variation in the range of -60.8 to 45.3%.

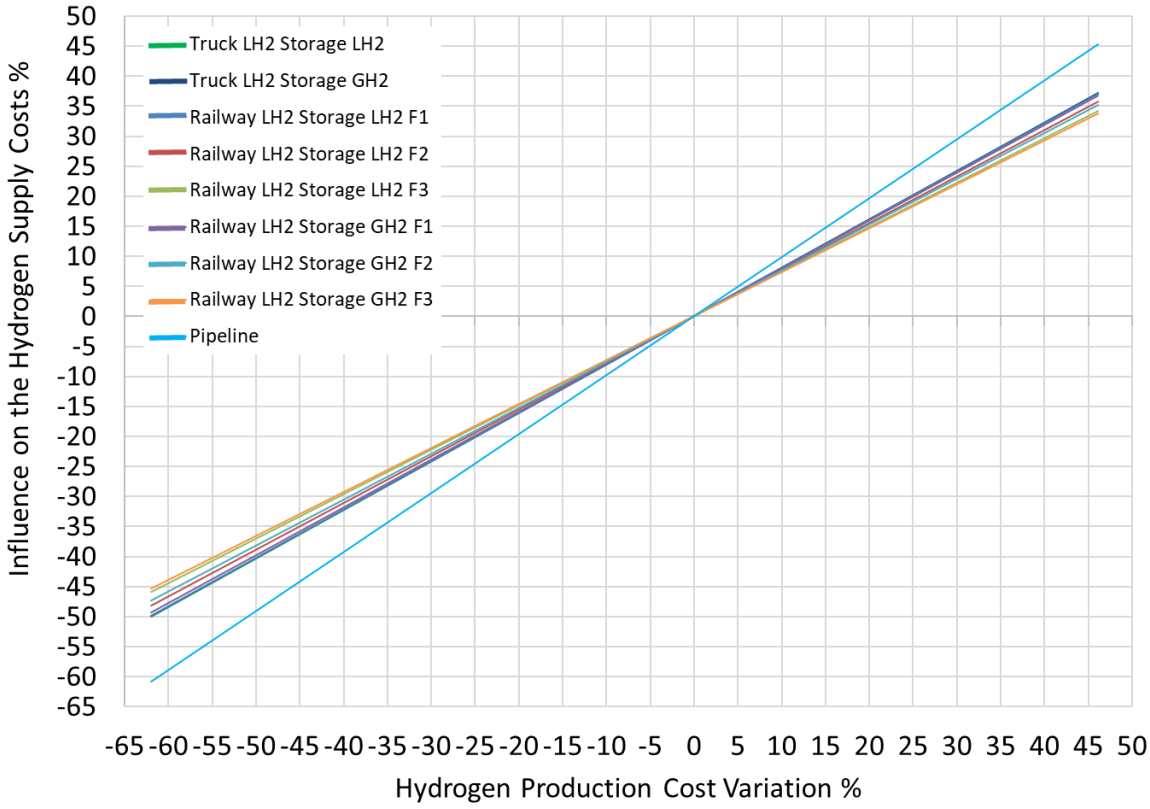


***Figure 35: Sensitivity analysis to investigate the influence of the hydrogen production costs on the hydrogen supply costs for the transport scenarios.***

# 6 CONCLUSION AND OUTLOOK

With the ongoing transformation of the industry the demand of low emission hydrogen will increase. The expansion of the hydrogen transport infrastructure is influenced by many factors and cannot always meet the requirements of the companies. Companies with a significant hydrogen requirement have to make a decision whether they rely on the future regional transport and distribution infrastructure or if they invest in an on-site production facility to obtain the hydrogen themselves. Under the investigated assumptions hydrogen production on-site could be competitive solution to purchasing the hydrogen from a supply point depending on the company size and requirements. Smaller companies may benefit from merchant hydrogen especially when they are close to a supply point or transport hub. For larger companies transport by pipeline seems to be favourable especially when the hydrogen is obtained directly from sources in Spain or Tunisia as stated by Kathan et al. and Rodgarkia-Dara et al. [4] or from Norway as expressed by Carels et al. [5]. On-site production could be beneficial to ensure supply security at reasonable costs when the regional transport infrastructure reaches its capacity limits or if no repurposed hydrogen pipeline connection is available. The use of an electrolyser together with a storage tank could be a cost-efficient solution by taking advantage of fluctuating electricity prices and further improving supply

security. The impact of this optimization depends strongly on the electricity price level and its fluctuations. Lower electricity price levels will improve the cost efficiency of on-site electrolysis and enable the use of smaller storage tanks. This could be covered by low pressure aboveground storage tanks which cause less costs and safety concerns. However high electricity price levels necessitate large storage capacities to be competitive. Those capacities will only be realized in underground storages due to costs and safety concerns. Increasing the storage capacity by compressing or liquifying the hydrogen cannot be recommended. The cost reducing effect of the capacity gain is nullified by the rising electricity costs and the advantage of reduced space consumption is assumed to be less important.

Future trends will strongly depend on the price for fossil energy carriers and $CO_2$ certificate costs which can slow the transformation as companies remain with existing processes. A positive incentive towards hydrogen utilization could be the intensive expansion of renewable energy which decreases electricity prices and improves the costs of on-site production through water electrolysis. Furthermore, learning curves and scale effects in electrolyzer technology, industrial hydrogen storage and hydrogen applications could improve the cost efficiency even more.

Looking into the future of the Austrian hydrogen supply a well-balanced hydrogen energy system is needed to meet the demands of all companies. This necessitates a well-developed hydrogen infrastructure including on-site electrolysis, transport, and storage options. On-site production could be a key component to enable the utilization of hydrogen in regions with a well-established electrical infrastructure and a lack of hydrogen transport infrastructure. The progressive development of electrolysis system efficiencies can further improve cost efficiency and reduce the load on the electricity grid. Moreover, electrolysis can mitigate peak loads in the growing hydrogen infrastructure and improve the utilization of renewable surplus power.

In a future techno-economic analysis, this model could be adapted to investigate a variety of companies with different requirements and load profiles and reevaluate the costs with new data created by the intensive research on electrolysis and hydrogen storage. Moreover, other electricity price profiles can be used to tailor the model accordingly to future price developments. Additionally, oxygen utilization for oxyfuel technologies together with CCU and a methanol synthesis could be added to investigate the cost impact on the overall system.

# 7 BIBLIOGRAPHY

[1] BUNDESMINISTERIUM FÜR KLIMASCHUTZ, UMWELT, ENERGIE, MOBILITÄT, INNOVATION UND TECHNOLOGIE: *Wasserstoffstrategie für Österreich* (2022). URL https://www.bmk.gv.at/themen/energie/energieversorgung/wasserstoff/strategie.html – Überprüfungsdatum 2024-03-16

[2] WANG A., JENS J., MAVINS D, MOULTAK M., SCHIMMEL M., VAN DER LAUN K., PETERS D., AND BUSEMAN M.: *European Hydrogen Backbone* : *Analysing future demand, supply, and transport of hydrogen* (2021)

[3] GANTER, Alissa ; GABRIELLI, Paolo ; SANSAVINI, Giovanni: *Near-term infrastructure rollout and investment strategies for net-zero hydrogen supply chains*. In: *Renewable and Sustainable Energy Reviews* 194 (2024), S. 114314

[4] JOHANNES KATHAN, JUDITH KAPELLER, STEFAN REUTER, PHILIPP ORTMANN, ARIA RODGARKIA-DARA, MAXIMILIANE REGER, GREGOR BRÄNDLE, CHRISTOPH GATZEN: *Importmöglichkeiten für Erneuerbaren Wasserstoff* (2022). URL https://publications.ait.ac.at/de/publications/importm%C3%B6glichkeiten-f%C3%BCr-erneuerbaren-wasserstoff-5 – Überprüfungsdatum 2024-03-28

[5] FABIAN CARELS, LUCAS SENS, PROF. DR.-ING. MARTIN KALTSCHMITT ; DR.-ING. LEANDRO JANKE, DR. MATTHIAS DEUTSCH: *Wasserstoff-Importoptionen für Deutschland* : *Analyse mit einer Vertiefung zu Synthetischem Erdgas (SNG) bei nahezu geschlossenem Kohlenstoffkreislauf* (2023). URL https://www.agora-energiewende.de/publikationen/wasserstoff-importoptionen-fuer-deutschland – Überprüfungsdatum 2024-04-14

[6] MORTIMER, Charles E. ; MÜLLER, Ulrich: *Chemie* : *Das Basiswissen der Chemie*. 13. vollständig überarbeitete Auflage. Stuttgart : Thieme, 2019

[7] NAJJAR, Yousef S.H.: *Hydrogen safety: The road toward green technology*. In: *International Journal of Hydrogen Energy* 38 (2013), Nr. 25, S. 10716–10728

[8] INGENIEURE, Verein Deutscher: *VDI-Wärmeatlas* : *Reference work*. 11., bearb. und erw. Aufl. Berlin, Heidelberg : Springer Vieweg, 2013

[9] LI, Xinfeng ; MA, Xianfeng ; ZHANG, Jin ; AKIYAMA, Eiji ; WANG, Yanfei ; SONG, Xiaolong: *Review of Hydrogen Embrittlement in Metals: Hydrogen Diffusion, Hydrogen Characterization, Hydrogen Embrittlement Mechanism and Prevention*. In: *Acta Metallurgica Sinica (English Letters)* 33 (2020), Nr. 6, S. 759–773

[10] LI, Xinfeng ; ZHANG, Jin ; FU, Qinqin ; SONG, Xiaolong ; SHEN, Sicong ; LI, Qizhen: *A comparative study of hydrogen embrittlement of 20SiMn2CrNiMo, PSB1080 and PH13-8Mo high strength steels*. In: *Materials Science and Engineering: A* 724 (2018), S. 518–528

[11] LI, Xinfeng ; ZHANG, Jin ; SHEN, Sicong ; WANG, Yanfei ; SONG, Xiaolong: *Effect of tempering temperature and inclusions on hydrogen-assisted fracture behaviors of a low alloy steel*. In: *Materials Science and Engineering: A* 682 (2017), S. 359–369

[12] NEERAJ, T. ; SRINIVASAN, R. ; LI, Ju: *Hydrogen embrittlement of ferritic steels: Observations on deformation microstructure, nanoscale dimples and failure by nanovoiding*. In: *Acta Materialia* 60 (2012), 13-14, S. 5160–5171

[13] ZHU, Xu ; LI, Wei ; HSU, T. Y. ; ZHOU, Shu ; WANG, Li ; JIN, Xuejun: *Improved resistance to hydrogen embrittlement in a high-strength steel by quenching–partitioning–tempering treatment*. In: *Scripta Materialia* 97 (2015), S. 21–24

[14] ZHAO, Tianliang ; LIU, Zhiyong ; XU, Xuexu ; LI, Yong ; DU, Cuiwei ; LIU, Xingbo: *Interaction between hydrogen and cyclic stress and its role in fatigue damage mechanism*. In: *Corrosion Science* 157 (2019), S. 146–156

[15] ZHOU, Pengwei ; LI, Wei ; ZHU, Xu ; LI, Yu ; JIN, Xuejun ; CHEN, Jian: *Graphene Containing Composite Coatings as a Protective Coatings against Hydrogen Embrittlement in Quenching & Partitioning High Strength Steel*. In: *Journal of The Electrochemical Society* 163 (2016), Nr. 5, D160-D166

[16] RONEVICH, Joseph A. ; SOMERDAY, Brian P. ; SAN MARCHI, Chris W.: *Effects of microstructure banding on hydrogen assisted fatigue crack growth in X65 pipeline steels*. In: *International Journal of Fatigue* 82 (2016), S. 497–504

[17] ALVARO, Antonio ; DI WAN ; OLDEN, Vigdis ; BARNOUSH, Afrooz: *Hydrogen enhanced fatigue crack growth rates in a ferritic Fe-3 wt%Si alloy and a X70 pipeline steel*. In: *Engineering Fracture Mechanics* 219 (2019), S. 106641

[18] OGAWA, Yuhei ; MATSUNAGA, Hisao ; YAMABE, Junichiro ; YOSHIKAWA, Michio ; MATSUOKA, Saburo: *Fatigue limit of carbon and Cr Mo steels as a small fatigue crack threshold in high-pressure hydrogen gas*. In: *International Journal of Hydrogen Energy* 43 (2018), Nr. 43, S. 20133–20142

[19] WANG, Rong: *Effects of hydrogen on the fracture toughness of a X70 pipeline steel*. In: *Corrosion Science* 51 (2009), Nr. 12, S. 2803–2810

[20] CHATZIDOUROS, E. V. ; TRAIDIA, A. ; DEVARAPALLI, R. S. ; PANTELIS, D. I. ; STERIOTIS, T. A. ; JOUIAD, M.: *Effect of hydrogen on fracture toughness properties of a pipeline steel under*

*simulated sour service conditions*. In: *International Journal of Hydrogen Energy* 43 (2018), Nr. 11, S. 5747–5759

[21] SONG, Yan ; CHAI, Mengyu ; YANG, Bin ; HAN, Zelin ; AI, Song ; LI, Yun: *Investigation of the Influence of Pre-Charged Hydrogen on Fracture Toughness of As-Received 2.25Cr1Mo0.25V Steel and Weld*. In: *Materials (Basel, Switzerland)* 11 (2018), Nr. 7

[22] BHUIYAN, Md. Shahnewaz ; TODA, Hiroyuki ; SHIMIZU, Kazuyuki ; SU, Hang ; UESUGI, Kentaro ; TAKEUCHI, Akihisa ; WATANABE, Yoshio: *The Role of Hydrogen on the Local Fracture Toughness Properties of 7XXX Aluminum Alloys*. In: *Metallurgical and Materials Transactions A* 49 (2018), Nr. 11, S. 5368–5381

[23] PALLASPURO, Sakari ; YU, Haiyang ; KISKO, Anna ; PORTER, David ; ZHANG, Zhiliang: *Fracture toughness of hydrogen charged as-quenched ultra-high-strength steels at low temperatures*. In: *Materials Science and Engineering: A* 688 (2017), S. 190–201

[24] YAMABE, Junichiro ; YOSHIKAWA, Michio ; MATSUNAGA, Hisao ; MATSUOKA, Saburo: *Effects of hydrogen pressure, test frequency and test temperature on fatigue crack growth properties of low-carbon steel in gaseous hydrogen*. In: *Procedia Structural Integrity* 2 (2016), S. 525–532

[25] INTERNATIONAL ENERGY AGENCY: *Global Hydrogen Review 2023* (2023), S. 18–98. URL https://www.iea.org/reports/global-hydrogen-review-2023 – Überprüfungsdatum 2024-03-16

[26] ZOU, Caineng ; LI, Jianming ; ZHANG, Xi ; JIN, Xu ; XIONG, Bo ; YU, Huidi ; LIU, Xiaodan ; WANG, Shanyu ; LI, Yiheng ; ZHANG, Lin ; MIAO, Sheng ; ZHENG, Dewen ; ZHOU, Hongjun ; SONG, Jiani ; PAN, Songqi: *Industrial status, technological progress, challenges, and prospects of hydrogen energy*. In: *Natural Gas Industry B* 9 (2022), Nr. 5, S. 439–442

[27] VALERA-MEDINA, Agustin (Hrsg.); BAÑARES ALCÁNTARA, René (Hrsg.): *Techno-economic challenges of green ammonia as energy vector*. London : Academic Press, 2021

[28] RÄUCHLE, Konstantin ; PLASS, Ludolf ; WERNICKE, Hans-Jürgen ; BERTAU, Martin: *Methanol for Renewable Energy Storage and Utilization*. In: *Energy Technology* 4 (2016), Nr. 1, S. 193–200

[29] STERNER, Michael: *Bioenergy and Renewable Power Methane in Integrated 100% Renewable Energy Systems* : *Limiting Global Warming by Transforming Energy Systems*, 2010

[30] EUROPEAN CEMENT RESEARCH ACADEMY GMBH: *The ECRA technology Papers 2022* : *State of the Art Cement Manufacturing Current technologies and their future development*

(2022), S. 149–155. URL https://ecra-online.org/research/technology-papers/ – Überprüfungsdatum 2024-03-18

[31] GÄRTNER, Sebastian ; RANK, Daniel ; HEBERL, Michael ; GADERER, Matthias ; DAWOUD, Belal ; HAUMER, Anton ; STERNER, Michael: *Simulation and Techno-Economic Analysis of a Power-to-Hydrogen Process for Oxyfuel Glass Melting*. In: *Energies* 14 (2021), Nr. 24, S. 8603

[32] PASCAL, Barthe ; CHAUGNY, Michel ; DELGADO SANCHO, Luis ; ROUDIER, Serge: *Best available techniques (BAT) reference document for the refining of mineral oil and gas industrial emissions* : *Industrial Emissions Directive 2010/75/EU (integrated pollution prevention and control)*. Luxembourg : Publications Office, 2015 (EUR, Scientific and technical research series 27140)

[33] MARKUS LEHNER, Robert Obenaus-Emler: *Untersuchung der nachhaltigen Verwertung von Kohlenstoff aus der Methanpyrolyse* : *WPx Methanpyrolyse*. In: *Berichte aus Energie- und Umweltforschung* (2021), S. 15–21. URL https://nachhaltigwirtschaften.at/en/publications/schriftenreihe-2023-63-methanpyrolyse.pdf – Überprüfungsdatum 2024-03-18

[34] EMANUELE TAIBI, HERIB BLANCO, RAUL MIRANDA, MARCELO CARMO: *Green hydrogen cost reduction* : *Scaling up electrolysers to meet the 1.5$^{o}$ C climate goal*. Abu Dhabi : IRENA, International Renewable Energy Agency, 2020

[35] ANDERSSON, Joakim ; GRÖNKVIST, Stefan: *Large-scale storage of hydrogen*. In: *International Journal of Hydrogen Energy* 44 (2019), Nr. 23, S. 11901–11919

[36] POHLMANN, Carsten ; RÖNTZSCH, Lars ; HEUBNER, Felix ; WEIßGÄRBER, Thomas ; KIEBACK, Bernd: *Solid-state hydrogen storage in Hydralloy–graphite composites*. In: *Journal of Power Sources* 231 (2013), S. 97–105

[37] BLANKENSHIP, L. Scott ; BALAHMAR, Norah ; MOKAYA, Robert: *Oxygen-rich microporous carbons with exceptional hydrogen storage capacity*. In: *Nature communications* 8 (2017), Nr. 1, S. 1545

[38] MARTIN KALTSCHMITT, WOLFGANG STREICHER, ANDREAS WIESE: *Erneuerbare Energien* : *Systemtechnik, wirtschaftlichkeit, umweltaspekte*. [Place of publication not identified] : MORGAN KAUFMANN, 2020

[39] HOLGER DÖRR, ANGELA BRANDES, MARTIN KRONENBERGER, NILS JANßEN, STEFAN GEHRMANN: *Wasserstoff in der Gasinfrastruktur* : *DVGW/Avacon- Pilotvorhaben mit bis zu 20% Wasserstoffeinspeisung in Erdgas-H2-20*. Abschlussbericht (2023). URL https://www.avacon-netz.de/content/dam/revu-global/avacon-

netz/documents/avacon_netz/forschungsprojekte/H2-20-Abschlussbericht-final.pdf – Überprüfungsdatum 2024-03-21

[40] ALZOHBI, G. ; ALMOAIKEL, A. ; ALSHUHAIL, L.: *An overview on the technologies used to store hydrogen*. In: *Energy Reports* 9 (2023), S. 28–34

[41] LANGMI, Henrietta W. ; ENGELBRECHT, Nicolaas ; MODISHA, Phillimon M. ; BESSARABOV, Dmitri: Hydrogen storage. In: *Electrochemical Power Sources: Fundamentals, Systems, and Applications* : Elsevier, 2022, S. 455–486

[42] ULF BOSSEL ; BALDUR ELIASSON: *Energy and the Hydrogen Economy* (2003)

[43] J.M. SMITH, H.C. VAN NESS, M.M. ABBOTT, M.T. SWIHART: *Introduction to chemical engineering thermodynamics*. New York : McGraw-Hill, 2018

[44] WOLF, Erik: Large-Scale Hydrogen Energy Storage. In: *Electrochemical Energy Storage for Renewable Sources and Grid Balancing* : Elsevier, 2015, S. 129–142

[45] CARDELLA, U. ; DECKER, L. ; KLEIN, H.: *Roadmap to economically viable hydrogen liquefaction*. In: *International Journal of Hydrogen Energy* 42 (2017), Nr. 19, S. 13329–13338

[46] VALENTI, G.: Hydrogen liquefaction and liquid hydrogen storage. In: *Compendium of Hydrogen Energy* : Elsevier, 2016, S. 27–51

[47] WILHELMSEN, Øivind ; BERSTAD, David ; AASEN, Ailo ; NEKSÅ, Petter ; SKAUGEN, Geir: *Reducing the exergy destruction in the cryogenic heat exchangers of hydrogen liquefaction processes*. In: *International Journal of Hydrogen Energy* 43 (2018), Nr. 10, S. 5033–5047

[48] BERSTAD, D. ; STANG, J. ; NEKSA, P.: *Comparison criteria for large-scale hydrogen liquefaction processes*. In: *International Journal of Hydrogen Energy* 34 (2009), Nr. 3, S. 1560–1568

[49] CARDELLA, U. ; DECKER, L. ; SUNDBERG, J. ; KLEIN, H.: *Process optimization for large-scale hydrogen liquefaction*. In: *International Journal of Hydrogen Energy* 42 (2017), Nr. 17, S. 12339–12354

[50] KLELL, Manfred: *Handbook of hydrogen storage* : *Storage of Hydrogen in the Pure Form*. Weinheim : Wiley-VCH, 2010

[51] GOEPPERT, Alain ; CZAUN, Miklos ; JONES, John-Paul ; SURYA PRAKASH, G. K. ; OLAH, George A.: *Recycling of carbon dioxide to methanol and derived products - closing the loop*. In: *Chemical Society reviews* 43 (2014), Nr. 23, S. 7995–8048

[52] KLERKE, Asbjørn ; CHRISTENSEN, Claus Hviid ; NØRSKOV, Jens K. ; VEGGE, Tejs: *Ammonia for hydrogen storage: challenges and opportunities*. In: *Journal of Materials Chemistry* 18 (2008), Nr. 20, S. 2304

[53] GRASEMANN, Martin ; LAURENCZY, Gábor: *Formic acid as a hydrogen source – recent developments and future trends*. In: *Energy & Environmental Science* 5 (2012), Nr. 8, S. 8171

[54] BLOOMBERG NEF: *Hydrogen Economy Outlook* : *Key Messages* (2020)

[55] IEA: *The Future of Hydrogen* : *Seizing todays opportunities*. Report prepared by the IEA for the G20, Japan (2019)

[56] DANISH ENERGY AGENCY AND ENERGINET: *Technology Data for Energy Transport* : *Technology descriptions and projections for long-term energy system planning* (2017), Nr. 0004

[57] OEMOF DEVELOPER GROUP: *Open Energy Modelling Framework (oemof)*. URL https://oemof.readthedocs.io/en/latest/#open-energy-modelling-framework-oemof – Überprüfungsdatum 2024-03-24

[58] OEMOF DEVELOPER GROUP: *oemof.solph* : *A model generator for energy system modelling and optimisation*. URL https://oemof-solph.readthedocs.io/en/stable/readme.html#documentation – Überprüfungsdatum 2024-03-24

[59] KRIEN, Uwe ; SCHÖNFELDT, Patrik ; LAUNER, Jann ; HILPERT, Simon ; KALDEMEYER, Cord ; PLEßMANN, Guido: *oemof.solph—A model generator for linear and mixed-integer linear optimisation of energy systems*. In: *Software Impacts* 6 (2020), S. 100028

[60] HART, William E. ; LAIRD, Carl D. ; WATSON, Jean-Paul ; WOODRUFF, David L. ; HACKEBEIL, Gabriel A. ; NICHOLSON, Bethany L. ; SIIROLA, John D.: *Pyomo Optimization Modeling in Python*. 2nd ed. 2017. Cham : Springer International Publishing; Imprint: Springer, 2017 (Springer Optimization and Its Applications 67)

[61] OEMOF DEVELOPER GROUP: *solph User's guide*. URL https://oemof-solph.readthedocs.io/en/stable/usage.html – Überprüfungsdatum 2024-03-24

[62] JOHN FORREST ; TED RALPHS ; HAROLDO GAMBINI SANTOS ; STEFAN VIGERSKE ; LOU HAFER ; BJARNI KRISTJANSSON ; JPFASANO ; EDWINSTRAVER ; MILES LUBIN ; JAN-WILLEM ; RLOUGEE ; JPGONCAL1 ; SAMUEL BRITO ; H-I-GASSMANN ; CRISTINA ; MATTHEW SALTZMAN ; TOSTTOST ; BRUNO PITRUS ; FUMIAKI MATSUSHIMA ; TO-ST: *coin-or/Cbc: Release releases/2.10.10* : Zenodo, 2023

[63] ANDREW MAKHORIN: *GNU Linear Programming Kit* : *Reference Manual for GLPK Version 5.0* (2020)

[64] ABDIN, Zainul ; KHALILPOUR, Kaveh ; CATCHPOLE, Kylie: *Projecting the levelized cost of large scale hydrogen storage for stationary applications*. In: *Energy Conversion and Management* 270 (2022), S. 116241

[65] BÖHM, Hans ; ZAUNER, Andreas ; ROSENFELD, Daniel C. ; TICHLER, Robert: *Projecting cost development for future large-scale power-to-gas implementations by scaling effects*. In: *Applied Energy* 264 (2020), S. 114780

[66] EUROPEAN COMISSION: *EU Reference Scenario 2020*. URL https://energy.ec.europa.eu/data-and-analysis/energy-modelling/eu-reference-scenario-2020_en – Überprüfungsdatum 2023-11-27

[67] DOCK, Johannes ; KIENBERGER, Thomas: *Techno-economic case study on Oxyfuel technology implementation in EAF steel mills – Concepts for waste heat recovery and carbon dioxide utilization*. In: *Cleaner Engineering and Technology* 9 (2022), S. 100525

[68] EUROPEAN ENVIRONMENT AGENCY: *Greenhouse gas emission intensity of electricity generation*. URL URL https://www.eea.europa.eu/data-and-maps/daviz/co2-emission-intensity-13#tab-googlechartid_chart_11 – Überprüfungsdatum 2023-12-05

[69] ATKINS, Peter William ; PAULA, Julio de: *Atkins' physical chemistry*. 8th ed. Oxford : Oxford University Press, 2006

[70] INSTITUT FÜR ELEKTRIZITÄTSWIRTSCHAFT UND ENERGIEINNOVATION - TU GRAZ ; LEHRSTUHL FÜR ENERGIEVERBUNDTECHNIK (EVT) - MONTANUNIVERSITÄT LEOBEN ; ÖSTERREICHISCHES INSTITUT FÜR WIRSCHAFTSFORSCHUNG (WIFO): *InfraTrans 2040* : *Szenarien und Ausbaupläne für ein nachhaltiges Wirtschaftssystem in Österreich.* (2023)

[71] WOGRIN, Sonja ; TEJADA-ARANGO, Diego Alejandro ; GAUGL, Robert ; KLATZER, Thomas ; BACHHIESL, Udo: *LEGO: The open-source Low-carbon Expansion Generation Optimization model*. In: *SoftwareX* 19 (2022), S. 101141

[72] IKB: *Wasser Preisblatt* : *Gültig ab 1. Jänner 2024*. URL https://www.ikb.at/fileadmin/user_upload/Dokumente/Wasser/Wasser-Abwasser-Preisblatt.pdf – Überprüfungsdatum 2024-03-28

[73] LAND OBERÖSTERREICH: *Was kostet Trinkwasser*. URL https://www.land-oberoesterreich.gv.at/19703.htm – Überprüfungsdatum 2024-03-28

[74] FLORIAN NIGBUR, MARTIN ROBINIUS, PATRICK WIENERT, MATTHIAS DEUTSCH: *Levelised cost of hydrogen* : *Making the application of the LCOH concept more consistent and more useful* (2023)

[75] HYDROGEN EUROPE - TECH: *Hydrogen Transport & Distribution* (2021). URL https://www.hydrogeneurope.eu/wp-content/uploads/2021/11/Tech-Overview_Hydrogen-Transport-Distribution.pdf

[76] RAIL CARGO GROUP ÖBB: *Gütertarif* : *Neuausgabe vom 15. Dezember 2021* (2021). URL https://www.railcargo.com/de/dms/tarife/oegt-2022.pdf

[77] EUROPEAN CENTRAL BANK: *Average exchange rate USD vs. EUR 2019*. URL https://www.ecb.europa.eu/stats/policy_and_exchange_rates/euro_reference_exchange_rates/html/eurofxref-graph-usd.en.html – Überprüfungsdatum 2024-05-05

[78] GUNAWAN, Tubagus Aryandi ; SINGLITICO, Alessandro ; BLOUNT, Paul ; BURCHILL, James ; CARTON, James G. ; MONAGHAN, Rory F. D.: *At What Cost Can Renewable Hydrogen Offset Fossil Fuel Use in Ireland's Gas Network?* In: *Energies* 13 (2020), Nr. 7, S. 4–8

[79] ELBERRY, Ahmed M. ; THAKUR, Jagruti ; SANTASALO-AARNIO, Annukka ; LARMI, Martti: *Large-scale compressed hydrogen storage as part of renewable electricity storage systems*. In: *International Journal of Hydrogen Energy* 46 (2021), Nr. 29, S. 15671–15690

# 8 APPENDIX

It must be mentioned that AI-Tools have been used in parts of this thesis to support linguistic revision such as grammar, translation or rephrasing and to simplify and improve program codes. Table 12 shows the extend of the use for the respective purposes. Furthermore, a document with examples of the generated prompts is provided at the Chair of Energy Network Technology.

***Table 12: Declaration of AI based tools.***

| Purpose | AI Contribution | AI Tool | Prompts |
|---|---|---|---|
| Translation | 15% | DeepL<br>ChatGPT 3.5 | Chair of Energy Network Technology |
| Grammar and linguistic correctness | 30% | Grammarly<br>DeepL<br>ChatGPT 3.5 | Chair of Energy Network Technology |
| Rephrasing | 30% | Grammarly<br>ChatGPT 3.5 | Chair of Energy Network Technology |
| Code generation | 10% | ChatGPT 3.5 | Chair of Energy Network Technology |
| Code simplification and improvement | 20% | ChatGPT 3.5 | Chair of Energy Network Technology |
| Troubleshooting and debugging | 65% | ChatGPT 3.5 | Chair of Energy Network Technology |